
Electronic Thesis and Dissertation Repository

8-17-2022 9:00 AM

Campylobacter jejuni Capsular Heptose: Moderation of Host Macrophages and Substrate Channeling During Synthesis

Matthew Myles, *The University of Western Ontario*

Supervisor: Creuzenet, Carole, *The University of Western Ontario*

A thesis submitted in partial fulfillment of the requirements for the Master of Science degree in Microbiology and Immunology

© Matthew Myles 2022

Follow this and additional works at: <https://ir.lib.uwo.ca/etd>



Part of the [Bacteriology Commons](#), and the [Immunology of Infectious Disease Commons](#)

Recommended Citation

Myles, Matthew, "Campylobacter jejuni Capsular Heptose: Moderation of Host Macrophages and Substrate Channeling During Synthesis" (2022). *Electronic Thesis and Dissertation Repository*. 8753. <https://ir.lib.uwo.ca/etd/8753>

This Dissertation/Thesis is brought to you for free and open access by Scholarship@Western. It has been accepted for inclusion in Electronic Thesis and Dissertation Repository by an authorized administrator of Scholarship@Western. For more information, please contact wlsadmin@uwo.ca.

Abstract

With the majority of Canadian *Campylobacter jejuni* infections resulting from contaminated poultry, I investigated how the strain NCTC 11168 capsular heptose modulates host macrophage activation, and bacterial clearance. I hypothesized that this sugar acts to dampen immune activation in both human and avian hosts, leading to diminished clearance by macrophages. The heptose was found to be immunosuppressive in chicken, but not human, macrophages and did not significantly impact clearance. Previous data also indicate that the capsular heptose biosynthesis enzymes have a means to limit degradation of unstable intermediates. As such, I hypothesized that these enzymes engage in substrate channeling in order to limit substrate degradation within the cytosol. Data indicate that enzymes in the heptose modification pathways can interact physically, potentially permitting channeling. This work determined how the capsular heptose alters the activity of host macrophages, while investigating if enzymatic interactions can be exploited to modulate heptose production.

Keywords

Campylobacter, *Campylobacter jejuni* (*C. jejuni*), capsule, bacteriology, enzymology, glycobiology, modified heptose, host-specificity, protein-protein interactions, macrophage, substrate channeling, phagocytosis, cytokines, gastroenteritis.

Summary for Lay Audience

Campylobacter jejuni is a common cause of diarrheal disease in humans, with most cases in Canada resulting from eating contaminated broiler chicken meat. The bacterium does not cause disease in poultry, and different effects across hosts potentially result from differences in the reaction of their immune systems. A key mediator of interactions with host cells may be a modified heptose sugar which branches off the backbone of the capsule, a sugar chain that decorates the outside of *C. jejuni* NCTC 11168. To study the role this heptose plays in moderating the host immune response, I have added *C. jejuni* mutants that differentially express their capsular heptose to human or chicken macrophages (white blood cells). This work allowed me to study immune activation by looking at the production of molecules that help kill bacteria. Bacterial clearance has been assessed by counting the bacteria after their interaction with macrophages. I hypothesized that the *C. jejuni* NCTC 11168 capsular heptose acts to tone down activation in both hosts, leading to less clearance by host macrophages. Data indicate that the capsular heptose reduces immune activation by chicken, but not human, macrophages. The capsule itself causes lower binding to and survival within chicken macrophages, while causing lower uptake by human macrophages.

I have also investigated how the proteins that produce the heptose interact, as previous data indicates that these proteins have a means to limit breakdown of production intermediates. I hypothesize this is accomplished through substrate channeling, a process by which proteins directly transfer intermediates by interacting physically. Using biochemical techniques, data was generated which indicate that enzymes within the heptose synthesis pathways can bind together.

These two subprojects merge with the goal of increasing clearance of *C. jejuni* from broiler chickens being raised for human consumption, limiting transmission to humans. I have investigated how the capsular heptose alters activation of host macrophages, and their ability to clear bacteria while determining if physical interactions between proteins can be exploited to decrease heptose production.

Co-Authorship Statement

Much of my research required the use of capsular heptose mutants that were previously generated by the Creuzenet lab [173]. Work using microscale thermophoresis was conducted by Olivier Lesouhaitier and Florian Defontaine at the University of Rouen, Normandy (France), using proteins that I expressed and provided. My clearance assays were also an extension of work completed by previous Honour's student Daniel Zimmermann. The data generated by Daniel Zimmermann are detailed in appendix 2.

Acknowledgments

I would like to start off by thanking my supervisor Dr. Carole Creuzenet for her help and support throughout my degree. Your faith in my abilities as a researcher truly helped me believe in myself more and more, every day I stepped into the lab. The lessons I have learned over the past 3 years are those that I will carry into the future. Your ability to teach in a kind, empathetic, and effective manner is something I hope to emulate, you are my role model. Thank you for choosing me as a student, I cannot imagine doing this work without you. I am also extremely grateful for the members of my advisory committee, Dr. David Heinrichs and Dr. Gary Shaw. Thank you for your time, expertise, and input on my work. You have helped to strengthen the contents of the next 100+ pages. I would additionally like to thank Dr. John McCormick for providing a Roche LDH kit, allowing preliminary study of LDH release.

I want to thank the members of the Creuzenet Lab, past and present. In my three years here, I have met many wonderful people. I would like to first thank Matthew McCallum, Anthony Wong, Natalie Fava, Heba Barnawi, and Daniel Zimmermann who have previously worked on this project. I could not have completed my work without those who have laid out the background for me. I would also like to thank Noor Salloum, Mohammad Mohiuddin, Yingxue Sun, and Daniel Zimmermann for training me on the techniques that I have used to complete my research. I would also like to thank Brian Yang and Mahmoud Mahmoudpour for their help in making SDS-PAGE gels and in the purification of my enzymes. Finally, I would like to thank all members of the Creuzenet Lab for welcoming me, chatting with me about research, and about life. Three years have flown by in good company.

I would also like to thank my father Edward Myles for his constant support. You've always believed in me and pushed me to excel. Thank you for sparking an interest in nature in me from a young age. You've raised someone who cares deeply about the world they live in. Finally, I'd like to thank my partner Stephen Nettles and one of my best friends, Ian Cleary, for spending time with me throughout the past two years. It has been a busy, stressful time and you have kept me anchored.

Table of Contents

Abstract.....	ii
Summary for Lay Audience.....	iii
Co-Authorship Statement.....	iv
Acknowledgments.....	v
Table of Contents.....	vi
List of Tables.....	viii
List of Figures.....	ix
List of abbreviations.....	x
Chapter 1.....	1
1 Introduction.....	1
1.1 Food and its enduring importance.....	1
1.2 Food and waterborne pathogens.....	1
1.3 <i>Campylobacter jejuni</i>	3
1.4 Overview of <i>C. jejuni</i> virulence factors.....	6
1.4.1 Capsule polysaccharide.....	8
1.5 <i>C. jejuni</i> and host macrophages.....	14
1.6 Substrate channelling.....	17
1.7 Rationale, Hypothesis, and Objectives.....	19
Chapter 2.....	22
2 Materials and methods.....	22
2.1 Culturing <i>C. jejuni</i> capsular heptose mutants.....	22
2.2 Culturing MQ-NCSU chicken macrophages.....	23
2.3 Culturing THP-1 human monocytes and macrophages.....	24
2.4 Plating host cells for lactate dehydrogenase release assay, Griess assay, TNF α ELISA, and cytokine multiplex assay.....	25
2.5 Griess assay.....	26
2.6 LDH release assay.....	27
2.7 TNF α ELISA.....	27
2.8 MOI assay.....	29
2.9 Cytokine multiplex.....	29
2.10qRT-PCR.....	29
2.11Reactive oxygen species fluorescence assay.....	33
2.12Adhesion, uptake, and intracellular survival assays.....	34
2.12.1 Adhesion assay.....	34
2.12.2 Uptake assay.....	35
2.12.3 Intracellular survival assay.....	35
2.13Expression and purification of His-tagged proteins.....	36
2.14Analysis of purified proteins (SDS-PAGE, Western blot, Bradford assay).....	37
2.15Surface plasmon resonance using carboxyl chips.....	39
2.16Statistical Analysis.....	40
Chapter 3.....	42
3 Results.....	42
3.1 Validating the multiplicity of infection for macrophage activation assays.....	42
3.2 <i>C. jejuni</i> does not confer significant cytotoxicity to host macrophages under conditions tested.....	44

3.3	The <i>C. jejuni</i> NCTC 11168 capsular heptose diminishes nitrite induction in chicken macrophages	45
3.4	<i>C. jejuni</i> NCTC 11168 diminishes the levels of ROS produced by host macrophages	47
3.5	The <i>C. jejuni</i> NCTC 11168 capsular heptose does not impact TNF α induction by human macrophages.....	50
3.6	The <i>C. jejuni</i> NCTC 11168 capsular heptose does not impact cytokine induction by human macrophages.....	51
3.7	Comparison of WT <i>C. jejuni</i> -mediated effector transcription in THP-1 and MQ-NCSU macrophages.....	55
3.8	Adhesion, uptake, and intracellular survival of <i>C. jejuni</i> NCTC 11168 upon culture with host macrophages.....	57
3.8.1	The <i>C. jejuni</i> NCTC 11168 CPS diminishes adhesion to chicken macrophages	59
3.8.2	Addition of MeOPN to the <i>C. jejuni</i> NCTC 11168 CPS increases uptake by human macrophages.....	62
3.8.3	The <i>C. jejuni</i> NCTC 11168 CPS diminishes survival within human and chicken macrophages	65
3.8.4	Overall trends and summary	68
3.9	DdahA, DdahB, and DdahC, are able to interact in pairs	72
3.9.1	SPR principle and preliminary data for DdahA/DdahB	72
3.9.2	Attempt at determining K_D for DdahA and DdahB interactions	74
3.9.3	Qualitative pairwise interactions, can DdahC interact with DdahA or DdahB?	80
3.10	Assessing interactions of enzymes in the Mlgh pathway	81
3.10.1	DdahA with MlghB and MlghC	82
3.10.2	WcaG with MlghB and MlghC.....	84
3.11	Microscale thermophoresis affirms formation of the DdahA/B complex	93
Chapter 4	95
4	Discussion	95
4.1	<i>C. jejuni</i> NCTC 11168 capsular heptose in the activation of host macrophages..	95
4.2	<i>C. jejuni</i> NCTC 11168 capsular heptose in interactions with host macrophages.	101
4.3	Capsular heptose biosynthesis enzymes are able to interact physically	107
4.4	Overall significance and conclusions.....	113
References	115
Appendix 1: qRT-PCR figures.....		129
Appendix 2: Macrophage clearance work accomplished by Daniel Zimmermann		132
Curriculum Vitae		133

List of Tables

Table 1: Composition of the <i>C. jejuni</i> NCTC 11168 CPS mutants.	23
Table 2: Gene specific primers used during qPCR on cDNA generated from human and chicken macrophages.	31
Table 3: conditions for the expression and purification of the capsular heptose biosynthesis enzymes.	37
Table 4: NMR spectroscopy analyses of hot water/phenol extracted CPS from the wild-type <i>C. jejuni</i> and its isogenic capsular mutants.	58
Table 5: Percentage of WT recovered from host macrophages and monocytes in adhesion, uptake, and intracellular survival assays.	69
Table 6: Summary of phenotypes displayed by <i>C. jejuni</i> capsular mutants in adhesion, uptake, and intracellular survival assays, across chicken and human macrophages/monocytes.	70
Table 7: Quantification of Ddah proteins used for SPR by Bradford Assay.	75
Table 8: Enzymatic interactions tested by surface plasmon resonance without regeneration.	82
Table 9: Quantification of Mlgh proteins used for SPR by Bradford Assay.	82
Supplemental Table 1: Macrophage clearance data generated by Daniel Zimmermann.	132

List of Figures

Figure 1: <i>C. jejuni</i> capsule polysaccharide synthesis.....	10
Figure 2: <i>C. jejuni</i> GDP-manno-heptose modification pathways.....	12
Figure 3: Creation of <i>C. jejuni</i> capsular heptose mutants.....	13
Figure 4: Impact of multiplicity of infection on effector induction by host macrophages co-cultured with wild-type <i>C. jejuni</i>	43
Figure 5: Host macrophage cytotoxicity induced by <i>C. jejuni</i> capsular heptose mutants.....	45
Figure 6: Nitrite induction in MQ-NCSU macrophages by <i>C. jejuni</i> capsular heptose mutants.....	47
Figure 7: Induction of reactive oxygen species in THP-1 human and MQ-NCSU chicken macrophage by <i>C. jejuni</i> capsular heptose mutants.....	50
Figure 8: TNF α induction in THP-1 macrophages by <i>C. jejuni</i> capsular heptose mutants....	51
Figure 9: Cytokine output from Human THP-1 macrophage co-cultured with <i>C. jejuni</i> capsular heptose mutants.....	54
Figure 10: Adhesion of <i>C. jejuni</i> capsular heptose mutants to chicken and human macrophage and/or monocytes.....	61
Figure 11: Uptake of <i>C. jejuni</i> capsular heptose mutants by chicken and human macrophage and/or monocytes.....	65
Figure 12: Intracellular survival of <i>C. jejuni</i> capsular heptose mutants within chicken and human macrophage and/or monocytes.....	67
Figure 13: SDS-PAGE gels of purified proteins from the Mlgh and Ddah pathways.....	73
Figure 14: SPR signal flowing DdahB over immobilized DdahA.....	74
Figure 15: Tracedrawer outputs for SPR detailing interactions between enzymes in the Ddah pathway.....	78
Figure 16: Attempted kinetic determinization for the interaction of enzymes in the Ddah biosynthetic pathway.....	80
Figure 17: Proposed method of interaction between enzymes in the Ddah pathway.....	81
Figure 18: Tracedrawer outputs for SPR detailing interactions with MlghB and MlghC.....	87
Figure 19: Attempted kinetic determinization for the interaction of enzymes in the Mlgh and Ddah biosynthetic pathways.....	90
Figure 20: Proposed interactions between enzymes in the Mlgh pathway.....	92
Figure 21: Microscale thermophoresis dose response curves assessing interactions between DdahA and DdahB.....	94
Supplemental Figure 1: Fold change in the expression of THP-1 macrophage cytokine mRNA upon challenge with WT <i>C. jejuni</i>	129
Supplemental Figure 2: Cycling threshold values for cDNA generated from the co-culture of wild-type <i>C. jejuni</i> with host macrophages.....	130
Supplemental Figure 3: Cycling threshold values for cDNA generated from the co-culture of wild-type <i>C. jejuni</i> with host macrophages, rerun with modifications.....	131

List of abbreviations

bp	Base pair(s)
BSA	Bovine serum albumin
CFU	Colony forming units
CPS	Capsule polysaccharide
DCF	2',7'-dichlorofluorescein
DCF-DA	2',7'-dichlorofluorescein diacetate
FBS	Fetal bovine serum
FPLC	Fast protein liquid chromatography
Gal	Galactose
GalN	galactosamine
GalNAc	N-acetyl galactosamine
Glc	glucose
GlcA	glucuronic acid
GroN	2-amino-2-deoxyglycerol
IL	Interleukin
LB	lysogeny broth (Luria Bertani broth)
LOS	Lipooligosaccharide
LPS	Lipopolysaccharide
Me	Methyl
MeOPN	Methylated phosphoramidate
MQ-NCSU/ NCSU	Muquarrab Qureshi-North Carolina State University chicken macrophage cell line
MST	Microscale thermophoresis
NO	Nitric oxide
OD ₆₀₀	Optical density at 600 nm
PBS	Phosphate buffered saline
PCR	Polymerase chain reaction
ROS	Reactive oxygen species
RT	Reverse transcription/ transcriptase
SPR	Surface plasmon resonance

TNF α	Tumor necrosis factor alpha
TSA	Trypticase soy agar
TSB	Trypticase soy broth
WT	Wild-type

Chapter 1

1 Introduction

1.1 Food and its enduring importance

To say food is important is truly an extreme understatement. Food is a necessity, required to support life – from worms, to birds, to humans, all organisms that can eat are in constant pursuit of nourishment. For humans, food has many additional dimensions of significance beyond the need for sustenance. Food is an important means of cultural expression, with the development of cuisines stemming from the intersection of the historical, religious, and agricultural landscape in any given region [127]. Food helps maintain and share one's cultural identity and is an important means of expression and communication. As such, an incredible amount of time and resources are invested into both food preparation and preservation.

Compared to the past, with every year, there are more and more people who need to eat. As such, humans have shifted from primarily hunting, gathering, and small-scale agricultural endeavours, to much of the world – primarily developed countries – relying on the large-scale production of the food industry. With an increase in food production through large agricultural and processing efforts, there has also been an increased need for safe food handling and preservation. Food preservation has occurred throughout history as a means to inhibit the growth of pathogenic microorganisms, including foodborne bacteria. Common means of preservation are classified as mechanical (e.g., milling and crystallizing), biological (e.g., fermenting and curdling), thermal (e.g., smoking, drying, and frying), and chemical (e.g., salting and pickling) [74]. The need to produce safe food is ever increasing.

1.2 Food and waterborne pathogens

Unfortunately, when food is not handled properly, it can become contaminated by pathogens (bacteria, viruses, parasites, and molds) that cause great harm to humans. Even with the rise of antimicrobials, diarrheal diseases remain a large challenge to global

health, being the second leading cause of death for children under the age of 5, resulting in 1.6 million deaths yearly [90]. On an even larger scale, the World Health Organization (WHO) estimates that more than 2 billion people worldwide suffer from diarrheal disease annually [120]. The most common bacterial pathogens that result in enteric disease include *Salmonella spp.*, *Shigella spp.*, enterotoxigenic *E. coli* (ETEC), and *Campylobacter spp.*, accounting for roughly 95 million, 88 million, 75 million, and 75 million cases annually, respectively [147,166]. Other notable enteric pathogens include *Listeria monocytogenes*, *Vibrio spp.*, *Clostridium perfringens*, *Yersinia enterocolitica*, *Staphylococcus aureus*, rotavirus, norovirus, hepatitis A, and *Giardia spp.* [111]. These pathogens share a commonality in that they induce diarrhea that can result in dehydration. This dehydration, if untreated and prolonged, is the most common way these pathogens confer mortality.

In addition to transmission by food, a large proportion of diarrheal disease worldwide is brought on by the consumption of contaminated drinking water. The WHO estimates that, currently, at least 1 in 10 people worldwide have no access to basic services needed to obtain clean drinking water [160]. This is primarily a concern in developing countries, with lower accessibility to clean water greatly impacting the health of children under the age of 5 [90]. Outbreaks of waterborne illness often follow periods of heavy rain or snowfall, with increased runoff collecting pathogens in the environment (from soil, animal feces) and depositing them within communal water supplies [38,107]. Therefore, it is important to consider climate and meteorological events, in addition to socioeconomic factors in disease prediction and prevention.

While yearly incidence tends to be higher in developing nations due to a lack of clean drinking water, enteric pathogens still create a large burden in developed countries, with food and waterborne illness estimated to cause roughly 9.4 million illnesses, 56,000 hospitalizations, and 1,400 deaths annually in the United States alone [17]. Additionally, it is important to recognize that there are underserved communities in all countries, and that the division of safe food and water is not always equivalent. For example, it is well documented that the indigenous population of Canada is disproportionately affected by food and waterborne pathogens compared to the general population [66]. In fact, a 2015

study looking at the incidence of foodborne illness in Inuit communities in Rigolet and Iqaluit, Nunavut, found the annual incidence of acute gastrointestinal illness to be as high as 2.9-3.9 cases/person per year, relative to about 1.0 cases cases/person per year for the general public in Ontario or British Columbia [50].

Scientists, governments, food industries, and the agricultural industries across many countries work tirelessly to control the spread of these pathogens. The control of food and waterborne pathogens is a major public health concern, with outbreaks of enteric disease not only affecting people at an individual level, but also often having economic implications as well. Foodborne illness costs the United States up to 90 billion dollars annually [133]. Still, it is undeniable that mortality rates from food and waterborne illness are much lower now than they were 100 years ago, due to improvements in food handling, water treatment, and the rise of antimicrobials [36]. However, this work is far from over, with the emergence of antibiotic resistance being seen within all of the bacterial species listed in this section [24,36,111]. As such, it is imperative that research continues to detail causative pathogens in a manner that can be exploited to control the spread of disease.

1.3 *Campylobacter jejuni*

Though likely observed as early as 1886 by Theodor Escherich, the *Campylobacter* genus was not described until 1963 [134,136]. *Campylobacters* are Gram negative, microaerophilic bacteria that possess a characteristic spiral or corkscrew morphology [113,140]. The bacteria within this genus range in size from 0.2–0.8 μm in width by 0.5–5 μm in length, and are typically catalase and oxidase positive with the ability to reduce nitrites, though select species differ [140,148]. The production of catalase and oxidase permit growth in the presence of oxygen and help deal with oxidative stress, while nitrite reductases help to resist nitrosative stress. These bacteria grow optimally at 42°C, mirroring the internal temperature of avian hosts, with a significant decrease in growth at temperatures below 37°C [84]. Stressors including changes in temperature, pH, osmolarity, oxygen levels, and nutrient availability induce *Campylobacters* to take on a

protective coccoid morphology, in which the bacteria are considered to be viable but non-culturable [52,61,87].

Campylobacter jejuni is one of the leading causes of bacterial enteritis worldwide. In humans, upon entering the body through the fecal-oral route, *C. jejuni* colonizes the small intestine before reaching its target organ, the colon [140,163]. Campylobacteriosis results within 1-5 days of exposure and is characterized by the onset of watery, potentially bloody, diarrhea. This is associated with abdominal pain, nausea, and vomiting, with acute symptoms generally lasting 5-7 days [142]. Though symptoms tend to be similar across pathogenic members of *Campylobacter spp.*, *C. jejuni* is of greatest interest as it is the most prevalent, causing between 60-80% of all pathogenic *Campylobacter* infections [67]. The second most prevalent species is *C. coli*, accounting for roughly 10% of *Campylobacter* infections in developed countries [136]. One of the most notable local outbreaks of campylobacteriosis occurred in May of the year 2000, in Walkerton, Ontario. Heavy, prolonged rainfall caused the runoff of *E. coli* O157:H7 and *Campylobacter* into the town's drinking water and surrounding wells, cumulatively resulting in over 2000 cases of disease and 6 deaths [10,31].

The long-term complications of campylobacteriosis include increased risk of several autoimmune disorders. Infection is most strongly associated with Guillain-Barre syndrome, a neurodegenerative disorder in which autoreactive antibodies bind to gangliosides found on myelin sheaths coating nerves, causing degradation [6]. Guillain-Barre syndrome is consistently listed as the first or second leading cause of acute flaccid paralysis, and occurs following approximately 3 of every 10,000 cases of campylobacteriosis [18,59,88,142]. The autoreactive antibodies that cause GBS arise against specific modifications to the bacterium's lipooligosaccharide (LOS) that act as a form of molecular mimicry [23]. These antibodies are thus cross reactive between the *C. jejuni* LOS and human gangliosides. A study from July 2020 also implicates *C. jejuni* in increasing the risk of post infection-irritable bowel syndrome (PI-IBS), with a risk 1.2 times higher in those who were infected with *C. jejuni* relative to those infected with *Salmonella spp.* [60]. *C. jejuni* had the highest association with PI-IBS of all bacterial agents studied, and was found in patients with the diarrheal or mixed subtype (diarrhea

and constipation). The association with IBS is thought to be in part caused by cytolethal distending toxin (Cdt), a secreted toxin that disrupts tight junction proteins leading to epithelial dysfunction, and may trigger immune responses leading to further dysregulation [164]. Finally, a population study of Finnish patients linked campylobacteriosis to the development of reactive arthritis (ReA), with an annual incidence of 4.3 per 100,000 [49]. Post-infection ReA was most commonly seen in adults and was independent of HLA-B27 expression, which is a human leukocyte antigen commonly associated with Rheumatoid arthritis [49]. Increased incidence of ReA has also been observed in populations following *C. jejuni* outbreaks [49].

As *C. jejuni* is an enteric pathogen, the majority of infections stem from the ingestion of contaminated meat, milk, or drinking water. The most clinically relevant form of transmission in developed countries is ingestion of contaminated poultry – mainly broiler chicken meat [142]. *C. jejuni* resides as a commensal in the gastrointestinal tract of broiler chickens with concentrations as high as 10^9 colony forming units (CFU) per gram of caecal matter [126]. Through the slaughtering process, *C. jejuni* can be released onto the meat, leading to contamination. The bacteria pose little risk if the contaminated meat is cooked to the recommended temperature of 165°F (74°C), but can easily confer pathogenesis if the meat undercooked, or if surfaces are cross-contaminated during food preparation [25]. In fact, as few as 500 CFU of *C. jejuni* need to be ingested in order for campylobacteriosis to occur [177]. As of 2013, *Campylobacter spp.* could be isolated from 32 to 76% of broiler chicken meat tested in Europe [180]. Although estimates of *Campylobacter* contaminated poultry were lower in Canada as of 2010 – ranging between 36 and 42% – chicken meat still contributes to 64.5% of all Canadian *Campylobacter* infections [1]. Peak infection rates are associated with the summer months in the Northern hemisphere, correlating to an increase in contaminated poultry found during the same period. [64,171].

Though incidence of campylobacteriosis varies year to year, estimates per 100,000 people range from 14.3 for the United States and 27.6 for Canada, to as high as 1512 in Japan [67,122,142]. While infections clear spontaneously in most cases, *C. jejuni* is a major burden to economic, healthcare, and social systems. In the United States alone,

Campylobacter contaminated poultry causes a 6.9 billion dollar economic burden annually [133]. Additionally, in the United States *C. jejuni* infection results in over 22,500 disability-adjusted life-years, which is a measure that accounts for the loss of life and health compared to “perfect” health [132]. It is possible that this number will increase in coming years: *C. jejuni* alone surpassed *Salmonella spp.* in numbers of American foodborne diarrheal disease in 2017 [91]. Increased risk comes with the rise of antibiotic resistance, with multidrug resistant strains seen in outbreaks as recently as December 2019 [26]. Additionally, the CDC states that in 2017, 28% of all isolates proved to be resistant to ciprofloxacin [24]. In 2017 the WHO listed Campylobacters as high priority pathogens due to the increased prevalence of fluoroquinolone-resistant isolates [4]. With the rise of antibiotic resistance looming, it is imperative to search for antimicrobials that lead to diminished colonization by impairing key virulence factors.

1.4 Overview of *C. jejuni* virulence factors

C. jejuni uses a wide range of virulence factors to colonize, and cause disease in, humans. One notable class of virulence factors includes the abundance of glycosylated proteins. Though glycoproteins are more common in eukaryotes than prokaryotes, *C. jejuni* is able to produce both O-linked glycosylated and N-linked glycosylated proteins [23]. O-linked glycosylation is specific to the serine and threonine residues found on flagellins, seeing the addition of pseudaminic acid and legionaminic acid, as well as derivatives containing acetyl and acetamidino groups [43,98,178]. It is known that this addition is required for flagellin polymerization, with impaired O-linked glycosylation resulting in decreased bacterial mobility, as well as decreased adherence and invasion of host cells [45,178].

N-linked glycosylation, classically thought to only occur in eukaryotes and archaea, is carried out on many secreted proteins across all strains of *C. jejuni* [155]. Glycosylation occurs on asparagine residues, with a consensus sequence of [aspartic acid/ glutamic acid – X – asparagine – X – serine/threonine], where X can be any amino acid except proline [79]. The sugar residues added typically include 5 N-acetyl galactosamine residues, a glucose, a bacillosamine, and an additional phosphoethanolamine, with the control of this addition being under control of the *pgl* operon [80]. Mutations affecting glycosylation of

these proteins affect adherence and invasion of host epithelial cells, chicken and mouse colonization, and the overall immunogenicity of many proteins [53,69,153]. Additionally, these modifications may decrease protein degradation by host proteases, and alter host cytokine induction by increasing binding to lectins found on the surface of immune cells [2,145].

The formation of the flagella, facilitated by protein glycosylation, is key to the virulence of *C. jejuni*. This structure allows for the bacterium's darting motility, with average speeds around 40 μm per second [138]. This motility permits the penetration of, and movement within, gastrointestinal mucosa. This seemingly increases contact with human epithelial cells, which may in turn increase adhesion and invasion [154]. Interestingly, when infecting patients with motile and non-motile phase variants, only motile bacteria were recovered from stool, indicating motility is essential for colonization. [19]. This structure is also vital as it acts as a flagellar type III secretion system, allowing for the secretion of both flagellar and non-flagellar proteins [174]. The production and secretion of Cia proteins (Campylobacter invasion antigens) is induced upon co-culture with host epithelial cells [75]. Delivered by the fT3SS , these proteins accumulate within the host epithelium and appear to play a role in epithelial invasion [28]. While there has been relative consensus that *C. jejuni* exclusively uses a microtubule-dependent manner to penetrate host cells, a recent paper indicates that CiaD is able to interact with the host protein IQGAP1, facilitating actin restructuring and bacterial entry into the epithelium [56,110].

Adherence to, and colonization of, host cells is bolstered by the production of adhesins. The two best characterized proteins are Campylobacter adhesion to fibronectin (CadF) and fibronectin-like protein A (FlpA), which bind to fibronectin on the basolateral side of human intestinal epithelial cells [77]. When these proteins are mutated *C. jejuni* displays decreased adhesion to, and invasion of, human epithelial cells, and decreased chicken gut colonization [40,76,81]. Other adhesins, including Campylobacter adhesion protein A (CapA), PEB1, and PEB4 also impact adherence to human and chicken intestinal epithelial cells, but are not as well characterized as the fibronectin binding proteins [8,9,72,114].

Another important virulence factor is the bacterium's lipooligosaccharide, or LOS. Many Gram-negatives have lipopolysaccharide (LPS) as a component of their cell walls, which is composed of an antigenic lipid A, anchoring the structure to the membrane, an inner and outer core composed of sugar residues, and an O-antigen, a chain of repeating sugar subunits that vary in length and composition [104]. The campylobacter LOS differs from traditional LPS in that it lacks the long O-antigens found in most Gram-negatives [23]. Campylobacters also differ in their LOS composition through the endogenous synthesis of sialic acid. This residue is incorporated into the outer core and is responsible for the aforementioned molecular mimicry to host gangliosides. As a benefit to the bacteria, these modifications decrease immunogenicity and increase serum resistance. Modifications to the LOS have been shown to alter invasiveness in a strain specific manner [23,48].

Another major virulence factor of *C. jejuni* is its capsule. As the capsule polysaccharide is the focus of the study, it is highlighted in detail in the next subsection.

1.4.1 Capsule polysaccharide

Broadly, bacterial capsules are polysaccharide layers that reside beyond the plasma membrane. These structures can confer different selective advantages such as resistance to desiccation, phagocytosis, or antibiotic uptake, dependant on the strain specific configuration of the CPS [106,109,150]. Expression of the *C. jejuni* CPS has been shown to increase invasion of host epithelial cells, increase chicken gut colonization, and decrease sensitivity to serum killing in a strain specific manner [11,12,44,70,173]. The CPS also seems to modulate the host immune system, with acapsular mutants inducing lower levels of cytokines from murine lamina propria lymphocytes and bone marrow-derived dendritic cells [92,130]. A recent study demonstrates that clinical isolates express elevated levels of transcripts required for CPS expression, compared to a common laboratory strain [78]. The association with virulence is strong enough that several groups are targeting the CPS in vaccine development [93,102,125]. These vaccines would be

serotype specific as strains vary in CPS composition, with 47 different serotypes described to date [23].

Generally, *C. jejuni* capsules are produced in a manner similar to class 2 capsules of *E. coli* K1 and K5, *N. meningitidis* and *H. influenzae*, involving the sequential polymerization of monosaccharides [46] (Figure 1). While capsular synthesis genes vary between strains, the organization of genes is generally conserved with 3 distinct regions. Regions 1 and 3 are well conserved between species, encoding for genes involved in capsular assembly and transport respectively [46,162]. Region 2, conversely, is variable between strains and encodes enzymes that synthesize and modify sugar precursors (methyl transferases, MeOPN biosynthesis enzymes, and MeOPN transferases), that define any given serotype [46,170]. These sugars are synthesized with attached nucleotide tri-, di-, or monophosphates, which allow binding to modifying enzymes, and are required for glycosyltransferases to polymerize the monosaccharides [162]. The addition of nucleotide anchors also help confer specificity to the enzymes that act on these sugars. While region 2 has the highest variability, there is still high conservation of genes involved in heptose precursor synthesis (*hddC*, *gmhA*, *hddA*) and deoxyheptose synthesis (*dmhA*) as well as genes involved in MeOPN biosynthesis (homologs of *cj1415c – 1418c*) [23,97]. In strain NCTC 11168, capsular assembly begins with addition of monosaccharides onto an endogenous phospholipid anchor, anchoring the chain to the cytoplasmic side of the inner membrane. Sugar residues are then added sequentially by glycosyltransferases, before chain termination and transfer to a dipalmitoyl-glycerophosphate phospholipid anchor [34]. The CPS is ultimately transported to the outer membrane via the ABC transporters KpsM and KpsT, where the CPS is exposed to the extracellular environment [141]. The *C. jejuni* CPS cluster is able to undergo phase variation by slipped strand mispairing, altering expression of the CPS as a whole, as well as altering the expression of constituents that modify the CPS (MeOPN, capsular heptose) in certain serotypes [12,47]. The ability for phase variation suggests that differential expression of the CPS is advantageous based on the environment [46].

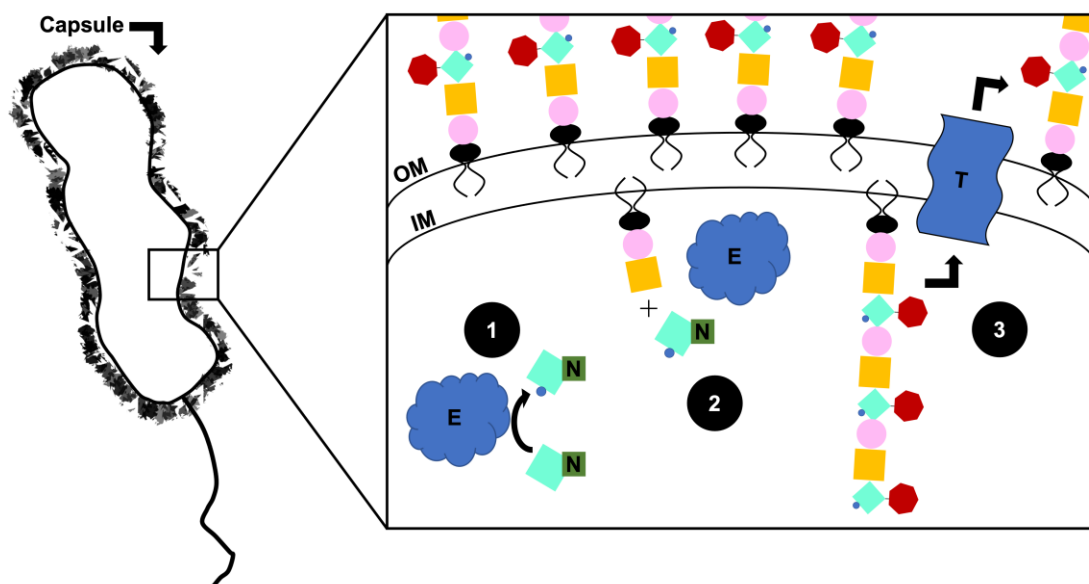


Figure 1: *C. jejuni* capsule polysaccharide synthesis. (1) Enzymes encoded by region 2 of the CPS synthesis cluster synthesize and modify sugar precursors that define a given serotype. These sugars are synthesized with attached nucleotide tri-, di-, or monophosphates, denoted by a green “N”. (2) Enzymes encoded by region 1 of the CPS cluster link the monosaccharides. Capsular assembly begins with addition of monosaccharides onto an endogenous phospholipid anchor, anchoring the chain to the cytoplasmic side of the inner membrane. Sugar residues are then added sequentially by glycosyltransferases, before chain termination. (3) Transporters encoded by region 3 of the CPS synthesis cluster export the fully generated CPS to the bacterial outer membrane. IM denotes the inner membrane while OM denotes the outer membrane. E= enzyme, T= a complex of several proteins acting to transport the CPS.

The *C. jejuni* CPS differs from other bacteria due to the inclusion of both variably linked O-methylated phosphoramidate (MeOPN) moieties and uniquely modified heptose residues [102]. The addition of the MeOPN has not been observed on the capsules of other bacteria and serves to moderate several aspects of virulence and survival. MeOPN is present in about 70% of *C. jejuni* strains and moderates bacteriophage entry into the cell, while decreasing invasiveness and increasing serum resistance in a strain specific manner [5,115,144]. Again however, this addition is not all that makes the *C. jejuni* CPS unique.

The Creuzenet Lab has previously characterized enzymes involved in the biosynthesis of the capsular heptose. In strain 81-176 the 6-deoxy-D-*altro*-heptose is produced through the Ddah pathway (Figure 2) [94,96]. The precursor sugar GDP-D-*glycero*-D-*manno*-

heptose is dehydrated at C4 and C6 by DdahA to form GDP-6-deoxy-4-keto-D-*lyxo*-heptose. This, in turn, is acted on by DdahB, which catalyzes a C3 epimerization event, producing GDP-6-deoxy-4-keto-D-*arabino*-heptose. Finally, the C4 reductase DdahC converts the penultimate sugar into GDP-6-deoxy-4-keto-D-*altro*-heptose. This heptose residue is always incorporated into the CPS backbone, and sometimes also branches off the backbone producing the HS:23/36 serotype (heat stable: 23/36) [68,102]. In strain NCTC 11168, the 6-O-Me-L-*gluco*-heptose is produced via the Mlgh pathway (Figure 2) [95,173]. This modified heptose has only been found in *C. jejuni* as well as a few other mucosal pathogens, namely *Yersinia pseudotuberculosis*, *Burkholderia pseudomallei*, and *Burkholderia mallei* [54]. It was originally thought that GDP-D-*glycero*-D-*manno*-heptose was oxidized at C4 by an unknown enzyme, MlghA, to form GDP-6-R-4-keto-D-*lyxo*-heptose. This product is epimerized at C3 and C5 by MlghB to form GDP-6-OMe-4-keto-L-*xylo*-heptose, which is ultimately reduced at C4 by MlghC to form GDP-6-OMe-4-keto-L-*gluco*-heptose. O-methylation is caused by the proposed methyltransferase MlghD, though it is presently unknown when this methylation event occurs. The heptose in NCTC 11168 is not incorporated into the CPS backbone and instead branches off the α -D-glucuronic acid residue, resulting in the HS:2 serotype [102]. A meta-analysis from 2021 placed HS:2 as the second most prevalent serotype worldwide, with a global pooled prevalence indicating this serotype accounts for 12.4% of all serotypes worldwide [32].

It was previously thought that WcaG, an enzyme found in both heptose biosynthesis pathways, acts as a scavenger reductase that competes for substrate with the epimerases (DdahB and MlghB) [94,96]. However, studies by Huddleston et al. published in 2020 demonstrate that WcaG likely acts as an oxidase *in vivo*, permitted by the presence of α -ketoglutarate which was absent in previous studies [57,58]. This cofactor causes the conversion of NADH to NAD⁺, permitting the WcaG mediated oxidation of GDP-D-*glycero*-D-*manno*-heptose to GDP-D-*glycero*-4-keto- α -D-*lyxo*-heptose, substrate of MlghB. These studies used mass spectroscopy and nuclear magnetic resonance (NMR), as well as co-crystallization of WcaG_{NCTC11168} with GDP and NADH to bridge a gap in knowledge. Interestingly, they were able to demonstrate through bioinformatic analysis that of the 484 *C. jejuni* genomes assessed, 24% contain homologs to WcaG (with 97%

sequence conservation), 36% contained DdahA homologs (with 91% sequence conservation), and 19% contained homologs of both [58]. Strains bearing exclusively a DdahA homolog only utilize the 6-deoxy moiety, while strains with DdahA and WcaG homologs possess both the 6-deoxy and the 6-hydroxy moieties. Presently, NCTC 11168 is the sole strain known to contain only the 6-hydroxy moiety, though the CPS structure is unknown for all other strains with only a WcaG homolog.

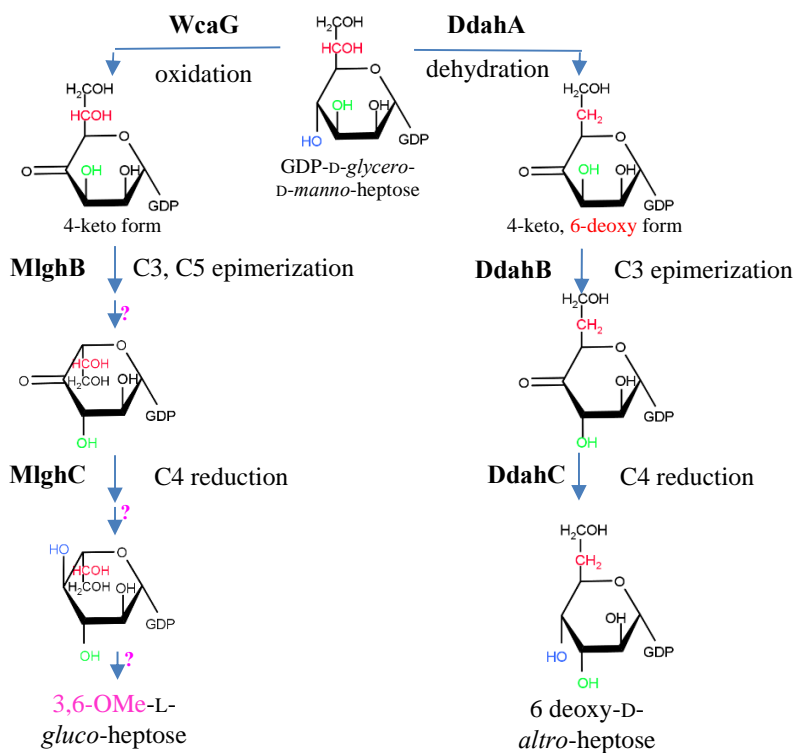


Figure 2: *C. jejuni* GDP-manno-heptose modification pathways. Biological pathways leading to 3,6-OMe-L-gluco-heptose in strain NCTC 11168 (left) and 6-deoxy-D-altro-heptose in strain 81-116 (right). The C4 oxidation and 3,6-O methylation steps necessary to generate 3,6-OMe-L-gluco-heptose have not yet been elucidated and are denoted by the “?”. Figure adapted from Barnawi et al. [15].

The Creuzenet lab has long been interested in studying the biological function of GDP-6-OMe-4-keto-L-gluco-heptose in strain NCTC 11168. This strain differs from other serotypes as the heptose residue only branches off the CPS, and is not incorporated into the backbone, allowing the residue to be knocked out without completely disrupting the CPS structure [173]. Branching of the heptose is thought to permit greater interaction with the environment, allowing for the potential of this residue to moderate interactions

with host cells. The Creuzenet lab has generated several knockout mutants in the Mlgh pathway permitting study of the heptose [173]. *wcaG::cat*, *mlghB::cat*, *mlghC::cat*, and *wcaG::catΔ* (*cat* denotes that a chloramphenicol resistance cassette was inserted into a given gene) all lack the capsular heptose residue, in line with the corrected biosynthetic pathway in which WcaG acts as the preliminary oxidase (Figure 3). These mutants differ in their expression of certain sugar modifications, with differential attachment of MeOPN and 2-amino-2-deoxyglycerol, in addition to differing in the overall amount of CPS produced. These mutants all have a single gene knockout except for *wcaG::catΔ*, which also lacks several methyltransferase and MeOPN transferase encoding genes. This prevents the MeOPN addition to N-acetylgalactosamine seen with *wcaG::cat*, *mlghC::cat*, and *mlghB::cat* that is not present on wild-type. As such, this mutant acts as a unique control for the addition of MeOPN. There is also *kpsM::kan* (*kan* denotes that a kanamycin resistance cassette was inserted into a given gene) which has a knockout for the ABC-transporter responsible for trafficking the CPS to the cell surface. As such, this mutant does not have a CPS, permitting study of the CPS as a whole in host cell interactions.

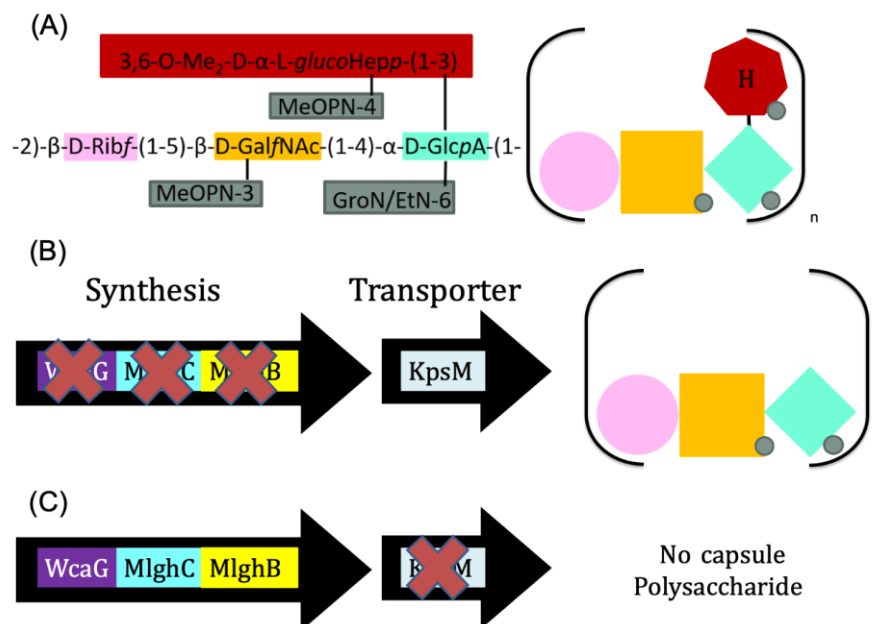


Figure 3: Creation of *C. jejuni* capsular heptose mutants.

(A) General CPS structure for wild-type *C. jejuni* NCTC 11168. (B) Knocking out genes involved in capsular heptose biosynthesis produces a CPS devoid of the capsular heptose. MlghC, MlghB, or WcaG knockouts all lack this residue, in addition to WcaG Δ which

contains a knockout for WcaG in addition to several methyltransferase and MeOPN transferase encoding genes. (C) Knocking out KpsM results in bacteria devoid of CPS. KpsM is a transporter required for delivering the CPS to the outer membrane, hence a knockout of this gene creates bacteria without this virulence factor.

Results from Wong et al. demonstrate key differences between the heptose biosynthesis knockout mutants, including increased susceptibility to bile salt killing for *mlghB::cat* and *mlghC::cat* [173]. The capsular heptose, and CPS as a whole seem to play a role in serum resistance, with all mutants being more susceptible to killing than WT in the presence of 20% serum. With regards to human epithelial cells grown *in vitro*, the acapsular mutant demonstrated increased adherence and invasion, while *mlghB::cat* and *mlghC::cat* demonstrated wild-type levels of adherence, but significantly reduced levels of invasion. This may indicate that the capsular heptose is important for invasion of the human gut epithelium. Finally, the paper demonstrated that all mutants were significantly impaired in colonizing the intestines of two-day old chicks, indicating that both the CPS and capsular heptose play a role in chicken gut colonization. While previous research has given insight into the role of the capsule in relation to host epithelial cells, little is known about how the capsular heptose interfaces with the immune cells.

1.5 *C. jejuni* and host macrophages

Upon colonization of the human or chicken gut, enteric bacteria are rapidly sensed by the host innate immune system. In both chicken and humans, M cells are present as part of the intestinal epithelium, readily transcytosing invading pathogens from the intestinal lumen to Peyer's patches [35]. These Peyer's patches are immune cell rich regions that are responsible for surveying microbes and antigens [65]. Cells present represent both the adaptive branch of the immune system, including T cells and B cells, as well as the innate immune system, involving dendritic cells, and most relevantly to this study, resident macrophages [65]. Macrophages are professional phagocytes and antigen presenting cells, capable of internalizing pathogens, killing them using intracellular compartments such as lysosomes, and processing their antigens for presentation to the adaptive immune system. Macrophages can either arise from circulating monocytes, differentiating as proinflammatory signals from other immune cells draw them towards the site of

infection, or they can be tissue resident, already differentiated for the specific niche in which they reside [85].

One of the largest pools of resident macrophages are those that line the intestinal basolateral membrane [165]. Macrophages residing in the Peyer's patches are characterized by the high expression of CD11c and MHCII, and have a predominately proinflammatory phenotype, secreting IL-1 β , IL-6 and TNF α , upon challenge with LPS [13,16,165]. However, other CD11c⁻ intestinal macrophages however, take on a more anti-inflammatory role, with little proinflammatory cytokine production and constitutive expression of the anti-inflammatory cytokine IL-10 [16,165]. This anti-inflammatory phenotype promotes lamina propria regulatory T cell expansion and aids in preventing excessive inflammation found in conditions such as irritable bowel disease [16,165]. The designation of proinflammatory macrophages to specific immune sentinel sites allows for the effective detection and presentation of antigens, without causing excessive, widespread inflammation. These macrophages interface with other immune cells in Peyer's patches, making their presence key for mounting a proper immune response upon the ingestion of pathogens. As such, the means by which enteric bacteria mitigate macrophage activation is likely to impact the clearance of these pathogens, and progression of pathogenesis.

When researching the impact pathogens have on host macrophages, cell lines are often used. The use of cell lines is beneficial in that cells are immortalized, allowing for prolonged use. Additionally, they are well characterized, and are less likely to have variations in behaviour relative to primary cells. One common lineage used for human macrophage studies is the THP-1 cell line. THP-1 cells are a monocytic cell line derived from a patient with childhood acute monocytic leukemia, and were therefore already immortalized upon collection [159]. While naturally monocytic in nature, these cells are commonly used for macrophage studies due to the fact they take on a macrophage-like phenotype upon treatment with phorbol-myristate-acetate [157]. When assessing chicken macrophages, Muquarrab Qureshi-North Carolina State University (MQ-NCSU) cells are a common model. MQ-NCSU cells are an immortalized macrophage cell line derived from the spleen of a 2-month-old female DeKalb XL chicken [124]. Immortalization was

attained by infecting cells with the JM/102W strain of the Marek's disease virus [124]. This cell line has largely been used for examining the induction of cytokines and nitric oxide when these cells are co-cultured with pathogens or treated with pathogen associated molecular patterns [14,172].

Although the role of the capsular heptose in host macrophage activation has yet to be elucidated, the response to WT *C. jejuni*, has been partially characterized. In response to *in vitro* challenge with NCTC 11168, human THP-1 macrophages have been shown to upregulate secretion of interleukin-1 α (IL-1 α), IL-1 β , IL-6, IL-8, and tumor necrosis factor alpha (TNF α) over 24 hours (multiplicity of infection [MOI] 100) [21,63,139]. Increased transcription of NLRP3 inflammasome components, NLRP3 and Caspase-1, have also been characterized in response to *C. jejuni* strain 108 (MOI 20) after 4 hours [21]. This generally indicates that upon sensing of the bacteria, human macrophages produce a strong proinflammatory immune response, leading to direct clearance by resident macrophages, and chemoattraction of other immune cells. Chicken MQ-NCSU cells upregulate transcription of IL-6, IL-8, IL-10, IL-12, and iNOS within 8 hours of exposure to *C. jejuni* strain 81116 (MOI 20) [161]. These cells have also demonstrated increased transcription of IL-1 β , IL-10, IL-18, IFN γ , CXCLi2, and iNOS in response to campylobacter-derived ligands including DNA, LOS, and outer membrane proteins [156]. TNF α production by MQ-NCSU cells in response to *C. jejuni* has not been characterized, as the existence of a functional TNF α in chickens is currently contentious. Many believe that only a truncated inactive sequence is encoded in the genome, though some argue that chicken TNF α transcription is induced in response to LPS [129]. Interestingly, transcription of IL-1 β , IL-6, and CXCLi2 is upregulated in the mucous membranes of chicken ileum infected with *C. jejuni* strain G1, though this change is caused by multiple cells in the environment, not just macrophages [143].

A previous study partially implicates the CPS and addition of MeOPN in the moderation of the host immune response. The absence of the CPS or MeOPN increased the transcription of the proinflammatory cytokine IL-6 and the anti-inflammatory cytokine IL-10 in murine bone-marrow derived macrophages [73]. This study utilized strain 11168H (a hypermotile derivative of *C. jejuni* NCTC 11168) and only observed this

phenotype with mouse, but not human or chicken, macrophages [73]. Still, this study implicates the CPS and capsular modification may play a role in immune evasion. A different study implicates the CPS in mitigating TLR2 and TLR4 signaling in human THP-1 macrophages with a KpsM/ capsule deficient conferring increased TLR signal [92]. As TLR2 and TLR4 are receptors on the host macrophages designed to sense LPS and bacterial lipoproteins, this study suggests that the strain 81-176 CPS is immunoprotective, hiding more immunostimulatory molecular patterns on the exterior of *C. jejuni*.

C. jejuni is not consistently able to survive within host macrophages. Several studies indicate that *C. jejuni* can survive within murine macrophages, but the 2015 study by Wong et al. found that this survival is likely strain specific [101]. Here, intracellular survival of strain NCTC 11168 decreased greatly within hours, with no difference between WT and mutants [173]. An increase in the engulfment of the KpsM knockout mutant, however, indicated that the CPS displays some antiphagocytic properties when interfacing with these macrophages [173]. A study by Wassenaar et al., utilizing macrophages derived from human peripheral monocytes, found that clearance was consistent across all strains tested, with the majority of donor macrophages being able to clear *C. jejuni* within 24-48 hours [167]. Interestingly, 10% of donors had macrophages incapable of clearing the bacteria, potentially leaving these individuals more susceptible to disease. Chicken peritoneal macrophages also demonstrate the ability to kill *C. jejuni*, with complete clearance of strains B540 and Clin 1 within 6 hours of phagocytosis [108]. The impact of the capsular heptose in mitigating clearance by host macrophages is presently unknown.

1.6 Substrate channelling

Substrate channelling, defined as “the process of direct transfer of an intermediate between the active sites of two enzymes that catalyze sequential reactions in a biosynthetic pathway” [100], may be occurring within the heptose biosynthesis pathway. Previous work by McCallum et al. demonstrates the extremely labile nature of select pathway intermediates, with products from both epimerases (DdahB and MlghB)

degrading within minutes of production, therefore being too unstable for analysis by NMR [95,96]. As such, I believe that *C. jejuni* capsular biosynthesis enzymes engage in substrate channeling as a means to limit substrate degradation in the cytosol. By directly transferring products between enzymes, degradation of products in the cytosol would be minimized, allowing for efficient production of products using unstable substrates.

Generally, there are 3 accepted methods by which substrate channeling occurs between two enzymes [37,137,169]. The first is by electrostatic guidance, in which a charged intermediate is drawn from the active site of one enzyme to the next based on a charge gradient. Substrate channelling can also occur in the case of an intramolecular tunnel being formed, in which the binding of two enzymes causes the formation of a tunnel that prohibits substrate diffusion into the cytosol. This tunnel may have a charge gradient, but regardless, flux increases by limiting the diffusion of the substrate. Finally, channeling can occur by chemical arm swings, in which the activity of the first enzyme causes a conformational change that brings the intermediate into a favourable position to be acted upon by the second enzyme in the series.

Substrate channelling has been hypothesized in several systems, with the most notable being the enzymes of the tricarboxylic acid cycle (TCA) and mitochondrial membrane proteins. It should be noted that substrate channelling is unlikely to increase the speed or efficiency of a reaction, as diffusion between enzyme active sites is generally not a rate limiting step [152]. Though efficiency would be increased in systems with exceedingly low concentrations of enzyme, it is more likely that metabolomic channels form to deal with labile or toxic intermediates, or to increase flux through a specific pathway [152]. The latter seems to be the case with TCA cycle enzymes, with enzyme kinetic and isotope labelling studies suggesting that certain enzymes channel in order to increase pathway flux [22,105,146,151]. More recent work has used affinity purification–mass spectrometry in order to identify that TCA cycle enzymes from *Bacillus subtilis* engage in protein-protein interactions [99]. Structural analysis of malate dehydrogenase, citrate synthase, and aconitase indicates that there are internal tunnels that can connect the malate dehydrogenase and citrate synthase active sites [175]. This tunneling between active sites is absolutely necessary for substrate channeling to occur, and these tunnels

have been demonstrated to self-assemble *in vitro* [22]. There is also a charge gradient between the two enzymes which draws the negatively charged intermediate to the active site of citrate synthase [169,175]. Interestingly, a mutagenesis experiment was conducted in which citrate synthase received a R65A mutation in a positively charged patch that connected its active site to malate dehydrogenase. This mutation decreased the probability of channeling from 0.99 to 0.023, disrupting the transport of the negatively charged intermediate [22]. Substrate channelling is also hypothesized in enzymes involved in purine nucleotide biosynthesis and glycolipid synthesis [82,152].

While evidence for substrate channelling in enzymes from *C. jejuni* does not presently exist, there is evidence for PRODH and P5CDH, which are proline biosynthesis enzymes found within Gram negative bacteria [131]. There is also presently very little research looking into channelling within capsule biosynthesis pathways, with the few papers discussing this topic ruling out the possibility of substrate channeling in their systems [71,116,179]. This is of little concern to this study as the enzymes studied in these papers do not have homology to the heptose biosynthesis enzymes and utilize different sugars. Substrate channelling would effectively explain how *C. jejuni* is able to deal with such labile intermediates and is currently supported by preliminary evidence, making this work novel.

1.7 Rationale, Hypothesis, and Objectives

The ultimate goal of this research is to gain an understanding of how capsular heptose expression alters the virulence of *C. jejuni*, with hopes of perturbing interactions between heptose biosynthesis enzymes in a manner that increases clearance by the host innate immune system. It should be noted that the capsular heptose biosynthesis enzymes are unique to Campylobacters and present in most species, making these attractive targets for targeting bacterial virulence [15]. As such, this research is broken into two subprojects: simultaneously investigating how the capsular heptose alters activation of, and clearance by, host macrophages and if physical interactions between enzymes can be exploited to modulate heptose production.

Host macrophage activation: I hypothesize that the *C. jejuni* NCTC 11168 capsular heptose residue acts to dampen activation in both human and avian hosts, leading to diminished clearance by host macrophages.

Substrate channeling during heptose synthesis: I hypothesize that *C. jejuni* capsular biosynthesis enzymes engage in substrate channeling in order to limit substrate degradation in the cytosol.

Objective 1: Assess expression of activation markers in chicken and human macrophages in response to *C. jejuni* capsular heptose mutants (Figure 3).

I hypothesize that the 6-O-Me-L-*gluco*-heptose residue generally acts to dampen immune activation. Several studies indicate that the capsule polysaccharide as a whole is immunostimulatory to murine lamina propria lymphocytes and bone marrow-derived dendritic cells, inducing the release of proinflammatory cytokines, such as TNF α and IL-6 [92,130]. Release of these cytokines would generally promote phagocytosis and bacterial clearance, and as such, it would be advantageous to the bacterium to produce structures such as 6-O-Me-L-*gluco*-heptose to minimize host cell activation while maintaining other protective functions.

By co-culturing host macrophages with the CPS and heptose mutants, I can collect samples at several time points and assess them for markers of macrophage activation via enzyme linked immunosorbent assays (ELISA), cytokine multiplexing, Griess assay, fluorescence assays, and qRT-PCR. The use of select assays also permits direct comparison between the response of host (chicken and human) macrophages.

Objective 2: Assess differences in clearance between chicken and human macrophages in response to *C. jejuni* capsular heptose mutants.

As I expect the capsular heptose to alter the expression of activation markers and effectors, I too expect the residue to alter the rate of phagocytosis by host macrophages. Exposure to proinflammatory cytokines, such as TNF α , increases the capacity of macrophages to phagocytose pathogens [7]. Therefore, if there is less cytokine release, there should also be a decrease in bacterial uptake and killing. Additionally, expression of

the capsular heptose may decrease the affinity for macrophage receptors or opsonizing proteins, which would also confer resistance to phagocytosis.

The interactions with host macrophages can be measured using 3 distinct assays – comparing adherence, invasion, and intracellular survival of capsular heptose mutants co-cultured with host macrophages. This permits comparison between capsular mutants and WT, as well as comparison between host macrophages in their ability to interact with WT or mutant *C. jejuni*.

Objective 3: Characterize protein-protein interactions between enzymes in capsular heptose biosynthesis pathways.

While the structure and function of each enzyme in the Mlgh and Ddah pathways has been elucidated, there are still unknowns regarding the flow of intermediates through these pathways. Work by McCallum et al. demonstrates the extremely labile nature of select pathway intermediates, with products from both epimerases (DdahB and MlghB) completely degrading within 10-30 minutes of production [95,96]. As such, I propose that *C. jejuni* capsular heptose biosynthesis enzymes participate in substrate channeling, directly transferring products between enzymes to minimize degradation of intermediates in the cytosol. This would allow for efficient production of products in systems containing unstable pathway intermediates. As the study of substrate channeling has primarily focused on enzymes within the tricarboxylic acid cycle, studying channelling in *C. jejuni* and channeling during capsular synthesis remains novel [22,105,146,151].

We propose testing enzymes in a pairwise manner using biochemical techniques such as surface plasmon resonance and microscale thermophoresis as a means to investigate physical interactions between proteins.

Chapter 2

2 Materials and methods

2.1 Culturing *C. jejuni* capsular heptose mutants

C. jejuni NCTC 11168 (ATCC 700819) freezer stocks (-80°C) were created by combining 50% glycerol with *C. jejuni* suspended in trypticase soy broth (TSB) in a ratio of 1:3. The original suspensions had an optical density at 600 nm (OD₆₀₀) of 4.0, ensuring a final OD₆₀₀ of 3.0 in the stocks. To start a culture, roughly 50 µL was taken from a freezer stock and deposited without spreading onto 5% sheep's blood trypticase soy agar (TSA) plates. All plates contained 10 µg/mL vancomycin and 5 µg/mL trimethoprim as background antibiotics. Concentrations of 15 µg/mL chloramphenicol was used for MlghB, MlghC, WcaG, and WcaGΔ knockout mutants, while 30 µg/mL kanamycin was used to select for the KpsM knockout mutant. All were cultured overnight at 37°C in micro-aerobic conditions (85% humidity, 10% CO₂ and 5% O₂). To expand *C. jejuni*, cultures were collected with sterile cotton swabs and resuspended in 1mL TSB. These suspensions were then diluted to an OD₆₀₀ of 0.01, of which 100 µL was spread on TSA background plates using sterile glass beads, and then incubated overnight, as above. All *C. jejuni* were collected in 1mL TSB and diluted to a specific OD₆₀₀ dependent on the subsequent experiment. In experiments including heat-killed *C. jejuni*, the WT was harvested and diluted as described, and then inactivated in a 57°C water bath for 45 minutes with intermittent shaking.

The capsular heptose mutants were previously generated by Creuzenet lab member Anthony Wong and Dirk Lange. Information on the antibiotic cassettes used to knockout genes encoding the capsular heptose biosynthesis enzymes can be found in Table 1, along with differences in CPS expression and composition as determined by Wong et al. [173].

Table 1: Composition of the *C. jejuni* NCTC 11168 CPS mutants.

	Antibiotic resistance cassette	GlcA	Hep	3,6-O-Me ₂ on Hep	MeOPN on GalNAc	Substituent on GlcA	CPS expression level	Growth relative to WT
WT	none	+	+	+	-	EtN	++	
MlghB	cat	+	-	-	+	EtN, GroN	+/-	+
MlghC	cat	+	-	-	trace	EtN, GroN	++++	+
WcaG	cat	+	-	-	+	EtN, GroN	++++	=
WcaGΔ	cat	+	-	-	-	EtN, GroN	+	+
KpsM	kan	N/A	N/A	N/A	N/A	N/A	Absent	+/-

Note: This table has been adapted from Wong et al., 2015 [173]. cat= chloramphenicol, kan = kanamycin. A plus (+) or minus (-) in the represent either the presence or the absence of the specified component respectively, as determined by NMR spectroscopy. GlcA, glucuronic acid; Hep, heptose; Me, methyl; MeOPN, O-methyl phosphoramidate; GalNAc, N-acetyl galactosamine; EtN, ethanolamine; GroN, 2-amino-2-deoxyglycerol. N/A = not analyzed as the CPS is not exported to the outer membrane in this mutant.

In all experiments using *C. jejuni*, inoculum colony forming units (CFU) values were measured by serially diluting bacterial suspensions tenfold in 0.85% saline 8 times. 10 μ L from each diluted sample was then spot-plated on background TSA plates in triplicate and incubated for 48 hours. The colonies were enumerated to back calculate the concentration of live CFU/mL.

2.2 Culturing MQ-NCSU chicken macrophages

Freezer stocks were created by first suspending MQ-NCSU cells (originally provided by Dr S. Sharif from the University of Guelph) in 90% heat-inactivated fetal bovine serum (FBS) (Multicell), 10% dimethyl sulfoxide to a final concentration of $\sim 2 \times 10^6$ cells/mL. To begin culturing, 1 mL stocks were thawed and added to 6 mL of fresh MQ-NCSU media (RPMI-1640 containing 2.05 mM L-Glutamine [Wisent Bioproducts], 10% heat-inactivated FBS, 100 units/mL penicillin, 100 μ g/mL streptomycin, 10mM HEPES, and 10 μ M β -mercaptoethanol [BME], 1% non-essential amino acids [Gibco]) before being centrifuged at 300g for 5 minutes. The supernatant was discarded, and the cell pellet was resuspended using 10 mL of the same media before being transferred to a T-25 flask. Flasks were incubated at 37°C under 5% CO₂ for 1-2 days. MQ-NCSU cells were maintained at concentrations up to 1×10^6 cells/mL, through passaging into T75 flasks, up to a maximum of 5 passages. As these cells are adherent in the presence of BME,

passaging of MQ-NCSU required washing with 3 mL 1x PBS pH 7.4 (137 mM NaCl, 2.7 mM KCl, 8 mM Na₂HPO₄, and 2 mM KH₂PO₄) and treatment with 3mL 0.25% trypsin-EDTA (Multicell) for 5 minutes at 37°C. The trypsinized cell suspension was added to 4mL MQ-NCSU media before centrifugation at 300g for 5 minutes. The pellet was resuspended in 7 mL of culture media and the cell suspension was diluted 1:1 in 0.4% Trypan blue exclusion dye to allow for counting of live (clear, undyed) cells via hemocytometry. New T75 flasks were seeded at 2x10⁵ cells/mL and the media was replaced every 2-3 days between passages, which were conducted when ~80% adherent confluency was achieved. Cells were then diluted in media and plated 24 hours before the start of an experiment at a concentration dependent on the assay being conducted.

2.3 Culturing THP-1 human monocytes and macrophages

Storage and culture initiation for THP-1 cells was the same as for MQ-NCSU cells (see above section). THP-1 macrophages (provided by Lydia Dafoe from Western University, ATCC TIB-202) were grown in RPMI-1640 containing 2.05 mM L-Glutamine, 10% heat-inactivated FBS, 100 units/mL penicillin, 100 µg/mL streptomycin, 1mM HEPES, 10 µM BME. Flasks were incubated at 37°C in a 5% CO₂ incubator for 1-2 days. Macrophages were maintained at concentrations between 2x10⁵ cells/mL and 1x10⁶ cells/mL (as measured by hemocytometry with Trypan blue exclusion dye), via the addition of new media or through passaging into T75 flasks. THP-1 monocytes are non-adherent and, as such, did not have to be trypsin treated or centrifuged between passages. Instead counts were taken directly from flasks, and new T75 flasks were seeded at concentrations of 2-4x10⁵ cells/mL. THP-1 cells were grown to a maximum of 5 passages.

After about two weeks of culturing, THP-1 monocytes were plated 24 hours before the start of an experiment, or differentiated into THP-1 macrophages, which are plated 72 hours before the start of an experiment to accommodate for the differentiation treatment. Suspensions of THP-1 cells in culture media to be differentiated were brought to a concentration of 250nM phorbol-myristate-acetate (PMA). This suspension was then

plated and incubated undisturbed for 48 hours before being washed twice with 1x PBS and resuspended in an antibiotic free media, for an additional 24-hour PMA-free incubation. The seeding density and type of plate used (96- or 24-well) were dependent on the assay conducted.

2.4 Plating host cells for lactate dehydrogenase release assay, Griess assay, TNF α ELISA, and cytokine multiplex assay

MQ-NCSU and THP-1 macrophages were seeded into 96 well plates in a similar manner for the lactate dehydrogenase (LDH) release assays, Griess assays, TNF α ELISAs, and the cytokine multiplex assay. MQ-NCSU macrophages were plated at a concentration of 6×10^4 cells/well 24 hours before the start of co-culture (target concentration of 8.5×10^5 cells/well at start of co-culture), while THP-1 macrophages were plated at a concentration of 8.5×10^5 cells/well in 72 hours before. PMA-treated THP-1 cells lose much of their proliferative capability, and as such were plated at the target concentration.

Wells were washed twice with 150 μ L 1x PBS pH 7.4 before antibiotic free RPMI media (same composition as THP-1 media, without antibiotics) was added. As the target MOI was 200, and a *C. jejuni* OD₆₀₀ of 1 is equivalent to 1×10^9 CFU/mL, 17 μ L of OD₆₀₀=1 suspensions were added to appropriate wells containing $\sim 8.5 \times 10^5$ MQ-NCSU macrophages. Only 8.5 μ L of OD₆₀₀=1 suspensions were added to appropriate wells containing $\sim 4.25 \times 10^5$ THP-1 macrophages. This is because roughly 50% of the plated monocytes were lost during PMA treatment (due to PMA induced toxicity or non-adherence during washes), which was initially unexpected. Some wells received 21 μ L of 0.1 mg/mL *E. coli* VW187 LPS, which acted as a positive control for activation in the TNF α ELISAs, and the Cytokine Multiplex Assay. Other wells containing macrophages received only media, acting as negative controls for activation. All samples were run in biological triplicates composed of technical triplicates, and each well had a final volume of 275 μ L. After all samples were loaded, interactions between *C. jejuni* and macrophages were synchronized by centrifugation at 300g for 2 minutes.

Plates were then incubated for various time points dependent on the assay being conducted and supernatants were collected for further analysis as follows. Two 50 μL supernatant samples were taken per well of MQ-NCSU at 30 minutes, 90 minutes, 5 hours of co-culture to be assessed by Griess assay. From the same wells, two 35 μL samples were taken at 5 hours for assessment in the LDH release assay. For THP-1 cells, two 115 μL supernatant samples were taken per well at 2, 5, 12, and 24 hours of co-culture to be assessed by TNF α ELISA. Two 35 μL samples were taken from wells at 5, 12, and 14 hours for assessment in the LDH release assay. Finally, as with the ELISA samples, two 115 μL supernatant samples were taken from well at 2, 5, 12, and 24 hours of co-culture to be assessed in the cytokine multiplex assay. While samples for all assays were taken from the same wells for MQ-NCSU cells, samples for THP-1 cell assays were taken from independent wells (i.e., MQ-NCSU Griess and LDH samples were derived from the same wells, but this is not so for THP-1 ELISA and LDH samples).

2.5 Griess assay

To detect levels of nitric oxide released by MQ-NCSU macrophages, 50 μL of tissue culture supernatants were collected as detailed in section 2.4 and frozen at -20°C for later use. A standard curve was made by serially diluting 400 μM sodium nitrite twofold in antibiotic free RPMI media to a concentration of 6.25 μM (7 concentrations). Like the experimental wells, all standard concentrations were created in triplicate. Controls without any sodium nitrite were also included. An additional 50 μL of 1% sulfanilamide in 5% phosphoric acid was added to all wells. After a 10-minute incubation at 26°C , wells received 50 μL of 0.1% N-1-naphthylethylenediamine dihydrochloride in water, followed by an additional 10-minute incubation which allowed samples to turn purple. The plates were read using a BioTek Eon microplate spectrophotometer at a wavelength of 535 nm. Using the data from the sodium nitrite standards, the microplate reader was able to generate a standard curve according to the equation $Y = (A-D)/(1+(X/C)^B) + D$, where Y is the OD₅₃₅, X is the nitrite concentration in μM , and A, B, C, and D are modifiers that alter the shape of the curve. Using this, the Eon software is able to convert

the OD readings to nitrite concentrations. Data were normalized to the average of the WT samples at each time point.

2.6 LDH release assay

To detect levels of cytotoxicity induced by strain NCTC and its capsular heptose mutants, wells containing 35 μ L of macrophage supernatant (stored at 4°C for up to 2 weeks) were diluted roughly threefold by adding 65 μ L 100 mM Tris (pH 7.5). As a positive control, wells containing macrophages were incubated at 37°C in 275 μ L of antibiotic free media with 0.45% Triton X-100 for 5 minutes, before collecting 35 μ L of lysate. A standard curve was made by serially diluting 1 U/mL LDH (Roche) threefold in 100 mM Tris (pH 7.5) to a concentration of 1.37×10^{-3} U/mL (7 concentrations). Like the experimental wells, all standard concentrations were created in triplicate. Controls without any LDH were also included. Sample LDH concentrations were assessed using a Roche Cytotoxicity Detection Kit, in which a reaction mixture was made by adding 250 μ L of the provided catalyst (Diaphorase/NAD⁺ mixture) with 11.25 mL of the provided dye (Iodotetrazolium chloride and sodium lactate). 100 μ L of this reaction mixture was then added to the diluted supernatants and standard. Plates were incubated at 37°C for 30 minutes, allowing samples to turn red. Plates were read using a Biotek Eon microplate spectrophotometer at a wavelength of 490 nm. Since a standard was constructed, the microplate reader was able to generate a standard curve according to the equation $Y = (A-D)/(1+(X/C)^B) + D$, where Y is the OD₄₉₀, X is the LDH concentration in U/mL, and A, B, C, and D are modifiers that alter the shape of the curve. Using this, the Eon software can convert the OD readings to LDH concentrations for the diluted samples. Values were ultimately multiplied by 2.86 to account for the initial sample dilution. Data were normalized to the average of the triton-containing samples (with maximal LDH release) at each time point.

2.7 TNF α ELISA

Human TNF α quantification was conducted using the Invitrogen Human TNF α ELISA kit. Wells were coated with 100 μ L of 1x capture antibody (diluted from 250x stock)

suspended in 1x coating buffer (diluted from 10x stock) overnight at 4°C. After washing 3 times with 200 µL 1x PBS containing 0.05% Tween-20 (PBS-T), wells were blocked with 200 µL 1x ELISA/ELISAPOT diluent (diluted from 5x stock) for 1 hour at room temperature. A standard was created by serially diluting 1 µg/mL of human TNF α twofold, 9 times to 1.95 pg/mL. Dilutions were done in 1x ELISA/ELISAPOT diluent, and extra wells were made containing concentrations of 750 pg/mL and 0 pg/mL to supplement the standard curve, and account for variation at the highest concentration. Plates were again washed before being loaded with 100 µL standard or 100 µL of 4x dilutes samples (25 µL of macrophage supernatant that had been added to 75 µL 1x ELISA/ELISAPOT diluent in a separate plate). Plates were incubated at room temperature with samples for 2 hours, before samples were removed and plates were washed 5 times with 200 µL PBS-T. Wells were loaded with 100 µL of 1x detection antibody (diluted from 250x stock) suspended in 1x ELISA/ELISAPOT diluent, then incubated for 1 hour at room temperature. Following an additional 3 washes, wells were loaded with 100 µL 1x streptavidin-horseradish peroxidase (diluted from 250x stock) and were allowed to incubate for 30 minutes at room temperature. Plates were washed 3 times and treated with 100 µL of 1x 3,3',5,5'-Tetramethylbenzidine (TMB) solution. After a 15-minute incubation at room temperature, stop solution (1 M H₃PO₄) was added, changing the colour from blue to yellow, and the plates were read using a Biotek Eon microplate spectrophotometer. The plates were read at two wavelengths, with values of 570 nM being subtracted from those of 450 nM. Since a standard was constructed, the microplate reader was able to generate a standard curve according to the equation $Y = (A - D)/(1 + (X/C)^B) + D$, where Y is the $\Delta OD_{450-570 \text{ nm}}$, X is the TNF α concentration in pg/mL, and A, B, C, and D are modifiers that alter the shape of the curve. Using this, the Eon software can convert the OD readings to TNF α concentrations for the diluted samples. Values were quadrupled to account for the initial sample dilution. Ultimately, data were normalized to the average value obtained with LPS (maximal activation) at each time point.

2.8 MOI assay

MOI assays were conducted to determine how the variability between actual WT MOI and the theoretical MOI of 200 impacted the induction of effectors. These MOI assays followed the same procedure as in section 2.4, where THP-1 and MQ-NCSU macrophages were plated, and supernatants were collected for further analysis. Here 17 μL of WT campylobacter with OD_{600} readings of 1.25, 1, 0.75, 0.5 and 0.25 were added to $\sim 8.5 \times 10^5$ chicken macrophages before incubating for 5 hours for the MQ-NCSU Griess assay. Only 8.5 μL of these suspensions were added to $\sim 4.25 \times 10^5$ human macrophages before incubating for 5, 12, or 24 hours for the THP-1 $\text{TNF}\alpha$ ELISA. Diluting these suspensions into a final volume of 275 μL using antibiotic free RPMI generated MOIs of 250, 200, 150, 100, and 50. Supernatants were then collected as noted in section 2.4 and samples were analyzed by Griess assay or ELISA as detailed in sections 2.5 and 2.7 respectively.

2.9 Cytokine multiplex

To detect the presence of human cytokines in THP-1 macrophage supernatants after co-culture with the capsular heptose mutants, samples were prepared as described in section 2.4, with both biological and technical replica being generated. Supernatants from triplicate wells within a replica were combined and 100 μL was set aside for analysis, (three biological triplicates, of pooled technical triplicates). Samples were sent to Eve Technologies in Calgary, Canada to quantify the amount of $\text{IL-1}\alpha$, $\text{IL-1}\beta$, IL-6 , IL-8 , IL-10 , IL-12p40 , IL-18 , and $\text{TNF}\alpha$ in solution. Like with the $\text{TNF}\alpha$ ELISA, data were normalized to the average value obtained with LPS (maximal activation) at each time point.

2.10 qRT-PCR

Reverse transcription and quantitative PCR were used to measure the transcription of cytokine and effector genes after co-culturing THP-1 or MQ-NCSU macrophages with WT *C. jejuni*. Twenty-four well plates were seeded with 7.5×10^5 MQ-NCSU cells/well 24

hours before the start of co-culture, or 1.25×10^6 THP-1 cells/well 72 hours before the start of co-culture (target of 1×10^6 cells/ well for both cell lines). THP-1 cells were differentiated into monocytes using PMA as described in section 2.3. For THP-1 cells, 6 wells were plated per time point, with 3 wells for samples containing WT, and 3 wells for the macrophage only samples (technical triplicates). Eighteen MQ-NCSU wells were plated per time point, as 3 wells were pooled per sample to increase transcript abundance before reverse transcription, based on preliminary data suggesting very low transcription levels of the assessed targets.

WT *C. jejuni* was grown and harvested as above, before being diluted to an OD_{600} of 0.4 in RPMI media. Wells containing macrophage were washed twice with 1x PBS pH 7.4 before 500 μ L of bacteria suspensions were added to achieve an MOI of 200 in each well. Cells were then co-cultured for 0.5, 1.5, 2.5, or 3.5 hours at 37°C and 5% CO₂. After co-culture, THP-1 cells were treated with 300 μ L of Trizol Reagent (Thermo Fisher), while wells containing MQ-NCSU cells were treated with 100 μ L Trizol each, with 3 wells being pooled for a total of 300 μ L. Plates with Trizol were placed in the incubator for 5 minutes before cells were homogenized by pipetting up and down, and lysate was stored at -80 °C for later analysis.

RNA was extracted by following the manufacturer's instructions for the Trizol reagent. 60 μ L of chloroform was added to each sample, with a 3-minute room temperature incubation before mixing by inversion and centrifugation at 12,000g for 15 minutes, 4°C. The aqueous phase of each sample was transferred to a new tube, to which 100 μ l of isopropanol was added to precipitate the RNA. After mixing the samples by inverting them 30 times, tubes were incubated at room temperature for 10 minutes. Samples were spun at 12,000g for 15 minutes, 4°C, before removing the supernatant and washing the pellet in 1 mL 75% ethanol. After additional pelleting at 7,000g for 15 minutes, 4°C, the supernatant was removed and the RNA pellet was air dried for 5-10 minutes. The pellet was resuspended in 25 μ L of DNase and RNase free water, and the concentration of RNA recovered was quantified using a Thermo Scientific NanoDrop 2000 spectrophotometer.

After RNA quantification, the equivalent of 1 μg THP-1 RNA or 3 μg MQ-NCSU RNA was added to tubes containing 1 μl of random hexamer primers (Thermo Scientific), which were brought to a final volume of 11 μl with DNase and RNase free water. Samples were placed in a thermocycler that maintained a temperature of 70 $^{\circ}\text{C}$ for 10 minutes, followed by primer annealing at 25 $^{\circ}\text{C}$ for 10 minutes. A master mix was made containing the following ratio, where quantities were multiplied by 1.1 times the number of samples: 2 μl of 0.1M DTT, 1 μl dNTP mix (10mM each), 4 μL of 5x SuperScript II reaction buffer, 1 μl DNase and RNase free water, and 1 μL of SuperScript II reverse transcriptase (invitrogen). 9 μL of this master mix was then added to each tube, before all tubes were placed in a thermocycler. Reverse transcription was conducted as follows: 25 $^{\circ}\text{C}$ for 10 minutes, 45 $^{\circ}\text{C}$ for 45 minutes, and 75 $^{\circ}\text{C}$ for 15 minutes. Samples of newly generated cDNA were stored at -20 $^{\circ}\text{C}$ for later use.

In order to conduct quantitative PCR (qPCR) a master mix was made containing the following ratio, where quantities were multiplied by 1.1 times the number of samples: 5 μl PowerUp SYBR green master mix (Applied Biosystems), 0.2 μL of each forward and reverse gene specific primers at 25 μM (Table 2), and 2.6-3.6 μL of DNase and RNase free water dependent on the amount of cDNA being added. This master mix was added to 1-2 μl of cDNA samples for a final volume of 10 μL . Samples were placed in a Corbett Rotorgene 6000 thermocycler, and run with the following settings: 50 $^{\circ}\text{C}$ for 2 minutes 95 $^{\circ}\text{C}$ for 2 minutes, followed by 40 cycles of denaturing at 95 $^{\circ}\text{C}$ for 15 seconds, annealing at 56 $^{\circ}\text{C}$ for 15 seconds, and extension at 72 $^{\circ}\text{C}$ for 1 minute. GAPDH and RPL37a were included as housekeeping genes to be used as internal references.

Table 2: Gene specific primers used during qPCR on cDNA generated from human and chicken macrophages.

Organism	Gene	F/R	Sequence	Amplicon size	Melting temperature $^{\circ}\text{C}^*$	Source **
Human	TNF α	F	TCAGCAAGGACAGCAGAGG	124	60	[176]
		R	GTATGTGAGAGGAAGAGAACC			
	IL-1 β	F	ATGGCTTATTACAGTGGCAATG	138	62	[176]
		R	GTAGTGGTGGTCGGAGATTC			
	IL-6	F	GTAGTGAGGAACAAGCCAGAG	240	64	[176]
		R	CATGCTACATTTGCCGAAGAG			
	IL-8	F	AACCATCTCACTGTGTGTAAC	66	62	[51]

		R	ATCAGGAAGGCTGCCAAGAG		62	
	IL-10	F	GAGGCTACGGCGCTGTCAT	60	62	[73]
		R	TGCTCCACGGCCTTGCTC		60	
	GAPDH	F	CAACGGATTTGGTCGTATTGG	72	62	[51]
		R	GCAACAATATCCACTTTACCAG		64	
	RPL37a	F	ATTGAAATCAGCCAGCACGC	94	60	[89]
		R	AGGAACCACAGTGCCAGATCC		66	
	ACTB	F	ATTGCCGACAGGATGCAGAA	150	60	[89]
		R	GCTGATCCACATCTGCTGGAA		64	
Chicken	IL-1 β	F	TGAGGCTCAACATTGCGCTG	213	62	[123]
		R	TGTCCAGGCGGTAGAAGATG		62	
	IL-6	F	CGTGTGCGAGAACAGCATGG	107	64	[123]
		R	GGCATTCTCCTCGTCAAG		62	
	IL-8	F	CCAAGCACACCTCTCTTCCA	176	62	[123]
		R	GCAAGGTAGGACGCTGGTAA		62	
	IL-10	F	CTTTGGCTGCCAGTCTGTGT	221	62	[156]
		R	TCATCCATCTTCTCGAACGTC		62	
	GAPDH	F	GCCGTCCTCTCTGGCAAAG	72	62	[161]
		R	GTAAACCATGTAGTTCAGATCG		62	
	iNOS	F	CAGCAGCGTCTCTATGACTTG	182	64	[156]
		R	ACTTTAGGCTGCCAGGTTG		62	
	RPL37a	F	ATTGAAATCAGCCAACACGC	94	58	**
		R	AGGACCCACAGTGCCAGATAC		68	
	ACTB	F	ATTGCTGACAGGATGCAGAA	150	58	**
		R	GCTGATCCACATCTGCTGGAA		64	

*Melting temperature was determined using GeneRunner version 6.5.52, representing the combined GC+AT melting temperature.

** Primers were selected from referenced primers. Some were modified to increase consistency of annealing temperature, or to minimize the formation of internal loops, by adding or removing complementary bases from the 5' and 3' ends

*** Primers were designed using NCBI primer blast, specifying primers must span one exon-exon junction

Fold change was analyzed using the equation, fold change = $2^{-\Delta\Delta Ct}$. This equation relies on the use of $\Delta\Delta Ct$ which can be derived using the equation: $\Delta\Delta Ct = \text{average } \Delta Ct \text{ (WT co-culture samples)} - \text{average } \Delta Ct \text{ (untreated samples)}$. ΔCt is in turn calculated using the equation: $\Delta Ct = Ct \text{ (gene of interest)} - Ct \text{ (housekeeping gene)}$, where Ct is the cycle at which cDNA is amplified to the point the fluorescence of a sample crosses the cycling threshold.

2.11 Reactive oxygen species fluorescence assay

To assess the induction of reactive oxygen species within host cells, 96 well plates were seeded with 6×10^4 MQ-NCSU cells/well 24 hours before the start of co-culture, or 1.6×10^5 THP-1 cells/well 72 hours before the start of co-culture. THP-1 cells were differentiated into monocytes using PMA as described in section 2.3. Higher numbers of THP-1 cells were used compared to previous assays to account for the cell death induced by PMA, with the goal of having 8.5×10^4 cell/well for both macrophages. *C. jejuni* was grown as described and harvested in 1 mL of TSB before being diluted to an OD₆₀₀ of 0.17 (1.7×10^8 cells/mL) in antibiotic free RPMI devoid of phenol red (containing 2.05 mM L-Glutamine and 10 mM HEPES) (Dpr-RPMI) (Wisent Bioproducts).

Wells with macrophage were washed twice with 1x PBS pH 7.4, before being incubated in 1x PBS pH 7.4 containing $50 \mu\text{M}$ 2',7'-dichlorofluorescein diacetate (DCF-DA) (Sigma) at 37°C (5% CO₂) for 30 minutes. Wells were again washed twice before adding $100 \mu\text{L}$ of *C. jejuni* suspended in Dpr-RPMI. Some macrophages received $100 \mu\text{L}$ of $7.5 \mu\text{g/mL}$ LPS in Dpr-RPMI as a positive control or $100 \mu\text{L}$ of Dpr-RPMI alone as negative control. Select wells had macrophages not treated with DCF-DA in Dpr-RPMI which gave readings of background fluorescence that were subsequently subtracted from the other readings. Finally, at this time point, wells without macrophages received DCF-DA in PBS as a measure of fluorescence inherent to the compound. Plates were incubated for either 30 or 90 minutes before samples were taken. $75 \mu\text{L}$ of supernatant was taken from each well and transferred to a fluorescence plate (black plastic with clear well bottoms, Invitrogen), after which the remaining supernatant was removed, and the wells were washed once with 1x PBS pH 7.4. Cells were treated with $100 \mu\text{L}$ of trypsin-EDTA at 37°C for 5 minutes, before being added to $100 \mu\text{L}$ of Dpr-RPMI in a fluorescence plate. Cells were pelleted by centrifugation at 300g for 5 minutes and were then resuspended in $100 \mu\text{L}$ of Dpr-RPMI. Plates were read using the BioTek Cytation 5 imaging reader at an excitation wavelength of 485 nm and an emission wavelength of 528 nm. Fluorescence intensities derived from the supernatant were multiplied by 4/3 to account for the fact that $75 \mu\text{L}$ was from $100 \mu\text{L}$ total. Like with the TNF α ELISA, data were normalized to the average value obtained with LPS (maximal activation) at each time point.

2.12 Adhesion, uptake, and intracellular survival assays

Plating of cells was consistent across all clearance assays, with culture information as described above. Following protocols laid out by prior Honours student Daniel Zimmermann, MQ-NCSU macrophage were seeded at a density of 2.5×10^5 cells/well 24 hours before the start of co-culture (500 μ l/well in 24 well plates). As both THP-1 macrophages and monocytes were used in this assay, THP-1 macrophages (cells treated with PMA) were seeded at 2.5×10^5 cells/well 72 hours before the start of co-culture, while monocytes were seeded at 1×10^5 cells/well at the same time point (500 μ l/well in 24 well plates). There were three wells per experimental condition in each biological replicate, comprising technical triplicates. In all experiments *C. jejuni* was normalized to an OD₆₀₀ of 1 in TSB before being diluted 1/100 into antibiotic free macrophage media. Samples of these suspensions were taken and diluted tenfold in 0.85% saline. Ten μ L of each dilution was spot-plated on background TSA plates to enumerate the CFU concentration for the inoculum. Before the start of co-culture, all wells were pelleted at 300g for 5 minutes and washed twice with 1x PBS pH 7.4, with centrifugation in between, removing any residual antibiotics in the wells. In all clearance assays, macrophages were enumerated using hemocytometry with trypan blue exclusion dye to determine the MOI. Data were normalized to the WT average of each researcher, at each time point tested.

2.12.1 Adhesion assay

To determine the ability of the capsular heptose mutants to adhere to host cells, 500 μ L of OD₆₀₀= 0.01 bacterial suspensions were added to plated macrophages (MQ-NCSU or THP-1 treated with PMA) and monocytes (THP-1 not treated with PMA). Interactions between *C. jejuni* and host cells were synchronized by centrifugation at 300g for 2 minutes, before incubation at 4°C for 30 minutes. Control samples were taken at this time to enumerate the bacteria in suspension, giving an indication of viability compared to the inoculum. Wells were washed 3 times with cold 1x PBS pH 7.4, with centrifugation at 300g for 5 minutes before each wash to prevent the loss of non-adherent monocytes. After washing, 200 μ l of ddH₂O was added to the wells and the plate was placed back into

the 37°C (5% CO₂) incubator for 20 minutes to lyse the host cells. After pipetting up and down to disrupt the macrophages, lysate was serially diluted tenfold in 0.85% saline. Ten µL of each dilution was spot-plated on background TSA plates to determine the CFU concentration for *C. jejuni* that had adhered to the host macrophage.

2.12.2 Uptake assay

To determine the ability of the capsular heptose mutants to resist uptake by host cells across two time points, 500 µL of OD₆₀₀=0.01 bacterial suspensions in RPMI were added to plated macrophages and monocytes. Cells were synchronized by centrifugation at 300g for 2 minutes before incubation at 37°C (5% CO₂) for either 1 or 3 hours. At the 1- and 3-hour time points, samples were taken to enumerate the number of bacteria in suspension. After this incubation, excess *C. jejuni* was removed with one wash of 1x PBS pH 7.4, with centrifugation at 300g for 5 minutes before washing to prevent the loss of non-adherent monocytes. Cells were then incubated with 500µL RPMI containing 200 µg/mL gentamicin (and 2.05 mM L-Glutamine, 10% heat-inactivated FBS, 10mM HEPES, and 10 µM 2-mercaptoethanol as with THP-1 media) for 1 hour at 37°C (5% CO₂) to kill all extracellular bacteria. Wells were then washed 3 times with 1x PBS pH 7.4 as described. As with the adhesion assay, wells were incubated with 200 µL of ddH₂O at 37°C (5% CO₂) for 20 minutes to lyse the host cells. Lysate was serially diluted as described in the adhesion assay and spot-plated to enumerate the intracellular bacteria.

2.12.3 Intracellular survival assay

To determine the ability of the capsular heptose mutants to survive within host cells, 500 µL of OD₆₀₀= 0.01 bacterial suspensions in RPMI were added to plated macrophages and monocytes. Cells were synchronized by centrifugation at 300g for 2 minutes before incubation at 37°C (5% CO₂) for 2 hours. After this incubation, excess *C. jejuni* was removed with one wash of 1x PBS pH 7.4, with centrifugation at 300g for 5 minutes before washing to prevent the loss of non-adherent monocytes. Cells were then incubated with 500µL RPMI containing 200 µg/mL gentamicin (and 2.05 mM L-Glutamine, 10% heat-inactivated FBS, 10mM HEPES, and 10 µM 2-mercaptoethanol as with THP-1 media) for 1 hour 37°C (5% CO₂) to kill all extracellular bacteria. Plates were then

washed 3 times with 1x PBS pH 7.4 before being resuspended in antibiotic free media and placed back in the incubator for 1 or 3 hours. Cells were then washed, lysed, and enumerated by spot-plating tenfold serial dilutions on background TSA plates.

2.13 Expression and purification of His-tagged proteins

E. coli expression strains, previously generated by the Creuzenet lab and differing in the enzyme they express (Table 3) were revived from freezer stocks by shaking overnight at 37°C in 20 mL of lysogeny broth (LB) [15,94–96]. The next morning cultures were diluted 1/50 into 300 mL of LB and placed back in the shaking incubator until an $OD_{600}=0.6$ was achieved. Protein induction was then induced by adding Isopropyl β -D-1-thiogalactopyranoside (IPTG) to a final concentration of 0.1mM and incubating at a time and temperature dependent on the protein (Table 3). Cells were then pelleted by centrifugation at 4500g and 4°C for 20 minutes, before washing in 20 mL 0.85% saline and pelleting again.

To prepare for purification, pellets were suspended in 20 mL of binding buffer (5 mM imidazole, 0.5 M NaCl, 20mM Tris, pH dependent on the protein, see Table 3) before being lysed using a Constant Systems CF1 cell disruptor. The lysate was then pelleted by centrifugation at 4750g and 4°C for 20 minutes. The supernatant was then filtered through a 0.8 μ m filter before being passed through a 3mL Novagen His bind quick column previously loaded with 15mL (5 column volumes [CVs]) of 50mM NiSO₄ and equilibrated with 5 CVs binding buffer. After passing the cell lysate, the column was washed with 12 mL (4 CVs) of binding buffer, followed by 9 mL (3 CVs) of wash buffer (60 mM imidazole, 0.5 M NaCl, 20mM Tris, pH dependent on the protein, see Table 3). Proteins were then eluted by adding 3 CVs of elution buffer (0.5 M NaCl, 20mM Tris, pH dependent on the protein, see Table 3) containing 200, 300, 400, 500, or 1000 mM imidazole.

Some proteins were purified by Fast protein liquid chromatography (FPLC). The cell lysate was prepared as above with the additional step of ultracentrifugation using a Beckman-Coulter Optima L 100K, at 100g (with the Beckman type 70.1 Ti rotor) for 15 minutes. After this, the supernatant was passed through a Poros nickel column (4.6mm x

100mm) which had been prepared with the sequential addition of 20mL of water, 20mL of binding buffer (as described previously), 20mL of 500mM NiSO₄, 20mL of binding buffer, 20mL of elution buffer (1M imidazole, 0.5 M NaCl, 20mM Tris, pH dependent on the protein), and 20mL binding buffer. After loading the lysate, weakly bound proteins were removed using 40mL of wash buffer. After this, a gradient ranging from 0 – 100% of the 1M elution buffer in binding buffer was passed through the column.

All fractions were diluted by half to a final concentration of 25% glycerol for storage at -20°C.

Table 3: conditions for the expression and purification of the capsular heptose biosynthesis enzymes

Protein	Mass (kDa)	Expression conditions	Purification pH
DdahA	40.5	BL21DE3pLys 37°C, 3 hours	8.0
DdahB	22.1	BL21DE3pLys 25°C, 3 hours	7.0
DdahC	41.7	ER2566 37°C, 3 hours	7.0
WcaG-PG	36.5	BL21DE3pLys 37°C, 3.5 hours	7.0
MlghB	22.2	BL21DE3pLys 37°C, 3 hours	8.0
MlghC	40.7	BL21DE3pLys 37°C, 3.5 hours	7.0

2.14 Analysis of purified proteins (SDS-PAGE, Western blot, Bradford assay)

As means to assess the presence of purified proteins, 40 µL protein samples were added to 13.3µL of a 4x loading buffer containing 625mM tris, 2% sodium dodecyl sulphate (SDS), 2% BME, 10% glycerol, and 0.002% bromophenol blue. These samples were boiled for 5 minutes before 20µL from each sample was loaded into the wells of a 15% polyacrylamide gel. Bio-Rad Precision Plus Protein All Blue Prestained Protein Standards and 0.25 µg/µL BSA were also loaded to serve as molecular weight standard and semi-quantitative loading references. Gels were run at 130V for 50-80 minutes in a running buffer containing 25mM Tris, 192mM glycine, and 0.1% SDS at pH 8.3. Bands

were then either visualized by staining with Coomassie brilliant blue dye or were analyzed by Western blotting [94].

Western blotting was conducted to assess the presence of proteins with His tags. Proteins were transferred from SDS-PAGE gels to nitrocellulose membranes in a transfer buffer containing 192mM glycine, 25mM Tris, 20% methanol, and 0.01% SDS at 180A for 45 minutes. Bands were then visualized by Ponceau S red staining before being washed with 1x PBS pH 7.4. The blot was then blocked with 20 mL of 10% skim milk in PBS overnight. The milk was then removed with 2 washes with 20 mL PBS containing 0.2% Tween-20 and 1 wash in PBS without tween. The blot was incubated with 20 mL Sigma mouse anti-polyhistidine clone His-1 monoclonal antibody (diluted 1/5000, concentration not supplied) for 1 hour at room temperature before being washed as described.

Afterwards, the blot was incubated in darkness with Molecular Probes goat anti-mouse IgG secondary antibody, alexa fluor 680 (diluted 1/5000, to 400 ng/mL) for 1 hour at room temperature. The blot was washed and subsequently imaged at 700 and 800 nm using the LI-COR Odessey CLx.

Densitometry was conducted on gels or blots using ImageJ (version 1.51 for MacOS) to roughly determine the concentration of proteins stored in glycerol. This was done by comparing the band intensity for bands of interest to a lane loaded with 5 µg of BSA.

Proteins concentration was further characterized using Bradford assays. This involved creating a standard curve by diluting a stock of BSA from concentrations ranging from 0-400 µg/mL. 10µL of these standards or purified protein samples were then added to 200µL diluted Bio-Rad Bradford reagent (1 part Bio-Rad Bradford reagent: 4 parts water) in a 96 well plate. This plate was then read at 595 nm using the BioTek Eon microplate spectrophotometer. As a standard was constructed, the microplate reader was able to generate a standard curve according to the equation $Y = (A-D)/(1+(X/C)^B) + D$, where Y is the OD₅₉₅, X is the protein concentration in µg/mL, and A, B, C, and D are modifiers that alter the shape of the curve. Using this, the Eon software can convert the OD readings to protein concentrations for the samples.

2.15 Surface plasmon resonance using carboxyl chips

Protein-protein interactions were assessed by SPR. To prevent bulk shift with injections of analytes that were preserved in the presence of 25% glycerol, 500 μL of protein stocks were loaded into Pall nanosep centrifugal devices with a 10 kDa cut-off. These units were centrifuged at 10,000 g, 4°C until $\sim 100\mu\text{l}$ was left in the upper chamber. The flow through was discarded and 400 μl of cold 1x PBS pH 7.4 was added to the upper chamber. The units were centrifuged at 10,000 g, 4°C until $\sim 100\mu\text{l}$ was left in the upper chamber. This was repeated 3 times before resuspending the protein in the upper chamber in a final volume of 500 μL , effectively removing the majority of the glycerol.

A carboxyl sensor chip was placed in the Nicoya OpenSPR Rev3 and was allowed to equilibrate with 1x PBS pH 7.4 running buffer by turning the flow rate up to 150 $\mu\text{L}/\text{minute}$ until the signal stabilized. Once the software began data collection, a standard bubble removal injection of 200 μL 80% isopropanol was performed, followed by a chip cleaning injection of 200 μL 10 mM HCl (pH 2). Both of these reagents had interaction times of 30 seconds, with running buffer flowing over the chip for one minute following injections. The flow rate was then lowered to 20 $\mu\text{L}/\text{minute}$, with all subsequent injections having a volume of 200 μL and a 5-minute interaction time. Aliquots of EDC (1-ethyl-3-(3-dimethylaminopropyl) carbodiimide hydrochloride) and NHS (N-hydroxysuccinimide), provided as part of the Nicoya amine coupling kit, were mixed in a 1:1 ratio. These reagents were then injected onto the chip with an interaction time of 5 minutes, allowing subsequent ligand immobilization. In all experiments the ligand was then diluted to a concentration of 50 $\mu\text{g}/\text{mL}$ (predicted from semi-quantitative SDS-PAGE analyses and densitometry of the stocks) in the provided activation buffer. The actual protein concentration was determined accurately by Bradford assays once all interaction assays were accomplished. As per the manufacturer's instruction, the ligand was injected immediately after the EDC/NHS injection, whereas running buffer was allowed to flow undisturbed between every other injection for 5 minutes. Proprietary blocking buffer was injected to prevent non-specific binding to unoccupied portions of the chip. To further minimize nonspecific binding, the 1x PBS buffer was swapped out with 1x PBS buffer containing 25 $\mu\text{g}/\text{mL}$ BSA, which would bind to any part of the chip

that was not properly blocked. The new buffer was allowed to equilibrate by flowing undisturbed for 25 minutes, and then remained in use for the duration of the experiment.

The analyte, suspended in PBS, was then injected at one of several concentrations dependent on the experiment. All analyte injections had a 5-minute interaction time. Regeneration was attempted, which involves injecting solutions to disrupt the interaction between analyte and ligand to bring the absorbance back to baseline. Regeneration solutions used included: 10-50 mM HCl, 1-4 M MgCl₂, 1% Triton X-100, 2 M MgCl₂ with 1% Triton X-100, and 100 mM glycine pH 3.0. After failed attempts of regeneration, the strategy was abandoned and a single chip with bound ligand was used for the injection of several analytes sequentially, in an attempt to further characterize interactions between enzymes.

Curves generated were then compiled and analyzed using the Tracedrawer software (version 1.6.1). Kinetic determination was conducted by defining the start of the rise and falls in signal, as well as detailing the analyte concentration in molarity. One-to-One local analysis was conducted for K_a and K_d determination, meaning that each curve was assessed independently, and not in reference to the other curves present in the analysis.

2.16 Statistical Analysis

One-way and Two-way ANOVAs with subsequent Dunnett tests were conducted to compare the effect of different groups. In most assays conducted, the samples are compared only to the WT samples, to see if the capsular heptose mutants caused differential effector induction. The notable exceptions to this include the LDH assay, and the MOI assay. In the LDH assay the macrophage only sample was the comparator, and a statistically significant difference would indicate differential lysis compared to the untreated condition. In the MOI assay, where the MOI of 200 was the comparator group, a statistically significant difference would indicate that the MOI causes different induction of effectors compared to an MOI of 200. In the case of the clearance assays, two-way ANOVAs with subsequent Bonferroni multiple comparisons tests were used to look at differences in the numeration of specific mutants over time. Dunnett's test runs multiple modified T-tests comparing WT and mutants and has high statistical power,

meaning it is capable of discovering relatively small but significant differences among groups. It is limited however, in that it can only look for differences between a noted control group (WT) and other experimental conditions (CPS mutants) [83]. As such, when comparing enumeration across time points Bonferroni tests were used. This test has a broader range of applications and can look at differences between several variables (mutants across time points for example) [83]. All analyses were conducted using PRISM for MacOS (Version 9.3.1), downloadable at: [graphpad.com/scientific-software/prism](https://www.graphpad.com/scientific-software/prism)

Chapter 3

3 Results

3.1 Validating the multiplicity of infection for macrophage activation assays

To measure the activation of host cells by *C. jejuni* capsular heptose mutants, Griess assays were used to assess the release of nitric oxide, while ELISAs were used to assess the release of TNF α . In these experiments, the target MOI was always 200, indicating there should be 200 bacteria for every macrophage present in the culture. Actual MOIs were calculated through the enumeration of bacteria and macrophages by spot plating and hemocytometry respectively. These actual MOIs often differed from the theoretical MOI of 200 due to variability in viability of both the bacteria and the macrophages across experiments and mutants. As such, Griess assays and ELISAs were run on supernatants from MQ-NCSU or THP-1 cells co-cultured with WT *C. jejuni* at MOIs ranging from 0-250.

When looking at the release of NO from MQ-NCSU at 5 hours, WT MOIs ranging from 50-250 did not cause significantly different levels of induction relative to MOI 200 (Figure 4A). However, while not significantly different from an MOI of 200, a WT MOI of 50 caused nitrite induction that was ~50% of what was seen with a WT MOI of 200. As such, MOIs below 100 were excluded, and if a mutant had an actual MOI between 100 and 250 in a given repeat, it was kept for analysis.

As seen with chicken macrophages, WT MOIs ranging from 50-250 did not induce significantly different levels of TNF α from human THP-1 macrophages, relative to an MOI of 200 at 5, 12 or 24 hours (Figure 4B). A different overall trend was seen in this cell type however, which showed that at all times tested, the higher the MOI, the lower the level of TNF α induction, and when tested, the MOI 50 differed significantly from MOI 250, only at 12 hours ($p=0.0332$). To maintain consistency with MQ-NCSU

analyses, MOIs between 100 and 250 were taken to be acceptable for analysis for THP-1 cells as well.

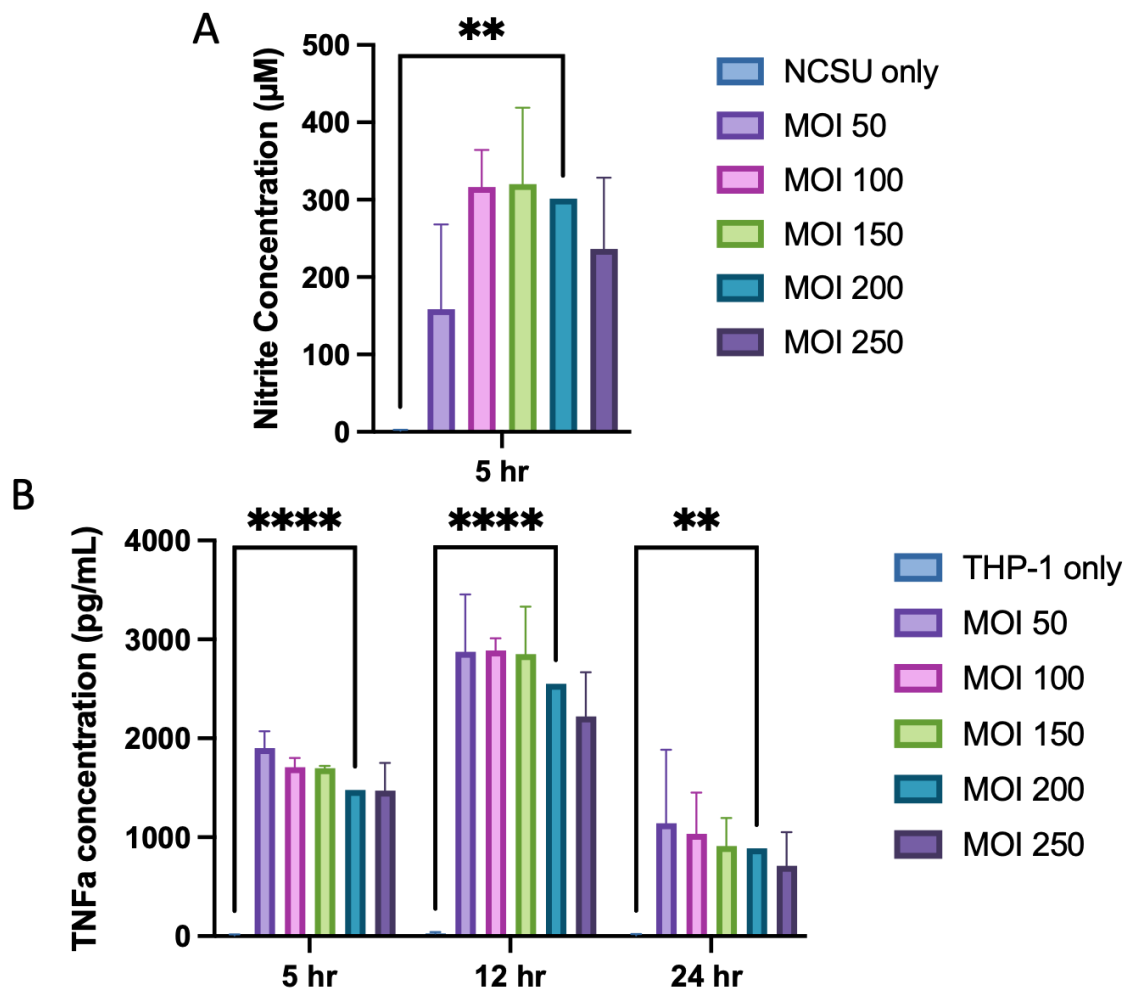


Figure 4: Impact of multiplicity of infection on effector induction by host macrophages co-cultured with wild-type *C. jejuni*. (A) MQ-NCSU cells (n=3), (B) THP-1 cells (5hr n=3, 12, 24 hr n=4). Tissue culture supernatants from host cells co-cultured with wild-type *C. jejuni* (at 37°C, 5% CO₂) were collected at several time points and assessed for the presence of nitrite by Griess assay or TNFα via ELISA. Samples were taken at 5 hours of co-culture for MQ-NCSU cells, and at 5, 12, and 24 hours for THP-1 cells. THP-1 cells were initially treated with 250nM PMA for 48 hours, followed by 24 hours of incubation without PMA. Statistical analysis was conducted by one-way ANOVA and subsequent Dunnett tests for MQ-NCSU cells. Analysis was conducted by two-way ANOVA with subsequent Dunnett tests for THP-1 cells. Each biological replica is comprised of three technical replicates. Error bars represent the standard deviation, all comparisons are to MOI 200. **=p<0.01, ****= p<0.0001.

3.2 *C. jejuni* does not confer significant cytotoxicity to host macrophages under conditions tested.

Before assessing activation by measuring effector levels, the cytotoxic effects of *C. jejuni* on host macrophage was examined. This is because *C. jejuni* induced cytotoxicity could alter the production of effectors: higher levels of cell death can decrease effector levels as cells may die before producing their effectors, or higher effector levels may be seen due to the release of damage associated molecular patterns (DAMPs) from lysed macrophages, which further promote an inflammatory response. An LDH release assay was used to assess cytotoxicity, which relies on the activity of LDH, an enzyme that normally resides in the cytosol, but will be found extracellularly if cells have been lysed. LDH is still active after release in the extracellular milieu. As such, the activity of extracellular LDH released upon cell death was used as a means of assessing cell death [128].

The data indicate that *C. jejuni* does not significantly induce cytotoxicity of either macrophage cell line, with no mutant or WT inducing significantly higher levels of LDH release than the negative control containing only macrophages (Figure 5A,B). In both cell lines, a significant difference was only seen with the addition of 0.45% triton, a detergent that acts to fully lyse all cells and thus release all of the LDH present in the cells. For MQ-NCSU cells, no mutant caused higher levels of LDH release than wells with macrophage only, while slightly higher levels of LDH were seen upon the co-culture of *C. jejuni* with THP-1 cells. Again, these differences were not significant, and LDH release was comparable between WT and mutants at all time points tested, indicating that differential cytotoxicity is not a contributing factor in the induction of effectors by WT *C. jejuni* or the capsular heptose mutants for either host cell line.

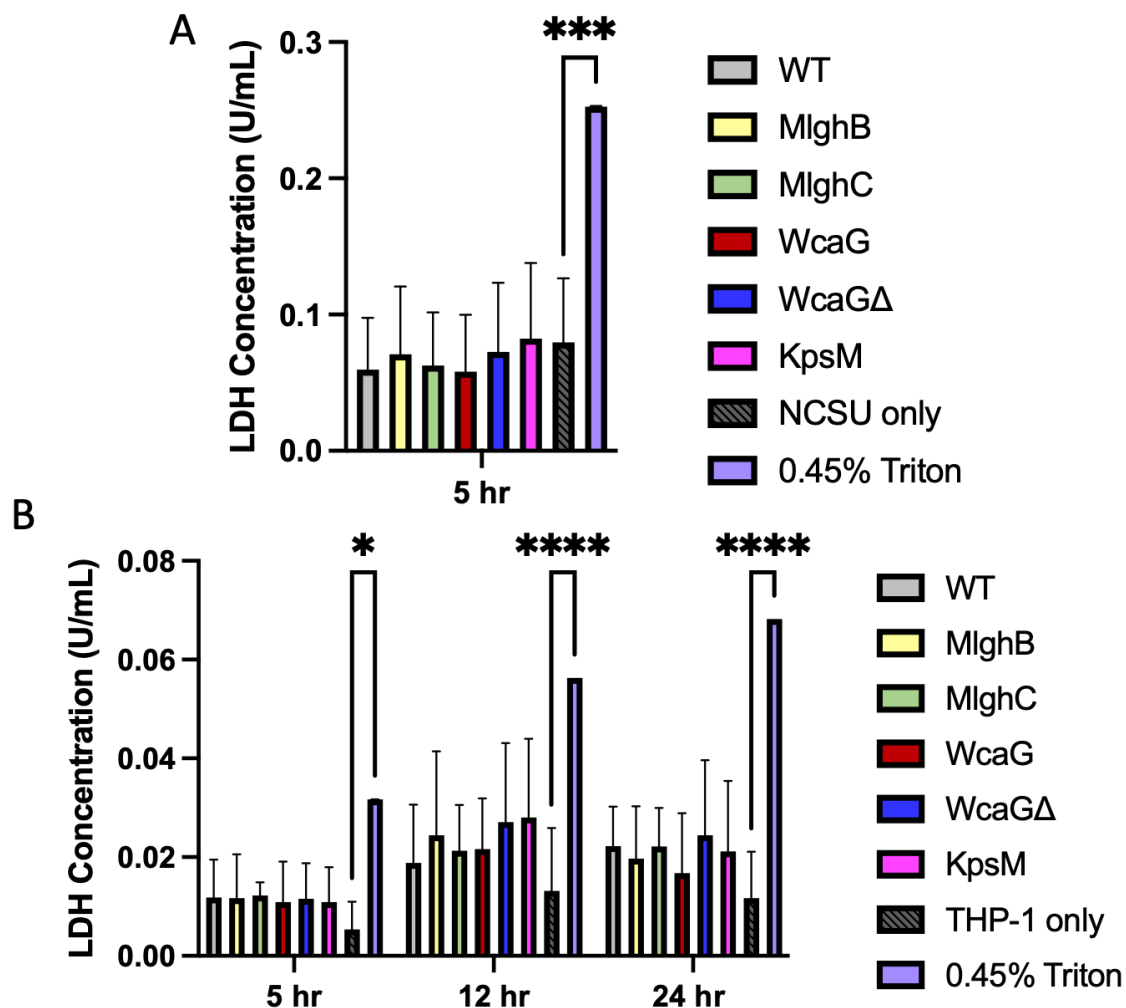


Figure 5: Host macrophage cytotoxicity induced by *C. jejuni* capsular heptose mutants.

(A) MQ-NCSU macrophages (n=3), (B) PMA-treated THP-1 macrophages (5, 12 hr n=3, 24hr n=4). Tissue culture supernatants from host cells co-cultured with *C. jejuni* (at 37°C, 5% CO₂) were collected at several time points and assessed for the presence of LDH via Roche LDH release assay. Samples were taken at 5 hours of co-culture for MQ-NCSU cells, and at 5, 12, and 24 hours for THP-1 cells. THP-1 cells were initially treated with 250nM PMA for 48 hours, followed by 24 hours of incubation without PMA. Statistical analysis was conducted by one-way ANOVA and subsequent Dunnett tests for MQ-NCSU cells. Analysis was conducted by two-way ANOVA with subsequent Dunnett tests for THP-1 cells. Each biological replica is comprised of three technical replicates. Error bars represent the standard deviation, all comparisons are to macrophage only. *= $p < 0.05$, ***= $p < 0.001$ ****= $p < 0.0001$.

3.3 The *C. jejuni* NCTC 11168 capsular heptose diminishes nitrite induction in chicken macrophages

As a means of evaluating activation in chicken macrophages, nitric oxide induction was assessed through the use of Griess assays, as conducted by Taha-Abdelaziz, 2020 [156]. Nitric oxide is an antimicrobial component released by host immune cells that can act to directly kill or impair invading pathogens. While the Griess assay does not directly measure NO, it is able to quantify the concentration of nitrites, the natural degradation products of NO, as a surrogate.

WT NCTC 11168 causes an induction of NO in MQ-NCSU macrophages, triggering a rise in nitrite concentration from undetectable levels in the macrophage only sample, to ~400 μ M after 5 hours of co-culture (Figure 6). Though levels were much lower earlier on, significant nitrite induction was found by the 90-minute time point.

Data indicate that the presence of the capsular heptose does in fact alter nitrite induction in MQ-NCSU cells, namely causing a reduction (Figure 6). As seen at the 5-hour time point, the MlghB, MlghC, WcaG, and WcaG Δ knockout mutants all had significantly elevated levels of nitrite induction relative to WT. This is notable as all 4 mutants still produce the capsule but lack the capsular heptose, which indicates that the normal addition of the heptose residue tones down nitrite induction in MQ-NCSU at 5 hours of co-culture. Conversely, the acapsular KpsM knockout mutant had diminished levels of nitrite induction relative to the WT, indicating that the normal addition of the CPS elevates levels of nitrite induction in WT at 5 hours of co-culture. These properties seem to be specific to live bacteria however, with the WT heat-killed sample causing no nitrite induction at any time point tested. Therefore, while the CPS on live *C. jejuni* induces nitrites in chicken macrophages, the presence of the capsular heptose is able to compensate, lowering nitrite induction.

Significantly differential nitrite induction between WT and any mutant was not observed at the 30- and 90-minute time points, with overall levels of induction being relatively low compared to what was observed at the 5-hour time point. Some trends observed at the 5-hour time point can be seen emerging at the 90-minute time point, with the MlghC mutant causing slightly higher levels of induction than WT *C. jejuni*.

A Griess assay was also attempted on THP-1 macrophages at 5 and 24 hours, despite their reportedly low nitrite induction. Nitrite levels in THP-1 supernatants were found to be undetectable or slightly above the level of detection, independent of capsule expression. As such, a full analysis could not be conducted with human macrophages.

Overall, this indicates that NO induction by MQ-NCSU macrophages in response to NCTC 11168 is a relatively slow process that is dependent on the viability of the bacteria and on the presence of the CPS and capsular heptose. The addition of the capsular heptose acts to dampen nitrite induction caused by live *C. jejuni*, while the addition of the CPS permits greater nitrite induction.

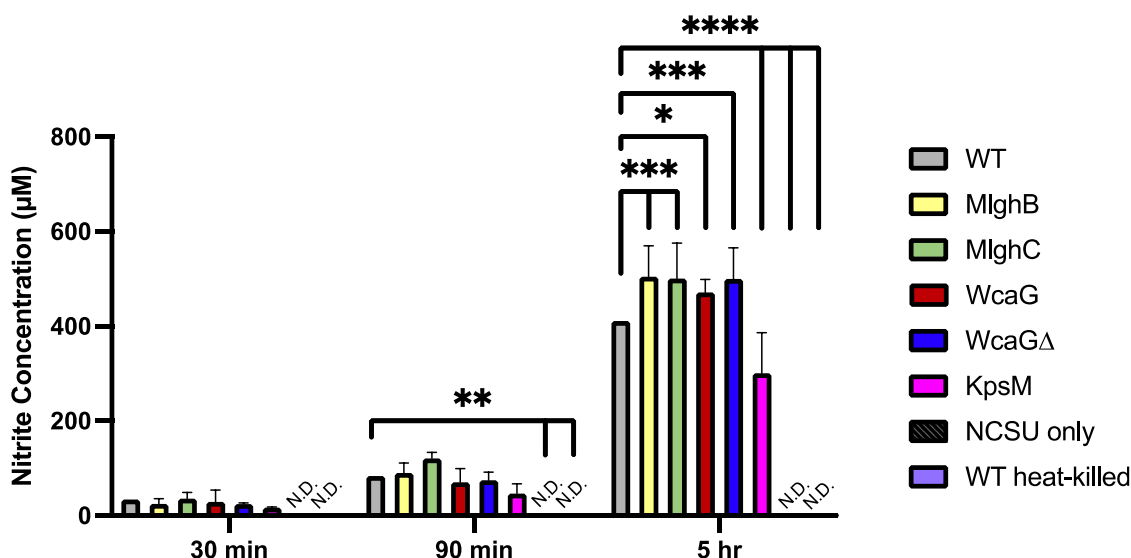


Figure 6: Nitrite induction in MQ-NCSU macrophages by *C. jejuni* capsular heptose mutants. Tissue culture supernatants from host cells co-cultured with *C. jejuni* (at 37°C, 5% CO₂, MOI 200) were collected at several time points and assessed for the presence of nitrites via Griess assay. Samples were taken at 30 minutes (n=3), 90 minutes (n=3), and 5 hours of co-culture (n=3 for all but WT, for which n=6). Analysis was conducted by two-way ANOVA with subsequent Dunnett tests. Each biological replica is comprised of three technical replicates. Error bars represent the standard deviation, all comparisons are to WT. N.D.= none detected *= $p < 0.05$, **= $p < 0.01$, ***= $p < 0.001$ ****= $p < 0.0001$.

3.4 *C. jejuni* NCTC 11168 diminishes the levels of ROS produced by host macrophages

Host macrophages were treated with DCF-DA before the start of co-culture with *C. jejuni* to determine how the capsular heptose mutants differentially induce ROS. This

compound is acted upon by host esterases, leaving it susceptible to oxidation by ROS, upon which, the fluorescent compound DCF is formed. As such, fluorescence intensity was compared between co-culture samples at 30 and 90 minutes to assess ROS induction.

Both co-culture supernatant and pelleted host cells were analyzed. The cells were trypsinized, pelleted by centrifugation, and resuspended in media before reading. The fluorescence intensity for the supernatant was consistently higher than what was seen from the cell fraction. The macrophage + DCF supernatants were ~100 fold higher than the cell fraction for THP-1 macrophages, and ~10 fold higher for MQ-NCSU macrophages. It should be noted readings from the supernatant still represent a measure of intracellular ROS, as DCF-DA must be converted to DCF within the cell. In ROS assays that use DCF, the whole well (cells + supernatant) is typically measured together, but that was not possible with the non-sterile fluorescence plates that were used.

Generally, it was observed that with regards to the supernatant specifically, the highest levels of fluorescence were observed in samples that did not contain live bacteria; those being macrophage only, heat-killed WT, or with the addition of LPS. WT differed significantly from the macrophage + DCF negative control only at 90 minutes for THP-1 cultures, though a marked reduction could be observed in both cell lines at all times tested (Figure 7A,B). This reduction in fluorescence intensity was also conserved in the supernatants derived from co-culture of the capsular heptose mutants. Interestingly, this phenotype is specific to live *C. jejuni*, as heat-killed WT caused slightly higher supernatant fluorescence than the negative control and induced significantly higher fluorescence than live WT across cell lines and time points tested (Figure 7A,B). The addition of LPS generally caused supernatant fluorescence near the level of the macrophage + DCF samples, displaying a significantly higher signal relative to live WT at 90 minutes in both cell lines. No significant differences in fluorescence intensity, and thereby ROS induction, were seen between WT and mutants in the supernatant of THP-1 or MQ-NCSU macrophages at 30 or 90 minutes of co-culture. This indicates that live NCTC 11168 is able to diminish the induction of ROS by host cells, and that this function is independent of heptose or CPS production.

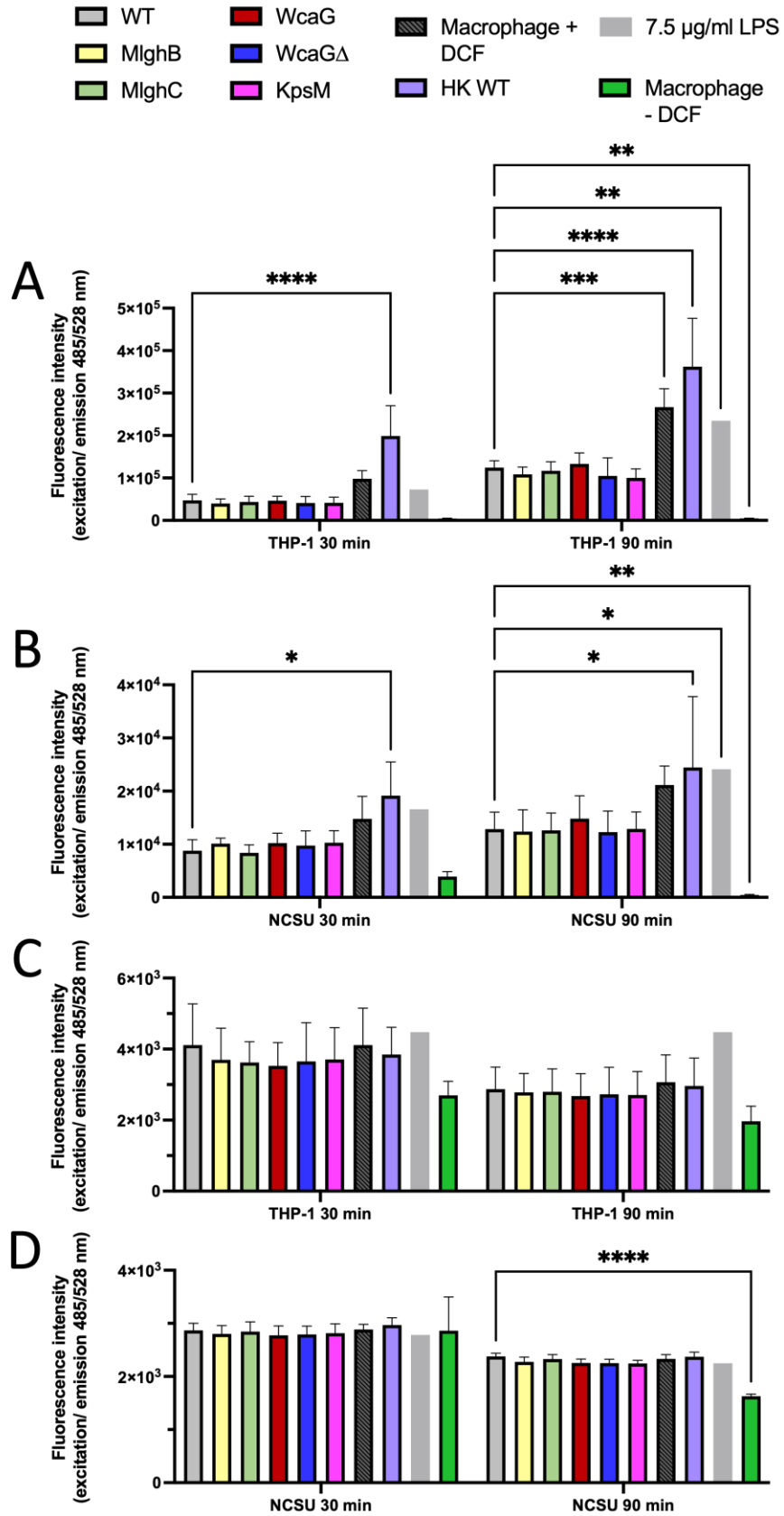


Figure 7: Induction of reactive oxygen species in THP-1 human and MQ-NCSU chicken macrophage by *C. jejuni* capsular heptose mutants. Cells were incubated at 37°C, 5% CO₂ with 100 μM 2',7'-dichlorodihydrofluorescein diacetate for 30 minutes before being washed twice with PBS. Cells were then challenged with wild-type *C. jejuni* or capsular heptose mutants (MOI=200) for 30 or 90 minutes. 75μL of (A) human supernatant or (B) chicken supernatant was collected from each well for analysis. Trypsinized (C) human cells or (D) chicken cells, were pelleted and subsequently resuspended in 75μL antibiotic free media. Plates were then read with emission and excitation wavelengths at 485 nm and 528 nm respectively. THP-1 cells were initially treated with 250nM PMA for 48 hours, followed by 24 hours of incubation without PMA. n=3, each biological replicate is comprised of three technical replicates. Error bars represent standard deviation. Analysis was conducted by two-way ANOVA with subsequent Dunnett tests, **=p<0.01, ***=p<0.001, ****=p<0.0001.

3.5 The *C. jejuni* NCTC 11168 capsular heptose does not impact TNFα induction by human macrophages

To measure the activation of THP-1 cells by capsular heptose mutants, TNFα secretion into the tissue culture supernatant was assessed using ELISAs. WT NCTC 11168 lead to elevated levels of TNFα induction at all time points tested, with a significant increase over the macrophage only samples (the negative control) at 5 and 12 hours of co-culture (Figure 8). TNFα induction in the WT peaked at 12 hours, at a concentration of ~2500 pg/mL. A significant difference was not seen at 2 or 24 hours, likely due to the fact that TNFα induction was quite low at these times compared to the intermediary time points. Maximal TNFα secretion was observed all time points with the addition of LPS (the positive control), which also peaked at 12 hours with a concentration of ~3700 pg/mL. Again, significance was not achieved at 2 hours, likely due to the overall low levels of induction.

Generally, data indicate the capsular heptose and CPS as a whole play little role in the induction of TNFα by these macrophages. At no time point did the four mutants lacking the capsular heptose (the MlghB, MlghC, WcaG, and WcaGΔ knockout mutants) differ significantly in their ability to induce TNFα. Additionally, a significant difference between WT and the KpsM mutant was only observed at the 12-hour time point, and not at any other time tested. Here, the KpsM mutant lacking the CPS led to diminished levels of TNFα relative to WT, indicating that, at 12 hours of co-culture, the CPS is slightly

immunostimulatory. This trend can also be seen at the 5-hour time point, but is less noticeable at 24 hours of co-culture.

Overall, these data indicate that the presence of the capsular heptose does not significantly impact the induction of TNF α in THP-1 cells, and that the normal addition of the CPS only slightly increases the induction of the cytokine at 12 hours after the start of co-culture.

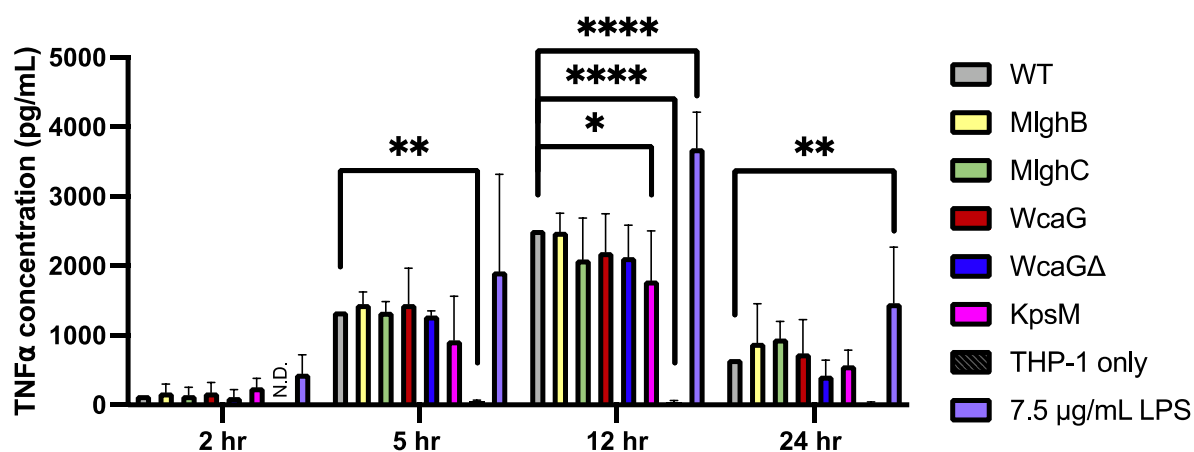


Figure 8: TNF α induction in THP-1 macrophages by *C. jejuni* capsular heptose mutants. Tissue culture supernatants from THP-1 cells co-cultured with *C. jejuni* (at 37°C, 5% CO₂, MOI 200) were collected at several time points and assessed for the presence of TNF α by ELISA. Samples were taken at 2 hours (n=3), 5 hours (n=2), 12 hours (n=3) and 24 hours (n=4 for all except MlghB where n=3) of co-culture. THP-1 cells were initially treated with 250nM PMA for 48 hours, followed by 24 hours of incubation without PMA. Analysis was conducted by two-way ANOVA with subsequent Dunnett tests. Each biological replica is comprised of three technical replicates. Error bars represent standard deviation, all comparisons are to WT. N.D.= none detected, *=p<0.05, **=p<0.001, ****= p<0.0001.

3.6 The *C. jejuni* NCTC 11168 capsular heptose does not impact cytokine induction by human macrophages

A cytokine multiplex assay was conducted to assess how the capsular heptose mutants differentially induce other cytokines than TNF α from THP-1 macrophages, namely the proinflammatory cytokines IL-1 α , IL-1 β , IL-6, IL-8, IL-12p40, IL-18, and the anti-inflammatory cytokine IL-10. This assay complements the in-house TNF α ELISA by

giving information on other proinflammatory, and anti-inflammatory, cytokines while also validating the results of the ELISA.

WT NCTC 11168 caused induction of nearly all tested cytokines (Figure 9). Significant differences between WT and the macrophage only samples were only seen at 5 hours in the induction of TNF α and IL-8 (Figure 9D,H). However, by 24 hours, a significant increase in induction was seen for all tested cytokines, except for IL-12p40, which had a slight trend of increased production. Cytokine concentrations peaked at 24 hours in most WT samples, with the exception of IL-8 and IL-18, peaking at 5 and 12 hours of co-culture, respectively (though levels for those two cytokines were fairly consistent across time). The addition of LPS also led to the induction of tested cytokines. Generally, cytokine concentrations induced by addition of LPS were fairly similar to WT induction, with WT NCTC 11168 and LPS samples not differing significantly in all but the 5-hour TNF α samples. In these samples, LPS led to significantly higher TNF α induction (Figure 9H). Though not significant, LPS consistently lead to notably lower induction of IL-1 α and IL-10 than WT, pointing to a potentially different mechanisms of induction (Figure 9A,E).

The TNF α output from this multiplex matches the results of the ELISA, with the mutants lacking the capsular heptose not differing significantly from the WT (Figure 8, 9H). Trends with the KpsM mutant were similar, with this mutant displaying only slightly diminished induction relative to the WT at the 12- and 24-hour time point. The notable difference between the two data sets is that the difference between WT and the KpsM knockout mutant was not significant at 12 hours in the multiplex, while it was in the ELISA. This points to the fact that while the addition of the CPS may cause some increased TNF α induction, this effect is relatively small.

Data indicate that normal addition of the capsular heptose, or CPS, does not significantly impact the induction of the tested cytokines. At no time point did any mutant differ significantly from WT in their ability to induce cytokines (with the exception of IL-1 α at 12 hours, with the MlghC mutant causing significantly higher signal compared to WT, but this was not conserved at other time points and had large error). Additionally, no

clear trends were observed with any mutant. For example, what was seen with IL-1 β and IL-18 release at 12 twelve hours of co-culture: the MlghB, MlghC, and WcaG knockout mutants induced lower levels of cytokines than WT, however, the high variability of the WT and the lack of this trend at other time points make it hard to create valid inferences.

Overall, these data indicate that the capsular heptose and CPS of *C. jejuni* NCTC 11168 do not significantly alter the induction of tested cytokines from THP-1 human macrophages.

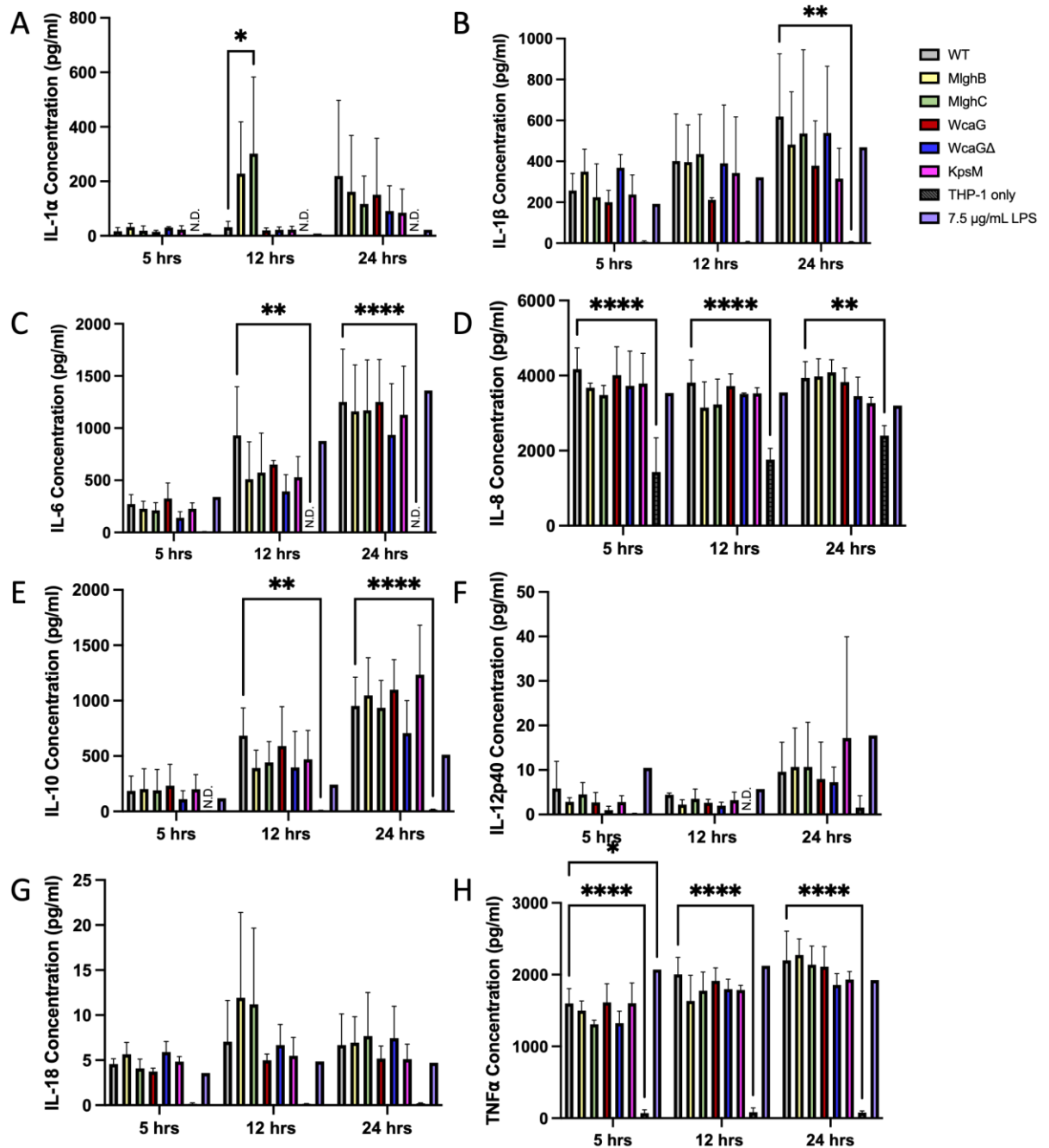


Figure 9: Cytokine output from Human THP-1 macrophage co-cultured with *C. jejuni* capsular heptose mutants. Tissue culture supernatants from THP-1 cells co-cultured with *C. jejuni* (at 37°C, 5% CO₂) were collected at 5, 12, and 24 hours and assessed for the presence of cytokines using a cytokine multiplex processed by Eve Technology (Calgary, Canada). (A) IL-1α, (B) IL-1β, (C) IL-6, (D) IL-8, (E) IL-10, (F) IL-12p40, (G) IL-18, (H) TNFα. THP-1 cells were initially treated with 250nM PMA for 48 hours, followed by 24 hours of incubation without PMA. MOI=200, n=3 for all times. Statistical analysis was conducted by two-way ANOVA and subsequent Dunnett's test, error bars represent standard deviation. All comparisons are to wild-type at each time point. N.D.= none detected, *= p<0.05, **=p<0.01, ***=p<0.001, ****= p<0.0001.

3.7 Comparison of WT *C. jejuni*-mediated effector transcription in THP-1 and MQ-NCSU macrophages

qRT-PCR was conducted to assess the production of effectors at the transcript level. A preliminary experiment looking at the production of transcripts induced by WT *C. jejuni* was attempted. Here, I tested the expression of GAPDH (a housekeeping gene), IL-1 β , IL-6, IL-8, IL-10, and TNF α in human cells, replacing TNF α with inducible nitric oxide synthase (iNOS) in chicken macrophages as chickens do not have a functional TNF α gene.

Gene specific qPCR primers were selected from previously published studies that demonstrated amplified transcript in THP-1 or MQ-NCSU cells, as listed in materials and methods section 2.10 [51,73,123,156,161,176]. Primers were modified to increase consistency of annealing temperature, or to minimize the formation of internal loops, by adding or removing complementary bases from the 5' and 3' ends. RNA samples were collected at 0.5, 1.5, 2.5, and 3.5 hours after the start of co-culture. This preliminary study was intended to allow us to select a time of co-culture to compare effector induction by the capsular heptose mutants.

Preliminary THP-1 data was promising with all cytokines tested showing upregulation by a factor >2 in at least three of the four tested time points (Supplemental Figure 1 in appendix 1). All cytokines tested had increased transcript abundance at 2.5 hours after the start of co-culture, making this a promising time point for comparing phenotypes induced by the capsular mutants.

Consistent amplification was not obtained for MQ-NCSU chicken macrophages, with cycling threshold values (C_t s) being quite high even for the housekeeping gene, indicating there was little transcript-specific cDNA in the samples. In many cases, cDNA amplification was not seen at all, especially for the macrophage only samples. This is an issue as a comparison must be made between the experimental samples and macrophage only samples in order to generate a fold change. In an attempt to fix this issue, the number of cells used for RNA extraction was increased, as were the amounts of RNA

reverse transcribed, and cDNA used in qPCR. cDNA from non-exposed macrophages was unable to be amplified consistently, and this was true for both the cytokine and housekeeping genes. Because of this, additional housekeeping genes were tested on cDNA generated from chicken macrophages: RPL37A (Ribosomal Protein L37a) and ACTB (actin beta). Human RPL37A and ACTB primers were selected from Maeß et al. 2010, while chicken RPL37A and ACTB primers were designed using NCBI primer blast, specifying primers must span one exon-exon junction [89]. If these worked, it would indicate that cytokine and GAPDH transcripts were being made in low abundance, and not that reverse transcription or qPCR were failing in some way.

The RPL37a primers worked well and amplified most samples derived from WT treated, and non-exposed MQ-NCSU macrophages, resolving a C_t for all of the 2.5- and 3.5-hour samples generated in a preliminary test. As such, one more test was conducted using WT only, with samples generated at 2.5 and 3.5 hours of co-culture for both human and chicken macrophages on the same day. These samples were all reverse transcribed on the same day, to give the most direct comparison between the human and chicken samples. The production of GAPDH, RPL37a, and IL-6 was assessed in both cell lines. Most human samples led to amplification of the housekeeping genes, but amplification was not seen for IL-6, which is inconsistent with the initial runs (Supplemental Figure 1, 2F,H). Rerunning these samples with a new dilution of IL-6 primers did not greatly improve the quality of the data (Supplemental Figure 3C,F). Testing another cytokine, TNF α , worked slightly better but still only yielded C_t in 6/12 samples (Supplemental Figure 3D,F).

The chicken macrophages performed poorly in the initial screen as well, with C_t s not being produced consistently for any primer set (Supplemental Figure 2A,B,C,F). As it was possible that contaminants were interfering with the qPCR reaction, cDNA was diluted by a factor of 3 or 9 and rerun. Interestingly, diluted samples had lower C_t s than the undiluted samples, indicating that diluting the samples was indeed beneficial. If this work is continued, cDNA will be diluted before being used in qPCR (Supplemental Figure 3A,B,E).

Overall, these data demonstrate that WT *C. jejuni* is capable of inducing the transcription of IL-1 β , IL-6, IL-8, IL-10, and TNF α in THP-1 cells in as little as 30 minutes of co-culture. However, the difficulty in obtaining consistent amplification with WT *C. jejuni* did not warrant continuing with the qRT-PCR study of the capsular heptose mutants in light of the potentially very subtle differences to be expected based on the ELISA and multiplex data. Also, the primary goal was to carry out a cross-species comparison, but failure to establish appropriate conditions for chicken macrophages prevented moving forward with this objective.

3.8 Adhesion, uptake, and intracellular survival of *C. jejuni* NCTC 11168 upon culture with host macrophages

To assess how the presence of the capsular heptose impacts the ability of *C. jejuni* to avoid clearance by host macrophage, several assays were run. These assays rely on the co-culture of host macrophage and monocytes with the capsular heptose mutants, to see if they behave differentially leading up to, during, and after internalization: 1) how well do they adhere to host cells, 2) how well are they taken up by host cells, and 3) how well do they survive within host cells?

The first assay relies on co-culture at 4°C to assess adhesion of *C. jejuni* to the host cells. Adherence is the stage in which pathogens bind receptors on the surface of macrophages, triggering uptake. The low temperature used in this assay interferes with polymerization of the macrophage cytoskeleton, preventing the uptake of bacteria into the cell [118,173]. After co-culture and washing off unbound bacteria, macrophages are lysed with distilled water, releasing bound *C. jejuni*, which are plated and counted.

The other two assays are similar to each other, with co-culturing at 37°C and the use of gentamicin to kill any bacteria that have not been internalized by the macrophage. Gentamicin is an antibiotic that is unable to enter eukaryotic cells, effectively protecting intracellular bacteria from its effects. In the uptake assay, the time of co-culture before gentamicin treatment is varied to obtain a time-course for the entry of bacteria into the macrophages. In contrast, the intracellular survival assay creates a time-course of

bacterial killing by having a constant time for initial co-culture and uptake, while varying the length of time after gentamicin treatment. As with the adhesion assay, macrophages are lysed with water, and bacterial cells are plated for CFU counting. All assays contain controls in which *C. jejuni* alone was incubated in tissue culture media, allowing for enumeration of bacteria that have not been exposed to host macrophages, and accounting for bacterial death or growth during incubation. Supernatant samples were also taken at points of co-culture, to see if incubation with host cells affects the overall viability of *C. jejuni* in suspension. These three assays collectively give a comprehensive description of how the capsular heptose affects different stages of interactions with host macrophages.

It should be noted that altering the expression of genes in the capsular biosynthesis pathway has an impact on other functions, such as overall capsular production. The differences between WT and CPS mutants can be found in Table 4, with the exception of the KpsM mutant that does not display CPS on its outer membrane, and thus could not be analyzed [173]. Generally, the MlghB and WcaG Δ mutants, in addition to lacking the heptose residue, had diminished CPS expression compared to WT. These mutants differ in the addition of MeOPN on GalNAc, only being seen in the MlghB mutant. Conversely the MlghC and WcaG mutants had elevated CPS expression relative to WT. Here, the WcaG adds MeOPN on GalNAc, while only trace amounts were seen with the MlghC mutant. These differences in CPS expression and MeOPN addition are critical to understanding the behaviour of *C. jejuni* in these assays.

Table 4: NMR spectroscopy analyses of hot water/phenol extracted CPS from the wild-type *C. jejuni* and its isogenic capsular mutants

Strain	Heptose	MeOPN on GalNAc	Substituent on GlcA	Total CPS expression
WT	+	--	EtN	++
MlghB	--	+	EtN, GroN	+/-
MlghC	--	Trace	EtN, GroN	++++
WcaG	--	+	EtN, GroN	++++
WcaG Δ	--	--	EtN, GroN	+

Note: Table adapted from Wong et al., courtesy of Dr. Carole Creuzenet [173]. A plus (+) or minus (-) represent the presence or the absence of the specified component

respectively. GalNAc, N-acetyl galactosamine; GlcA, glucuronic acid; MeOPN, O-methyl phosphoramidate; EtN, ethanolamine; GroN, 2-amino-2-deoxyglycerol.

3.8.1 The *C. jejuni* NCTC 11168 CPS diminishes adhesion to chicken macrophages

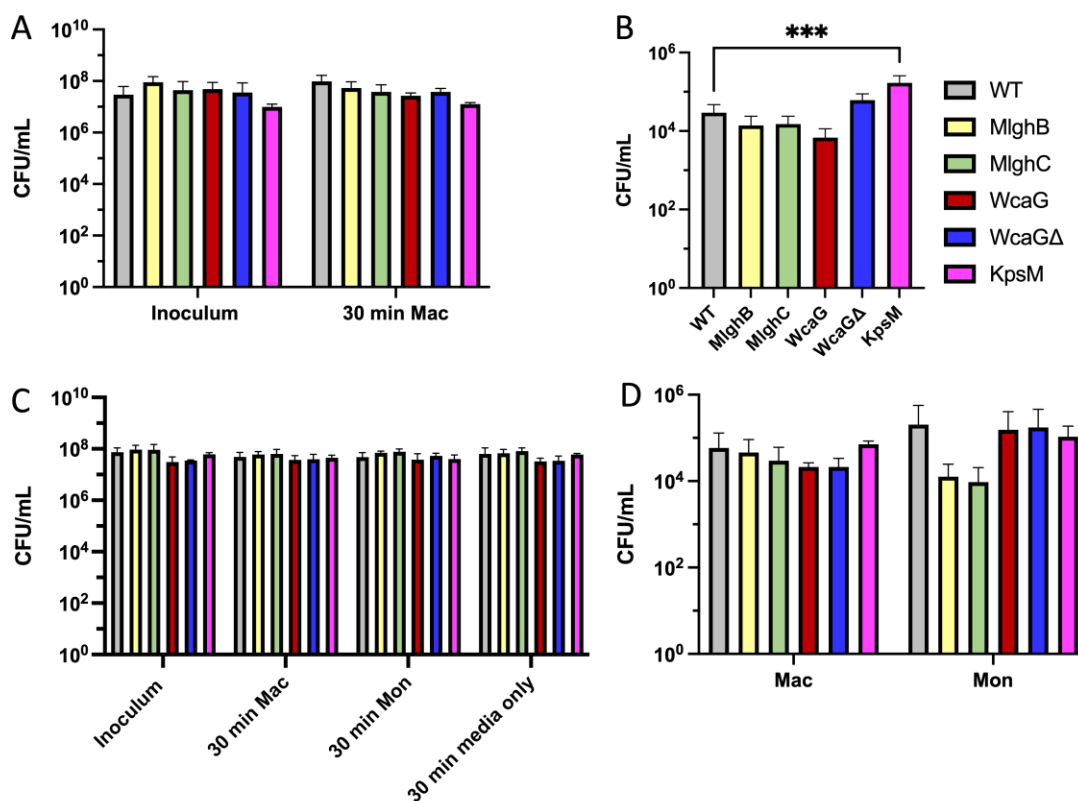
In all assays, controls were taken to ensure consistency in the amount of each mutant inoculated, which would demonstrate that differences in the phenotypes observed are due to intrinsic properties of the mutants, and not differences in inoculum. In this assay no mutant differed significantly in inoculum values from WT, indicating consistent loading in experiments with either human or chicken macrophages (Figure 10A,C). Samples of culture media were taken at certain time points to assess if co-culture conditions affected the viability of the bacteria. When assessing adhesion, supernatant samples were taken at 30 minutes of co-culture with MQ-NCSU macrophages, THP-1 macrophages, THP-1 monocytes, or tissue culture media alone. This is the length of time in which the cells are co-cultured before washing away unbound bacteria, lysing the macrophage and enumerating the bound bacteria. Under none of these conditions did the CFU/mL output for WT *C. jejuni* or any mutant differ from the initial inoculum, indicating that co-culture conditions did not affect the overall viability of the bacteria in suspension.

Enumerating the bacteria bound to chicken MQ-NCSU macrophages revealed that WT adhesion was quite low, with recovered bacteria representing 0.06% of the initial inoculum (Figure 10A,B). Data also demonstrate that the presence of the capsular heptose has little effect on the ability of these macrophages to adhere to *C. jejuni* (Figure 10B). Mutants lacking the capsular heptose (the MlghB, MlghC, WcaG, and WcaGΔ knockout mutants) did not differ significantly from WT in their ability to bind. Conversely, the presence CPS partially mitigates binding to the chicken macrophages, as demonstrated by the acapsular KpsM mutant binding at significantly higher levels than WT, though its original inoculum was ~10% lower. Therefore, it is the normal addition of the CPS that brings binding down to WT-like levels.

Adhesion of WT to THP-1 cells was higher than what was seen with MQ-NCSU cells, representing 0.08% of inoculum for macrophages, and 0.27% for monocytes (Figure

10C,D). Like with MQ-NCSU cells however, the presence of the capsular heptose does not affect the adhesion of *C. jejuni* to THP-1 macrophages, as mutants devoid of the capsular heptose were bound in similar levels to WT (Figure 10D). Looking at THP-1 monocytes however, there was a reduction in binding of the MlghB and MlghC knockout mutants by slightly more than 1 log, though significance was not attained by ANOVA. This may indicate that having intact *mlghB* and *mlghC* sequences helps *C. jejuni* to bind to human monocytes, with reduced binding when knocked out. Additionally, the presence of the CPS does not seem to impact levels of adhesion to either THP-1 host macrophage or monocytes, with the KspM mutant not differing significantly from WT.

Overall, these data indicate that the capsular heptose does not impact the adhesion of *C. jejuni* to either MQ-NCSU or THP-1 macrophages, though the normal expression of MlghB and MlghC may slightly improve binding to THP-1 monocytes. Additionally, the CPS was demonstrated to decrease binding to chicken, but not human, macrophages.



Repeats	MQ-NCSU studies	THP-1 studies
WT	n=6	n=8
MlghB	n=4	n=3
MlghC	n=3	n=3
WcaG	n=3	n=3
WcaGΔ	n=3	n=3
KpsM	n=3	n=3

Figure 10: Adhesion of *C. jejuni* capsular heptose mutants to chicken and human macrophage and/or monocytes. (A) Inoculum and culture controls for MQ-NCSU chicken macrophage. (B) Adhesion of capsular heptose mutants to MQ-NCSU chicken macrophages. (C) Inoculum and culture controls for THP-1 human macrophage and monocytes. (D) Adhesion of capsular heptose mutants to THP-1 human macrophage (Mac) and monocytes (Mon). The number of repeats for each mutant is found in the key, with select repeats completed by Daniel Zimmermann as detailed in appendix 2. Cells were co-cultured (MOI=100) for 30 minutes at 4°C under atmospheric conditions before 3 washes with PBS to remove unbound bacteria. Supernatant was taken before washing to enumerate live bacteria in culture. Cells were then lysed with distilled water and samples were spot-plated for counting. Each biological replicate is comprised of three technical replicates. Error bars represent standard deviation. Statistical analysis for panels B was conducted by one-way ANOVA and subsequent Dunnett tests, while panels A, C, and D were analyzed by two-way ANOVA. Subsequent Dunnett tests were used to compare between WT and mutants. Subsequent Bonferroni tests were used in panels A and C to identify differences between inoculum and culture controls. ***= $p < 0.001$.

3.8.2 Addition of MeOPN to the *C. jejuni* NCTC 11168 CPS increases uptake by human macrophages

As with the adhesion assay, inoculum CFU/mL readings did not differ significantly between WT and any mutant for MQ-NCSU or THP-1 experiments (Figure 10A,C). Likewise, there were no significant differences in viability between the inoculum and the control samples taken during co-culture with macrophages. Here, samples were collected after 1 or 3 hours of culturing, as these were the durations of co-culture before gentamicin treatment. Overall, this indicates differences in the uptake of the capsular heptose mutants are caused by intrinsic properties of the bacteria and are not due to inconsistent loading of bacteria or loss of viability.

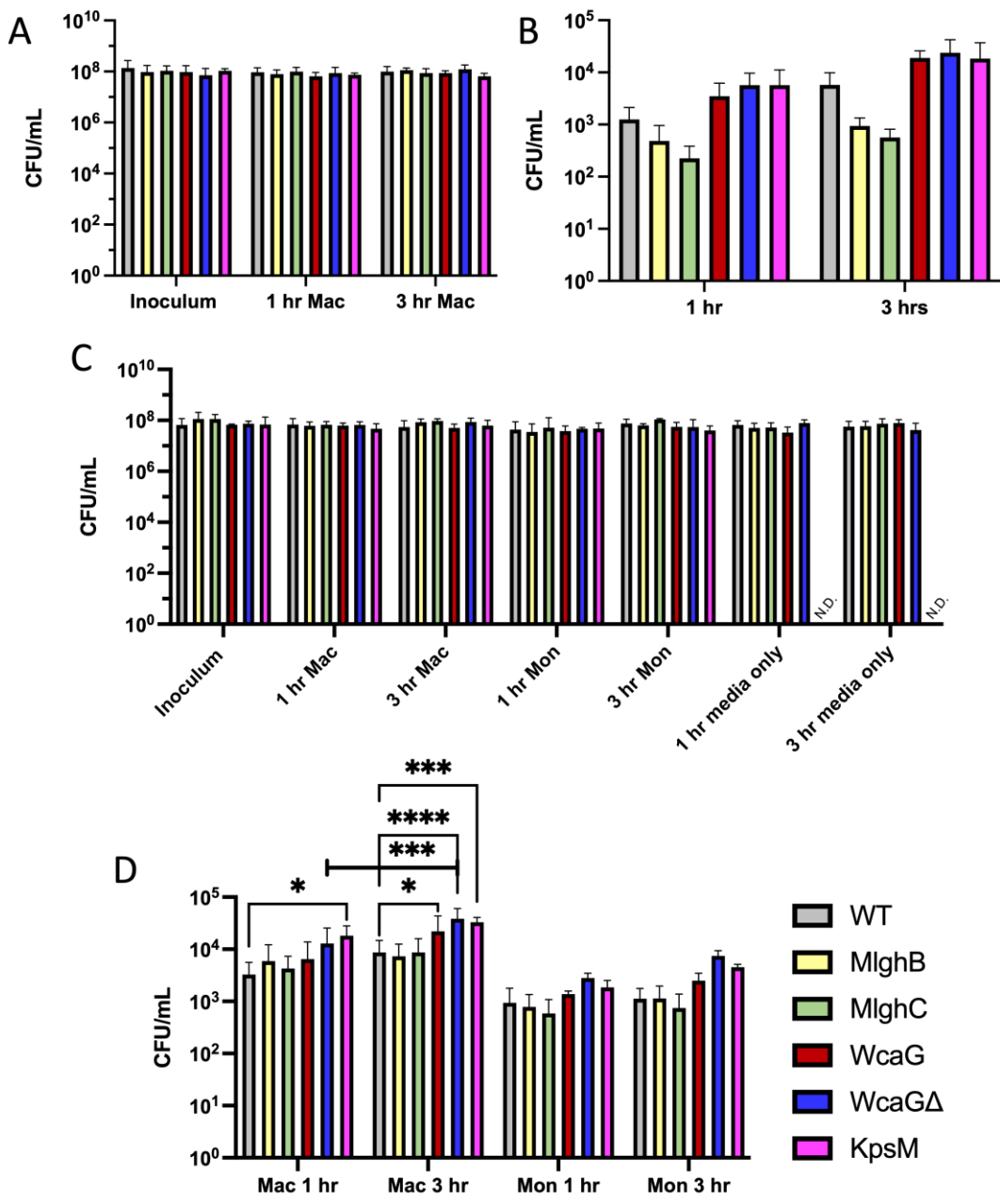
Examining the counts of internalized bacteria after gentamicin treatment for MQ-NCSU chicken macrophages revealed that 0.0009% of the initial inoculum was recovered after 1 hour, while 0.004% was recovered after 3 hours (Figure 11A,B). Counts of the KpsM mutant were elevated relative to WT at both time points, though significance was not reached (Figure 11B). Enumeration of WcaG and WcaG Δ mutants was slightly higher than WT, at around the same levels of the KpsM mutant, though these differences are also insignificant. Interestingly, though insignificant, the MlghB and MlghC mutants had diminished levels of uptake indicating that the activity of these two enzymes may slightly increase the propensity of *C. jejuni* to be internalized by chicken macrophages. This reduction in uptake was most notable at the 3-hour time point, with mutant recovery being roughly one log lower than WT. Uptake did not differ significantly between the time points for any mutant or WT tested, though there was a trend of increased enumeration for WT and all mutants tested. This increase was least notable for the MlghB and MlghC mutants.

As for uptake by THP-1 macrophages, counts of intracellular WT were much higher than chicken macrophages, representing 0.005% of inoculum at 1 hour, rising to 0.013% by 3 hours (Figure 11C,D). Uptake of the acapsular KpsM mutant was significantly elevated in THP-1 macrophages at 1 and 3 hours of co-culture, which indicates CPS decreases uptake by these macrophages. When examining the capsular heptose mutants, the WcaG

and WcaGΔ mutants had significantly elevated levels of uptake relative to WT at the 3-hour time point (Figure 11D). Like the KpsM mutant, the WcaGΔ mutant had diminished capsule production relative to the WT, potentially explaining its increased uptake [173]. A significant increase in uptake of the WcaGΔ mutant was seen between the 1- and 3-hour time points as well, indicating the reduction in capsule increases uptake more slowly than when the CPS is completely absent. Conversely, the WcaG mutant produces higher levels of CPS than WT, but still had increased uptake. This mutant differs in its addition of MeOPN onto GalNAc, indicating that the addition of MeOPN is detrimental, as higher uptake was seen when it is present. This was not true for the MlghB mutant, which adds MeOPN to its CPS, but overall has diminished CPS production. Therefore, it seems that MeOPN is detrimental, increasing uptake, only when large amounts of CPS are produced.

THP-1 human monocytes took up fewer bacteria than their macrophage counterparts, with WT recovery at 0.0014% of inoculum at 1 hour, only rising to 0.0017% at 3 hours (Figure 11C,D). Values presented reflect the increased phagocytic capacity of differentiated macrophage. THP-1 monocytes displayed a similar trend to their macrophage counterparts with increased, though ultimately insignificant, uptake of the WcaG, WcaGΔ, and KpsM mutants (Figure 11D). Uptake did not increase significantly for any mutant between the tested time points, though a trend of increased enumeration was observed.

Overall, these data indicate that the production of the CPS is protective to *C. jejuni* NCTC 11168, in that it decreases uptake by THP-1 macrophages. The addition of MeOPN on GalNAc conversely increases uptake, only when the CPS is produced at high levels. Similar trends were observed in MQ-NCSU macrophages and, more notably, in THP-1 monocytes. Significance was attained only between mutants in their uptake by THP-1 macrophages.



Repeats	MQ-NCSU studies	THP-1 inoculum, 1- and 3-hour macrophage controls and uptake output	THP-1 1-hour monocyte controls and 1- and 3-hour uptake output	THP-1 3-hour monocyte	1- and 3-hour media only controls
WT	n=3	n=8	n=6	n=6	n=4
MlghB	n=3	n=5	n=3	n=2	n=4
MlghC	n=3	n=5	n=3	n=2	n=4
WcaG	n=3	n=4	n=2	n=3	n=3
WcaGΔ	n=3	n=4	n=2	n=3	n=3
KpsM	n=3	n=3	n=3	n=3	n=0

Figure 11: Uptake of *C. jejuni* capsular heptose mutants by chicken and human macrophage and/or monocytes. (A) Inoculum and culture controls for MQ-NCSU chicken macrophage. (B) Uptake of capsular heptose mutants by MQ-NCSU chicken macrophages. (C) Inoculum and culture controls for THP-1 human macrophage and monocytes. (D) Uptake of capsular heptose mutants by THP-1 human macrophage (Mac) and monocytes (Mon). The number of repeats for each mutant is found in the key, with select repeats completed by Daniel Zimmermann as detailed in appendix 2. Cells were co-cultured (MOI=100) at 37°C, 5% CO₂ for 1 or 3 hours before being treated with 200µg/mL gentamicin for one hour. Supernatant was taken before gentamicin treatment to enumerate live bacteria in culture. Macrophages were then lysed with distilled water and spread plated for counting. Three PBS washes occurred between each step to remove unbound bacteria or gentamicin. Each biological replicate represents three technical replicates. Error bars represent standard deviation. Statistical analysis was conducted by two-way ANOVA. Subsequent Dunnett tests were used to compare WT to mutants, while Bonferroni tests were used to compare levels of mutants between inoculum and controls, and between time points in the uptake output. N.D. = not determined, *=p<0.05, ***=p<0.001, ****=p<0.0001.

3.8.3 The *C. jejuni* NCTC 11168 CPS diminishes survival within human and chicken macrophages

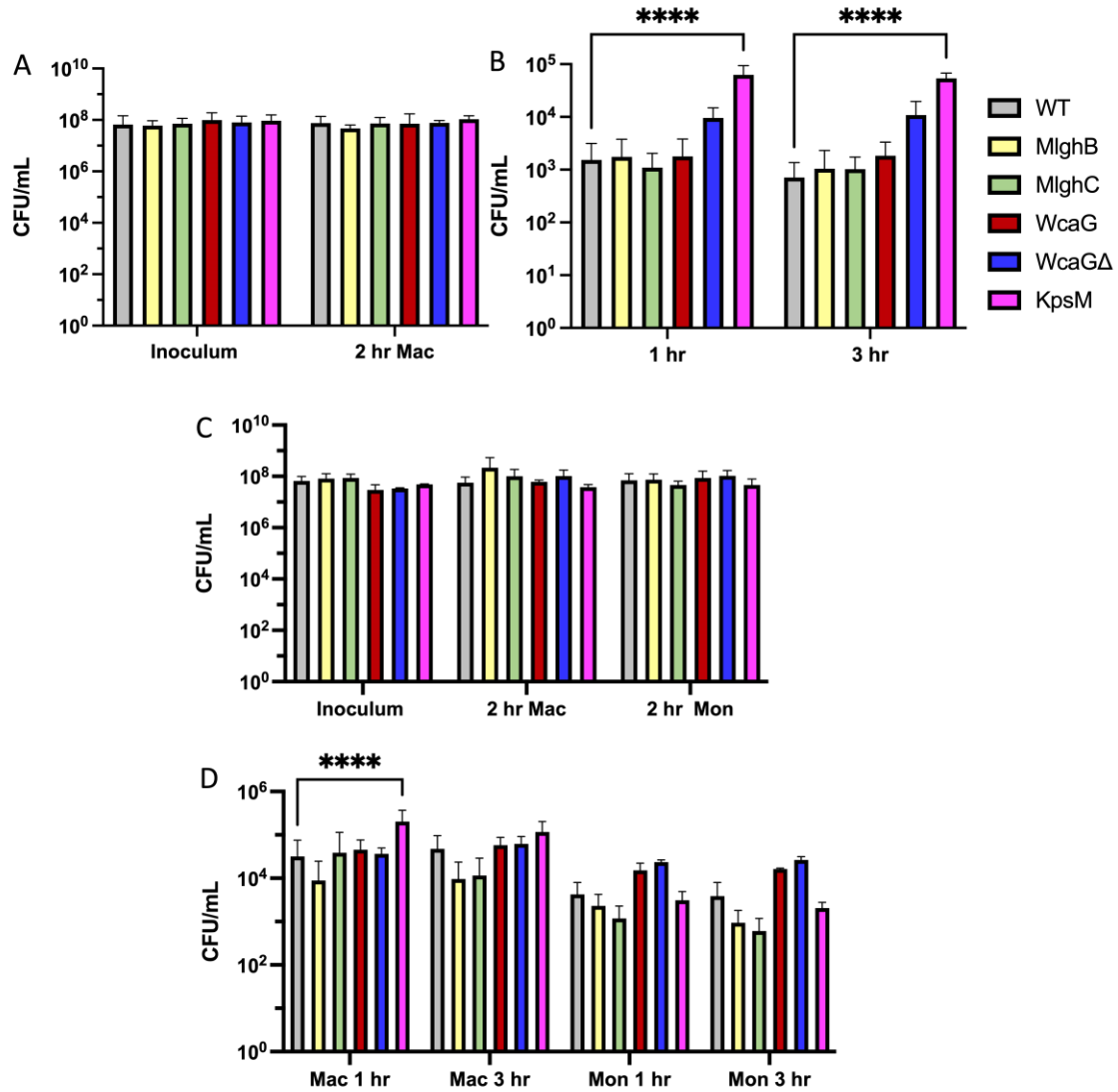
Examining intracellular survival of WT *C. jejuni* revealed that 0.0023% of the initial inoculum could be found in MQ-NCSU macrophage 1 hour after gentamicin treatment, with counts lowering to 0.001% at 3 hours (Figure 12A,B). Even with this decrease, no significant differences were seen in the enumeration of WT or any mutant between the 1- and 3-hour time points. This indicates that there was not a large degree of bacterial death within chicken macrophages within this 2-hour interval. The KpsM mutant displayed significantly increased survival relative to WT at 1 and 3 hours, indicating that the CPS is detrimental to the survival of NCTC 11168 within these chicken macrophages. Assessing the capsular heptose mutants, only the WcaGΔ mutant displayed elevated counts, though significance was not attained at either time point (Figure 12B). This correlates well with its slightly increased uptake caused by diminished capsule production.

Lysis of THP-1 macrophages revealed that 0.047% of the WT inoculum survived intracellularly after 1 hour of gentamicin treatment, with 0.071% seen at 3 hours (Figure 12C,D). This small increase in enumeration was not statistically significant for the WT, nor was it for any of the CPS mutants. The acapsular mutant had significantly elevated counts at the 1-hour time point indicating that, like with chicken macrophages, the

presence of the CPS diminishes survival within THP-1 macrophages, though this seems to be exclusive to earlier times for this cell line (Figure 12D). None of the capsular heptose mutants displayed significant differential survival to WT at the time points tested, though the MlghB and MlghC mutants showed a trend towards decreased survival especially at the 3-hour time point.

Compared to their macrophage counterparts, THP-1 monocytes had lower numbers of internalized WT, corresponding to 0.0063% of the initial inoculum at 1 hour post gentamicin treatment, and 0.0057% at 3 hours (Figure 12C,D). This is again likely due to macrophages having increased phagocytic capabilities. The KpsM mutant had similar levels to WT, signifying that the presence of the capsule has little impact on the survival of NCTC 11168 within human monocytes (Figure 12D). The capsular heptose mutants did have differential counts to WT, though significance was not attained (Figure 12D). The MlghB and MlghC knockout mutants had diminished survival, with ~1 log reductions compared to WT at the 3-hour time point, indicating that normal expression of these genes may be somewhat advantageous to the intracellular survival of *C. jejuni*. The WcaG and WcaG Δ mutants had ~1 log increases relative to WT enumeration, which indicates that the normal expression of WcaG may be somewhat detrimental for survival in THP-1 monocytes, though increased enumeration could result from increased uptake.

Overall, these data indicate that the CPS significantly diminishes survival in chicken macrophages at both times tested, and in human macrophages, 1 hour after gentamicin treatment. The normal expression of MlghB and MlghC may increase survival in human monocytes, while the normal expression of WcaG may decrease survival.



Repeats	MQ-NCSU studies	THP-1 inoculum, 1- and 3-hour monocyte survival output and 1 hour macrophage survival output	THP-1 3-hour macrophage survival output	THP-1 2-hour monocyte and macrophage controls	2-hour media only control
WT	n=6	n=9	n=9	n=7	n=6
MlghB	n=3	n=4	n=3	n=3	n=3
MlghC	n=3	n=3	n=3	n=3	n=3
WcaG	n=3	n=2	n=2	n=2	n=4
WcaGΔ	n=3	n=2	n=2	n=2	n=4
KpsM	n=3	n=3	n=3	n=3	n=3

Figure 12: Intracellular survival of *C. jejuni* capsular heptose mutants within chicken and human macrophage and/or monocytes. (A) Inoculum and culture controls for MQ-NCSU chicken macrophage. (B) Intracellular survival of capsular heptose mutants within MQ-NCSU chicken macrophages. (C) Inoculum and culture controls for

THP-1 human macrophage and monocytes. (D) Intracellular survival of capsular heptose mutants within THP-1 human macrophage (Mac) and monocytes (Mon). The number of repeats for each mutant is found in the key, with select repeats completed by Daniel Zimmermann as detailed in appendix 2. Cells were co-cultured (MOI=100) at 37°C, 5% CO₂ for 2 hours before being treated with 200µg/mL gentamicin for 1 hour. Supernatant was taken before gentamicin treatment to enumerate live bacteria in culture. After treatment, the media was replaced with antibiotic free media and incubated for 1 or 3 hours. Finally, macrophages were lysed with distilled water and spread plated for counting. Three PBS washes occurred between each step to remove unbound bacteria or gentamicin. Each biological replicate represents three technical replicates. Error bars represent standard deviation. Statistical analysis was conducted by two-way ANOVA. Subsequent Dunnett tests were used to compare WT to mutants, while Bonferroni tests were used to compare levels of mutants between inoculum and controls, and between time points in the survival output. ****=p<0.0001.

3.8.4 Overall trends and summary

There were some notable trends in the behaviour of the WT between host cells (Table 5). As stated, the percent of recovered WT relative to the initial inoculum was generally higher for THP-1 macrophages than monocytes in the uptake and intracellular survival assays, caused by the increased phagocytic capability upon differentiation. Interestingly, WT displayed higher adhesion to THP-1 monocytes than to THP-1 macrophages (at 0.27% and 0.08% of inoculum respectively). This indicates that while *C. jejuni* binds at higher rates to THP-1 monocytes, much lower levels were internalized compared to macrophages. There was also some host specificity in the behaviour of the WT across assays, with THP-1 macrophages having a higher percentage of WT inoculum enumerated across all assays compared to MQ-NCSU macrophages. This is in line with *C. jejuni* as a commensal in chickens, where the macrophages would likely be more tolerant and not act to clear the bacteria. In contrast, higher adherence to and enumeration within THP-1 macrophages points to *C. jejuni* as a human pathogen, where macrophages would actively attempt to eliminate the bacteria. It should be noted that values should not be compared directly across assays, as they were conducted independently, and thus CFU values enumerated must be compared to their initial inoculum. For THP-1 macrophage and monocytes, the highest percent inoculum was seen in the intracellular survival assays, where cells were co-cultured for 2 hours, treated with gentamicin for 1 hour and then left for 1 or 3 hours. Counts at the 1-hour survival time point were even higher than

what was seen at the 3-hour time point in the uptake assay, indicating WT *C. jejuni* NCTC 11168 may be proliferating within these human cells. Previous lab members have shown no *C. jejuni* were recovered at later points following gentamicin treatment, indicating that killing is indeed happening, with sufficient time needed to clear the pathogen.

Table 5: Percentage of WT recovered from host macrophages and monocytes in adhesion, uptake, and intracellular survival assays.

WT % of inoculum	Chicken Macrophages	THP-1 Macrophages	THP-1 Monocytes
Adhesion assay	0.06%	0.08%	0.27%
Uptake assay	0.0009 to 0.004%	0.005% to 0.013%	0.0014 to 0.0017%
Intracellular survival assay	0.0023% to 0.001%	0.047% to 0.071%	0.0063 to 0.0057%

The MQ-NCSU chicken macrophages had noteworthy trends across assays (Table 6). The KpsM knockout is interesting as it had significantly elevated levels of adhesion and survival, but only a trend of increased uptake. The difference between the WT and KpsM mutant is most notable in the survival assay however, with the difference in bacterial recovery being roughly 2 logs at the 3-hour time point. This indicates that capsule production protects against adherence to these chicken macrophages, but the lack of a CPS confers a significant survival advantage within these cells. While MlghB and MlghC knockouts had diminished uptake relative to WT, they demonstrated roughly equivalent or slightly higher levels of intracellular survival. This may indicate that these mutants have some survival advantage within the cell, with less internalization and higher survival combining to create a WT-like output. While WcaG and WcaGΔ knockouts did not have significantly different levels of adhesion than WT, an elevation in WcaGΔ counts was seen in both the uptake and survival assays. Higher uptake of this mutant was likely a result of decreased capsule production, and higher survival likely being a consequence of increased uptake. Significance was not attained for this mutant in either assay.

Table 6: Summary of phenotypes displayed by *C. jejuni* capsular mutants in adhesion, uptake, and intracellular survival assays, across chicken and human macrophages/monocytes.

Strain	Assay	Chicken Macrophage	THP-1 Macrophage	THP-1 Monocytes
MlghB	Adhesion			--
	Uptake 1 hr	-		
	Uptake 3 hr	--		
	Intracellular survival 1 hr		--	-
	Intracellular survival 3 hr		--	--
MlghC	Adhesion			--
	Uptake 1 hr	-		
	Uptake 3 hr	--		
	Intracellular survival 1 hr			-
	Intracellular survival 3 hr		--	--
WcaG	Adhesion	-		
	Uptake 1 hr	+		
	Uptake 3 hr	+	+*	+
	Intracellular survival 1 hr			++
	Intracellular survival 3 hr			++
WcaGΔ	Adhesion			
	Uptake 1 hr	+		+
	Uptake 3 hr	+	+*	++
	Intracellular survival 1 hr	+		++
	Intracellular survival 3 hr	+		++
KpsM	Adhesion	++*		
	Uptake 1 hr	+	++*	
	Uptake 3 hr	+	++*	++
	Intracellular survival 1 hr	++*	++	
	Intracellular survival 3 hr	++*	++	

* denotes a significant difference, while +/- denotes an increase or decrease relative to WT. -/+ signifies a smaller change than -/+.

The THP-1 macrophages displayed quite different trends, pointing to host specificity in interactions with NCTC 11168 (Table 6). Generally, there were no notable differences between WT and mutants in the adhesion assay. The acapsular mutant had significantly elevated levels of uptake at both time-points tested and demonstrated significantly elevated survival only at 1-hour post-gentamicin treatment. The increase in the survival of the KpsM mutant may be caused by increased uptake, or because the lack of the capsule confers a survival advantage early on. Regardless, it is apparent that the lack of the capsule is protective when looking at uptake by THP-1 macrophages as *C. jejuni* is

taken up in significantly higher levels when it is absent, even though it does not impact adherence. Additionally, the MlghB and MlghC knockouts demonstrated diminished intracellular survival, indicating the normal functioning of these genes help to resist killing upon phagocytosis. While the WcaG and WcaG Δ mutants were taken up in significantly higher amounts by THP-1 macrophages at 3 hours, there were no notable differences in intracellular survival compared to WT. These mutants are thus likely both taken up and killed at higher rates than WT which cumulatively creates WT-like intracellular recovery. With respect to the WcaG mutant, it was noted that even though it had high capsule production, it was taken up at high rates likely due to the addition of MeOPN. Additionally, the high abundance of MeOPN is likely impairing intracellular survival. Conversely, the WcaG Δ mutant had low capsule production conferring increased uptake, but the amount of capsule is likely not low enough to be protective internally as with the KpsM mutant.

THP-1 monocytes displayed some different trends to their macrophage counterparts (Table 6). The KpsM mutant only displayed notable differences in the uptake assay, having increased uptake relative to WT. This indicates that, like with THP-1 macrophages, the addition of the CPS may reduce uptake by THP-1 monocytes. The MlghB and MlghC mutants had a ~ 1 log reduction relative to WT in the adhesion assay, and at 3 hours in the intracellular survival assay. These differences were insignificant, but may indicate that the normal production of these enzymes increase binding to human monocytes, and also aid in increasing survival when internalized. As noted in the WT, while binding was higher to human monocytes than macrophages, internalization was much lower overall. Besides the MlghB and MlghC knockouts, no other mutant demonstrated altered adhesion to these monocytes. The WcaG and WcaG Δ mutants had increased uptake and intracellular survival in these cells, with the increased counts in the survival assay likely being a consequence of increased uptake. As with THP-1 macrophages, the increased uptake of the WcaG Δ mutant is likely due to a reduction in capsule, while the WcaG mutant is likely taken up at higher levels due to the abundance of MeOPN it presents.

3.9 DdahA, DdahB, and DdahC, are able to interact in pairs

3.9.1 SPR principle and preliminary data for DdahA/DdahB

To assess the hypothesis that enzymes in the capsular heptose biosynthesis pathways engage in substrate channelling, physical interactions between these enzymes first had to be established. This was accomplished by surface plasmon resonance (SPR), a method that assesses interactions by flowing an analyte over a ligand that has been immobilized onto a chip. Carboxyl chips were used as they allow the physical immobilization of ligand to the chip. This is important as all enzymes analyzed were His-tagged, meaning that analytes would compete with the ligand for binding to the sensor surface, if a nickel affinity chip was used. Within the SPR machine, light is reflected at different angles depending on the mass of materials bound to the chip, and this is detected by a sensor. Once the ligand has been covalently bound, a blocking buffer is injected, which prevents non-specific binding to unoccupied portions of the chip. As such, the only mass change after blocking should result from analyte binding to the ligand. Using this information, the SPR software is able to generate a binding curve in real time and can calculate association and dissociation constants using multiple curves obtained from running different concentrations of analyte over the same concentration of ligand.

Proteins were first overexpressed and purified for subsequent use in SPR experiments as detailed in chapter 2.13 to 2.14. While yield varied between enzymes, nickel affinity purification yielded fractions that were quite pure, with little co-elution of other proteins found in the *E. coli* expression strains that were used (Figure 13).

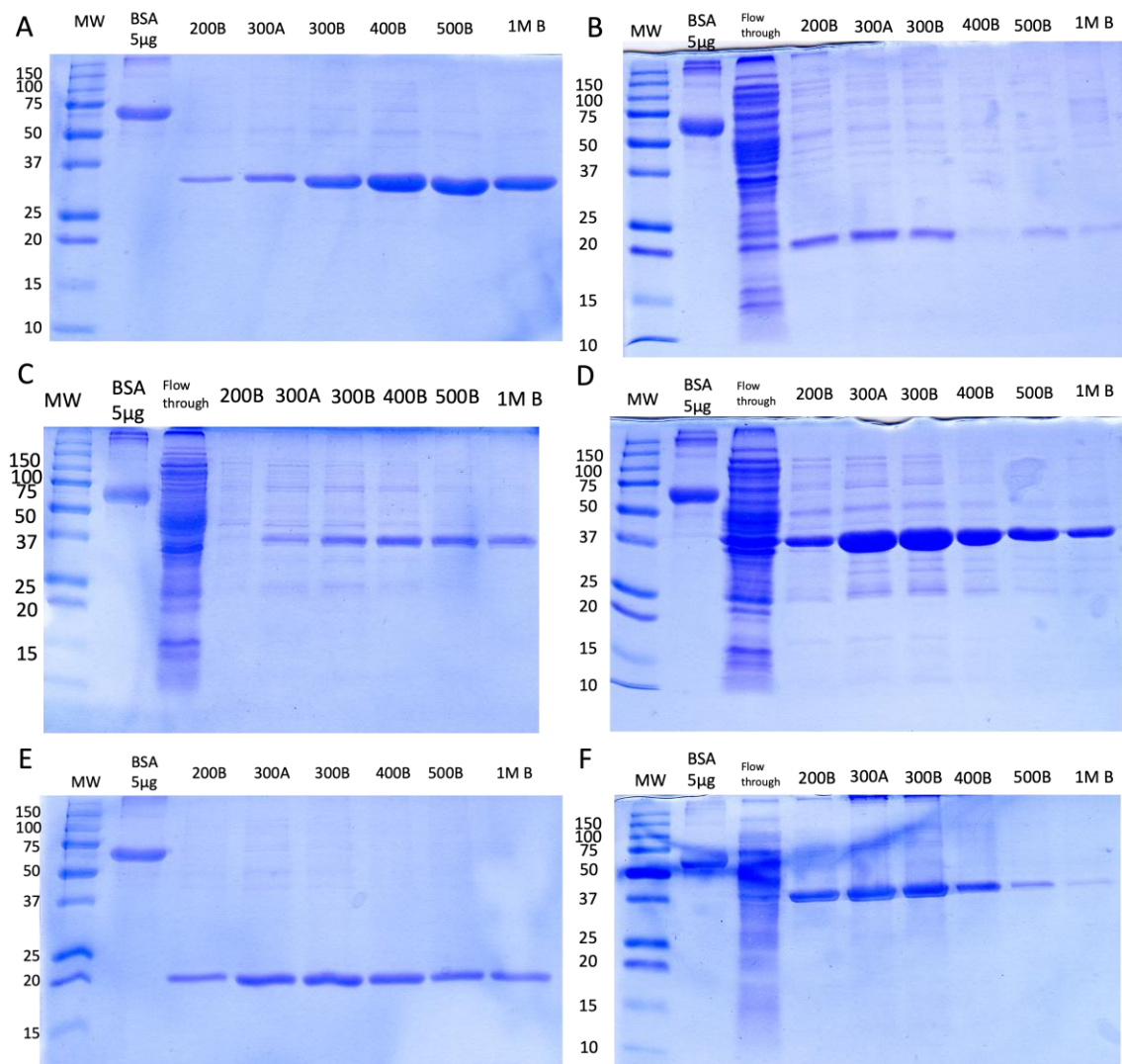


Figure 13: Representative examples of SDS-PAGE gels of purified proteins from the Mlgh and Ddah pathways.

(A) WcaG (36.5 kDa, from strain 81-176), (B) MlghB (22.2 kDa), (C) MlghC (40.7 kDa), (D) DdahA (40.5 kDa), (E) DdahB (22.1 kDa), (F) DdahC (41.7 kDa). Proteins were purified with nickel-NTA columns using buffers with increasing concentrations of imidazole, ranging from 200 μ M to 1 M. MW denotes the lane containing the molecular weight markers, with values on the left side of the gels denoting the mass of the markers in kDa. Gels were composed of 16% acrylamide and wells were loaded with 20 μ L of sample before being run at 130V for ~50 minutes.

An initial SPR run, presented in Figure 14, was conducted to look for interactions between DdahA and DdahB. Here, an injection containing 200 μ L of crosslinking reagent followed by 200 μ L of DdahA, at a theoretical concentration of 50 μ g/mL determined by densitometry from an SDS-PAGE gel, was used to immobilize the protein to the chip. After blocking the chip using blocking buffer and adding BSA to the media, 200 μ L of DdahB

at a theoretical concentration of 50 $\mu\text{g}/\text{mL}$ was injected. This caused a stable increase in signal after the 5-minute interaction period, indicating these two enzymes are able to interact.

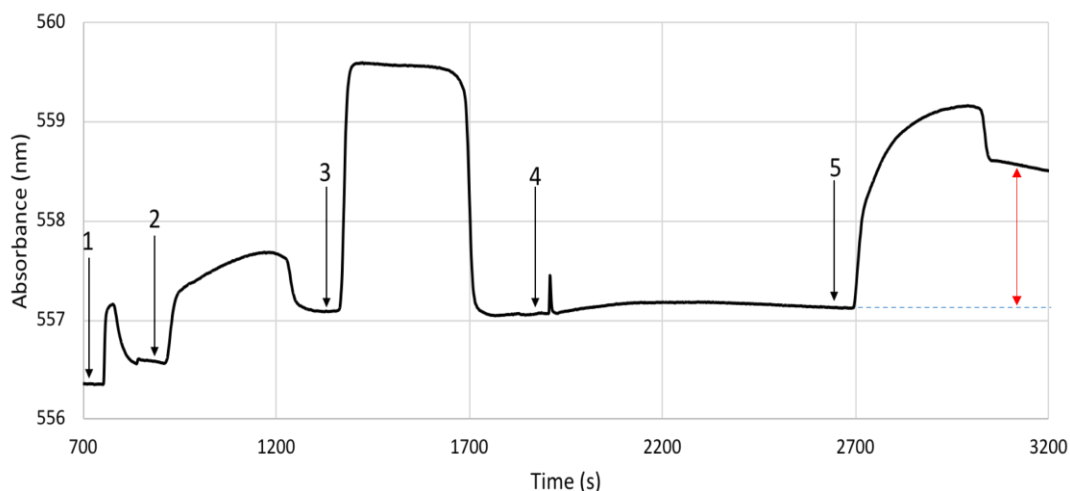


Figure 14: SPR signal flowing DdahB over immobilized DdahA. 1: Injection of EDC/NHS provided by Nicoya, which covalently links proteins to the SPR sensor chip. 2: Injection of DdahA ($\sim 50 \mu\text{g}/\text{mL}$ suspended in Nicoya’s activation buffer). 3: Injection of blocking buffer provided by Nicoya, which prevents non-specific binding of other molecules to the chip. 4: Addition of bovine serum albumin to the buffer flowing over the sensor (final concentration 25 $\mu\text{g}/\text{mL}$), as a control for nonspecific binding. 5: Injection of DdahB ($\sim 50 \mu\text{g}/\text{mL}$ suspended in 1x PBS pH 7.4). The sustained increase in absorbance, denoted by the red arrow, corresponds to a change in the reflection of light related to the binding of DdahB onto immobilized DdahA.

One limitation of this method deals with the concept of “regeneration”, in which the analyte should be able to dissociate from the ligand so that multiple curves can be gained with a single chip. All of the regeneration solutions tried have either resulted in incomplete regeneration of the tested DdahA/B complex or have denatured the ligand. Solutions tested include: 10-50 mM HCl, 1-4 M MgCl_2 , 1% Triton X-100, 2 M MgCl_2 with 1% Triton X-100, and 100 mM glycine pH 3.0.

3.9.2 Attempt at determining K_D for DdahA and DdahB interactions

In light of failed regeneration of chips following DdahA/DdahB interactions, multiple chips were used to generate binding curves between these enzymes, in which DdahA was immobilized on a new chip for each run.

To determine binding constants between DdahA and DdahB, at least 5 runs with serially diluted DdahB had to be conducted. To minimize variation between runs, all were completed with the same serially diluted proteins within two days after concentration and glycerol removal using centrifugal filters with a 10 kDa cut off.

A Bradford assay was used to quantify proteins used in SPR runs. As seen in Table 7, the concentration of DdahA and DdahB were much lower and higher than expected based on densitometry, respectively. Even with this low DdahA concentration, high signal was seen immobilizing this protein to the chip (Figure 15A).

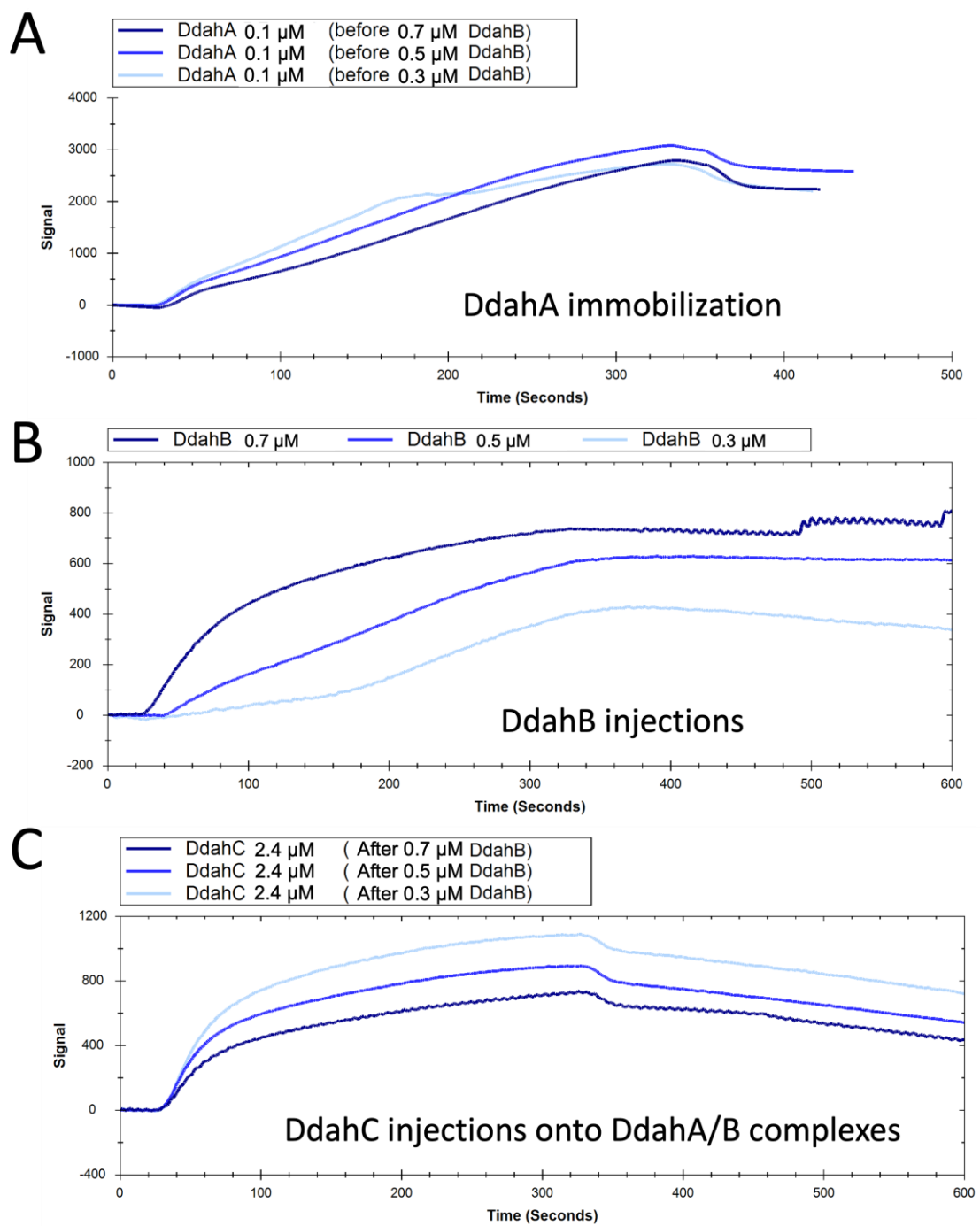
Table 7: Quantification of Ddah proteins used for SPR by Bradford Assay.

	Concentration by Densitometry of stocks ($\mu\text{g/mL}$)	Concentration by Bradford ($\mu\text{g/mL}$)	Concentration used in SPR based on Bradford ($\mu\text{g/mL}$)	Mass (kDA)	Molar concentration
DdahA	169	19.3	5.7	40.5	0.1 μM
DdahB	124	86.0	34.7 (or lower, with multiple dilutions, seen in Figure 15B)	22.1	1.6 μM
DdahC	130	262.0	100.1	41.7	2.4 μM

With this preparation only a few consistent runs were achieved, in which higher concentrations of DdahB led to larger rises in absorbance (Figure 15B). This was due largely to significant aggregation of DdahB that occurred at tested concentrations of $\sim 23 \mu\text{g/mL}$ or greater. It should be noted that immobilization of DdahA was inconsistent, with the DdahA signal corresponding to the highest concentration of DdahB being lower than what was seen on the other chips (Figure 15A). Still, this run had the highest rise in DdahB signal, demonstrating that an increased DdahB concentration led to more binding,

even in the presence of slightly less DdahA (ranging in signal by ~10% between the highest and lowest immobilization).

Determination of kinetics was attempted using the Tracedrawer software. As stated, the number of analyte dilutions needed for high accuracy was not achieved, but fitting was conducted to get a rough order of magnitude for the K_D of enzyme interactions observed. As only three DdahA/B curves were generated, local analysis as opposed to global analysis was used, which gave fits that were more accurate to the curves generated due to the low number of curves. Analysis revealed the interaction of DdahA and DdahB has a K_D in an order of magnitude of $\sim 10^{-8}$ M, which is quite strong (Figure 16A,D). While one curve gave a magnitude of 10^{-10} , it had quite a large error, making the two curves in the order of $\sim 10^{-8}$ M likely to be more accurate.



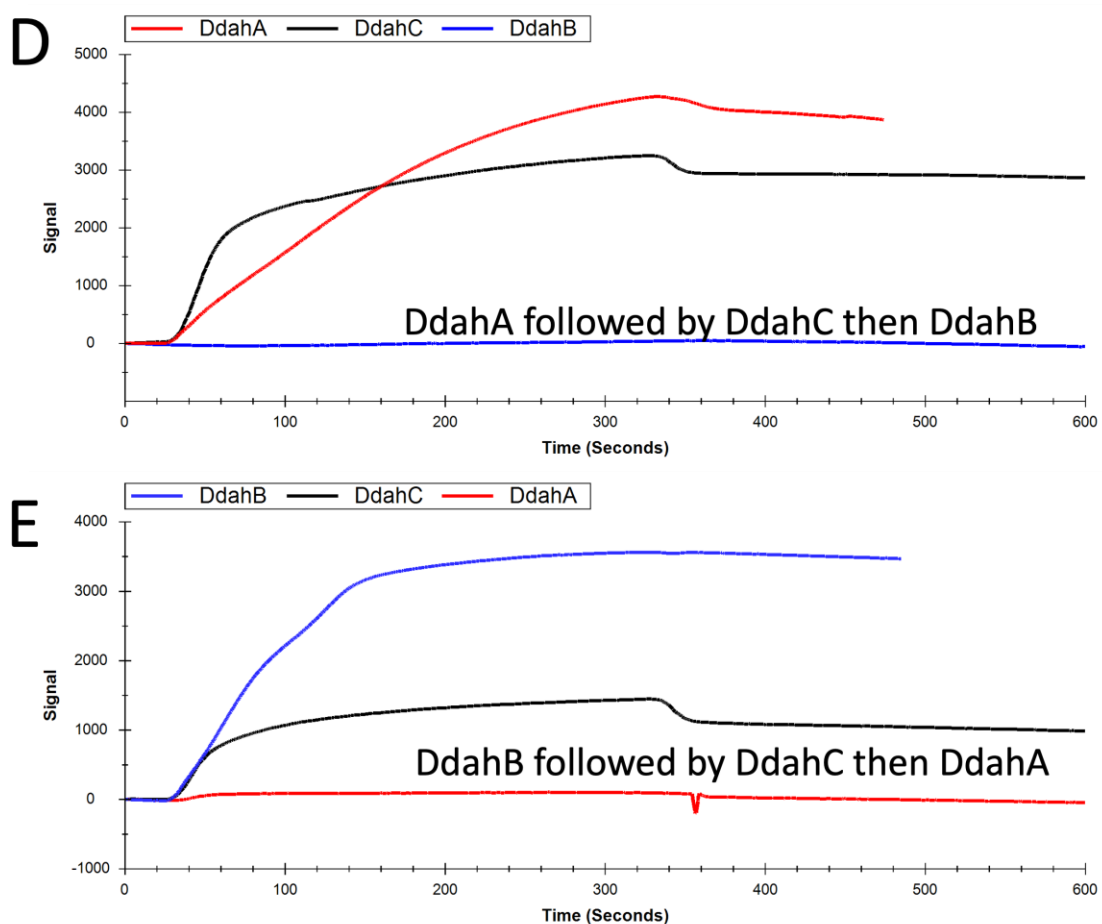
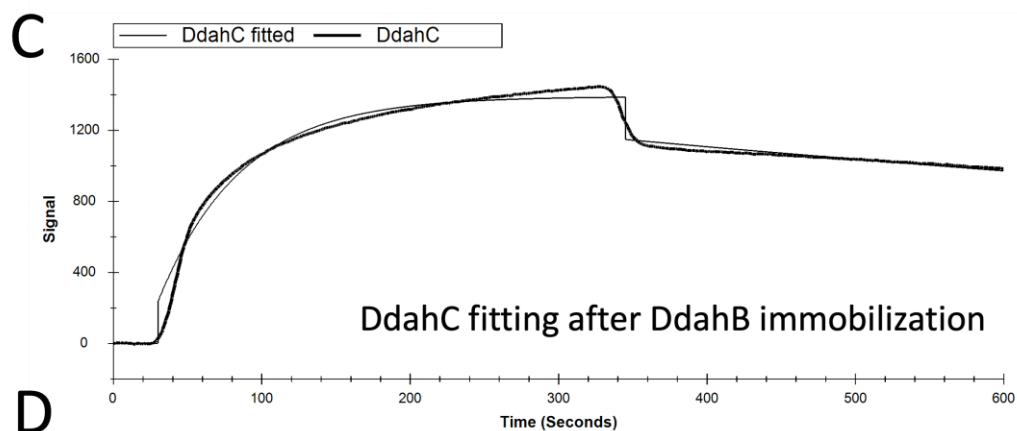
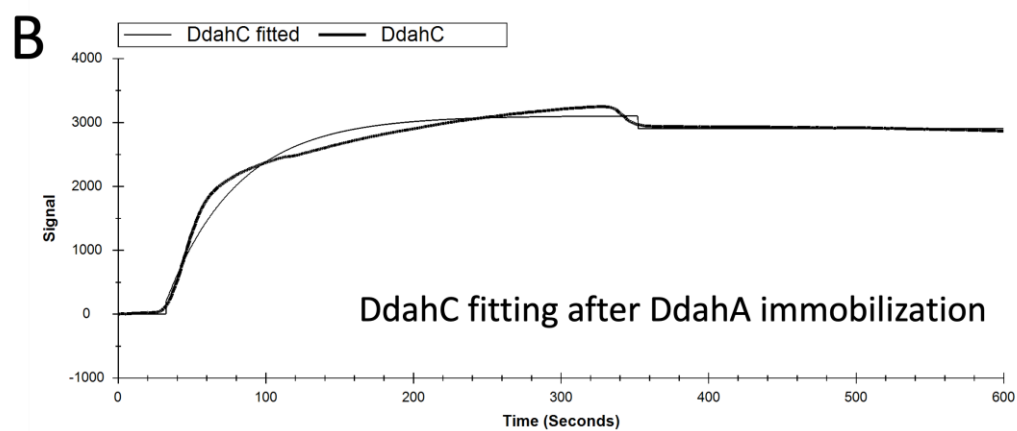
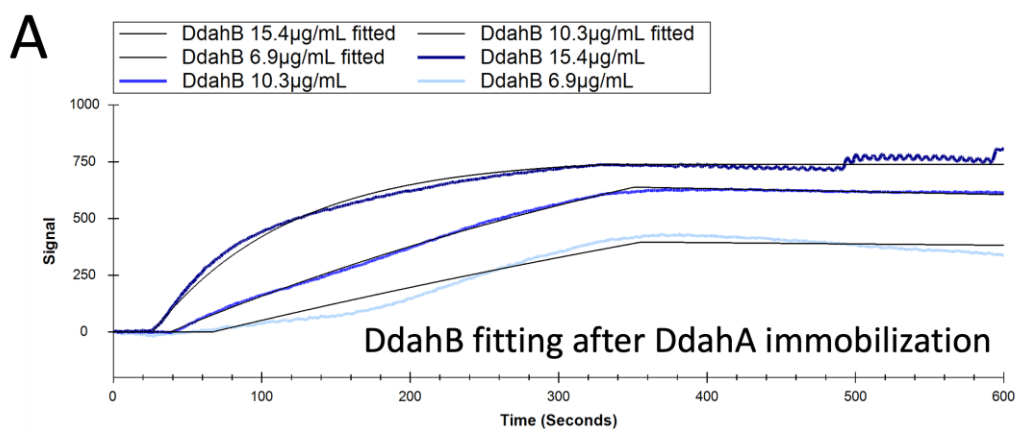


Figure 15: Tracedrawer outputs for SPR detailing interactions between enzymes in the Ddah pathway. (A) Immobilization of DdahA (injected at $0.1\mu\text{M}$ suspended in Nicoya activation buffer). Curves of the same colour in panels A, B, and C correspond to the same run. Values in brackets seen in the key indicate the concentration of DdahB injected (in μM) after the addition of DdahA. (B) Injections of DdahB onto immobilized DdahA. Coloured curves correspond to concentrations injected as seen in the key. (C) Injections of $2.4\mu\text{M}$ DdahC onto previously formed DdahA and DdahB complexes seen in panel B. Values in brackets seen in the key indicate the concentration of DdahB previously injected (in μM) before the addition of DdahC. (D) Curves detailing the immobilization of DdahA, and subsequent injections of DdahC followed by DdahB. Protein concentrations can be found in Table 5. (E) Curves detailing the immobilization of DdahB, and subsequent injections of DdahC followed by DdahA. Protein concentrations can be found in Table 5. The buffer used in all experiments was 1x PBS pH 7.4, and all samples had $200\mu\text{L}$ injected with an interaction time of 5 minutes.



D

Immobilized ligand	Analyte	analyte mass (kDa)	analyte concentration (nM)	k_a (1/(M*s))	error	k_d (1/s)	error	K_D (M)	error
DdahA	DdahB	22.1	310	2.97E+03	9.79E+01	2.49E-04	1.02E-04	8.40E-08	3.74E-08
	DdahB	22.1	465	3.17E+03	2.61E+01	2.69E-04	7.07E-06	8.48E-08	2.93E-09
	DdahB	22.1	698	1.66E+04	1.11E+02	9.79E-06	1.49E-03	5.91E-10	8.97E-08
DdahA	DdahC	40.1	2400	8.80E+03	9.64E+02	5.24E-05	1.12E-04	5.95E-09	1.35E-08
DdahB	DdahC	40.1	2400	7.21E+03	3.90E+02	6.54E-04	3.63E-05	9.08E-08	9.98E-09

Figure 16: Attempted kinetic determination for the interaction of enzymes in the Ddah biosynthetic pathway. (A) Injections of DdahB onto immobilized DdahA. (B) Injection of DdahC onto immobilized DdahA (C) Injection of DdahC onto immobilized DdahA. (D) Tracedrawer output of kinetic constants based on curve fittings and defined analyte concentrations. Analyte concentrations seen in panels A-C can be found in panel D, with all analytes being added to immobilized DdahA (injected at 0.1 μ M suspended in Nicoya activation buffer). The buffer used in all experiments was 1x PBS pH 7.4, and all samples had 200 μ L injected with an interaction time of 5 minutes.

3.9.3 Qualitative pairwise interactions, can DdahC interact with DdahA or DdahB?

In each run of the prior experiment, after flowing DdahB over DdahA, subsequent injections of DdahC (200 μ l, 2.4 μ M) were performed to generate more data. DdahC consistently caused an increase in absorbance, indicating DdahC can interact with either DdahA, DdahB, or both in a heterotrimer complex. Interestingly, as the amount of DdahB bound to DdahA increased, the amount of DdahC bound decreased (Figure 15C). This initially led to the belief that DdahC can bind to DdahA, but not DdahB.

After this experiment, other tests were run to further explain what was observed with DdahC. As seen in panel D of Figure 15, injecting DdahC onto freshly immobilized DdahA led to an increase in absorbance, indicative of binding. DdahB was injected afterwards and did not lead to a rise in absorbance, suggesting that the DdahB cannot interact with DdahA once the DdahA/DdahC complex has formed. Next, DdahC was injected onto freshly immobilized DdahB, which also caused an increase in absorbance, indicating that DdahB and DdahC can also interact if not previously engaged in interaction with DdahA (Figure 15E). Subsequent injection of DdahA onto the DdahB/DdahC complex did not lead to an increase in absorbance, although DdahA has been shown to bind to DdahB and to DdahC separately.

Tracedrawer analysis gives some potentially interesting insights into the affinity these enzymes have for each other. As reported in section 3.9.2, the DdahA/B complex had a K_D with a rough order of magnitude of 10^{-8} M (Figure 16A,D). The DdahA/C complex was shown to be slightly stronger with a K_D in the order of 10^{-9} M (though the error was one magnitude larger), with the DdahB/C complex being weaker with a K_D of roughly 10^{-

⁷M (Figure 16B,C,D). This is interesting as there was not a specific trend in increasing affinity along the cognate pathway as might be assumed with substrate channeling, though it is important to note this analysis was based on a limited number of curves, with varying fit quality.

These findings cumulatively demonstrate that DdahA, DdahB, and DdahC are able to interact, but that a complex of the three enzymes is not favoured. This potentially indicates that these three enzymes bind using the same domain, or that the binding domains are distinct but are configured in a manner that only permits one interaction at a time (Figure 17).

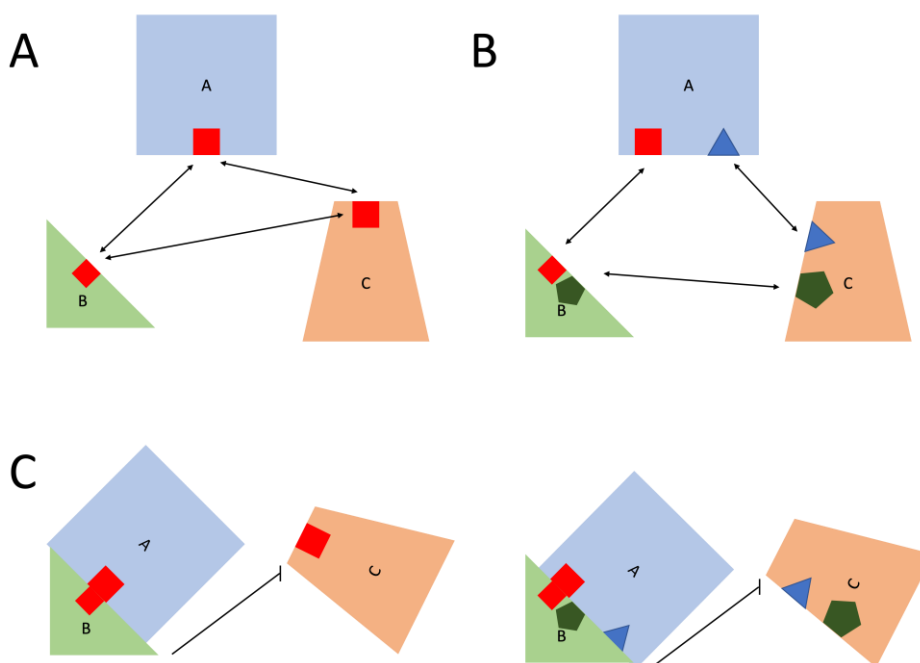


Figure 17: Proposed method of interaction between enzymes in the Ddah pathway. (A) Enzymes in the Ddah pathway may contain a common binding domain or (B) Enzymes in the Ddah pathway contain multiple domains that permit interactions. (C) In either case, the interaction of any two enzymes hinders the binding of the other enzyme in the series by hiding a previously available binding domain.

3.10 Assessing interactions of enzymes in the MlgH pathway

After determining that enzymes in the Ddah series are able to interact, a series of SPR runs utilizing carboxyl chips were conducted in order to look for interactions within the

Mlgh series, and between enzymes in the Mlgh and Ddah series. Generally, the first injection of an analyte was the most important for looking at interactions, while subsequent analytes were injected to generate additional data. It should be noted that regeneration is still not possible, so subsequent analytes are in many cases flowing over a ligand-analyte complex. The interactions tested are outlined in the following table:

Table 8: Enzymatic interactions tested by surface plasmon resonance without regeneration.

Ligand immobilized	Analyte 1	Analyte 2	Analyte 3	Analyte 4	Analyte 5
DdahA	MlghB-1	MlghC	WcaG-PG	DdahB	
DdahA	MlghC	MlghB-1			
WcaG-PG	MlghB-1	MlghC	DdahB	DdahC	
WcaG-PG	MlghB-2	MlghC	DdahB	DdahC	DdahA
MlghB-2	MlghC	WcaG			

* MlghB-1 and MlghB-2 refer to separate preparations of MlghB. These were taken from the same stock but were ultra-filtered on centricon devices separately for concentration and glycerol removal.

Diluted protein samples used in SPR were run on a gel, and a Bradford assay was used to quantify centriconned protein stocks. Most of the enzymes were not quite at the target of 50 μ g/mL (Table 9), but these concentrations do not alter the interpretations of the findings as explained in the subsequent sections.

Table 9: Quantification of Mlgh proteins used for SPR by Bradford Assay.

	Concentration by Densitometry of stocks (μ g/mL)	Concentration by Bradford (μ g/mL)	Concentration used in SPR based on Bradford (μ g/mL)	Mass (kDA)	Molar concentration
DdahA	264	55	10.5	40.5	0.3 μ M
DdahB	174	103	29.6	22.1	1.3 μ M
DdahC	155	194	62.6	41.7	1.5 μ M
MlghB-1	112	288	128.3	22.6	3.0 μ M
MlghB-2	112	154	68.7	22.6	1.7 μ M
MlghC	110	26	11.7	40.7	0.3 μ M
WcaG	289	144	24.9	40.5	0.6 μ M

3.10.1 DdahA with MlghB and MlghC

While DdahA is not part of the Mlgh series, subsequent enzymes MlghB and MlghC can act upon its product, and this property was exploited to characterize these enzymes while the initial oxidase had not been identified [15,95]. As such, interactions between DdahA and the Mlgh series epimerase and reductase were assessed by SPR. The first run in which DdahA was immobilized demonstrated a small interaction with MlghB, with a subsequent MlghC injection causing ~3 times the signal increase seen with MlghB (figure 19A). This indicates that DdahA binds to MlghC with greater affinity than MlghB, as MlghC led to a higher signal though it was injected second. Considering the actual molar concentrations presented in Table 9, MlghB was injected in higher amounts but still led to less binding, affirming greater interactions of MlghC with DdahA. Additionally, even though MlghC is twice the size of MlghB, it was injected at $\sim 1/10^{\text{th}}$ the concentration, indicating that the size of the analyte was not the reason for higher signal. Subsequent injections with WcaG or DdahB led to no rise in signal, indicating WcaG and DdahA do not interact, and/or that the binding sites of DdahA were occupied as was seen when assessing interactions between DdahA, B, and C.

The next immobilization looked at DdahA in conjunction with MlghB and MlghC, this time testing MlghC first to confirm trends in the previous run (figure 19B). Even with the order of the MlghC and MlghB analytes reversed, very similar signals were attained with these two enzymes as in figure 19, panel A. Within the Ddah series, it was observed that all 3 of these enzymes can form complexes in a pairwise manner, but the interaction of any two hinders the binding of the other enzyme in the series. This does not seem to be the case with MlghB and MlghC, at least at the concentrations tested, as it appears that there are still sites present on DdahA available for Mlgh binding after the first analyte injection, independent of injection order. This could also be caused by a reduction in the amount of DdahA immobilized in figure 19A,B, relative to figure 16A, causing less crowding on the chip and permitting more binding.

Kinetic determination revealed that the DdahA/MlghC complex had a K_D with an order of magnitude between 10^{-8} to 10^{-9} M, while the DdahA/MlghB complex had an order of magnitude of 10^{-7} M (figure 20A,B,F). This affirms the notion that DdahA interacts more strongly with MlghC than MlghB.

3.10.2 WcaG with MlghB and MlghC

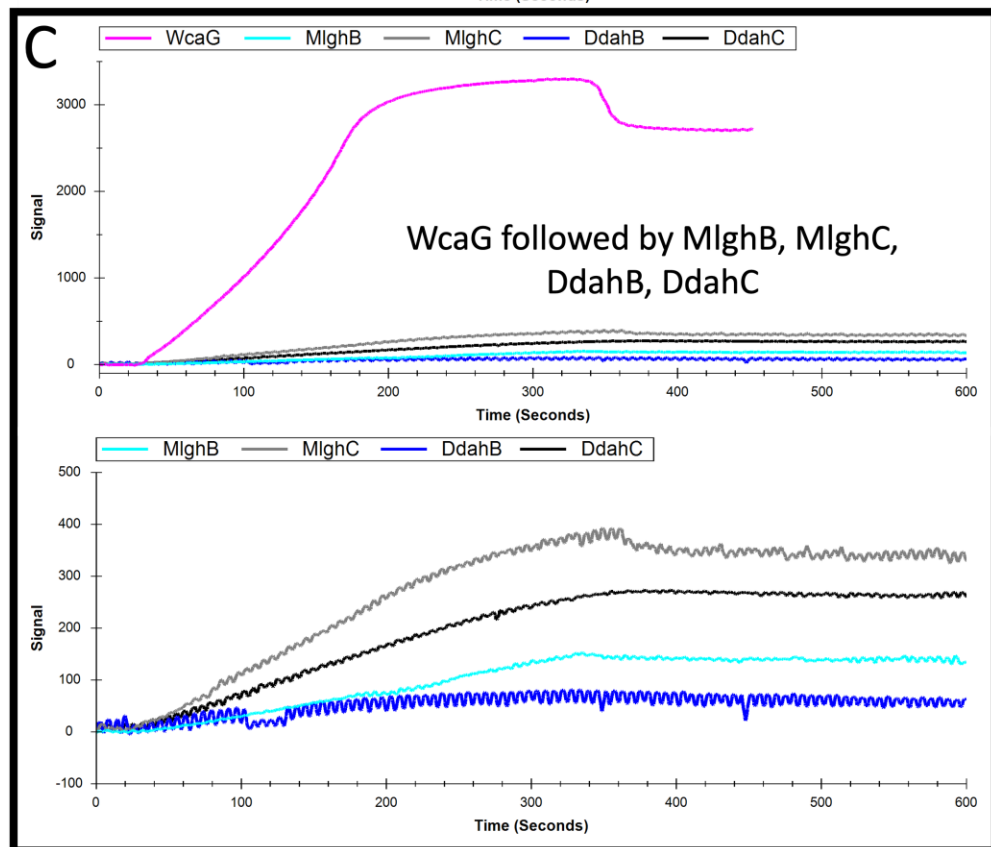
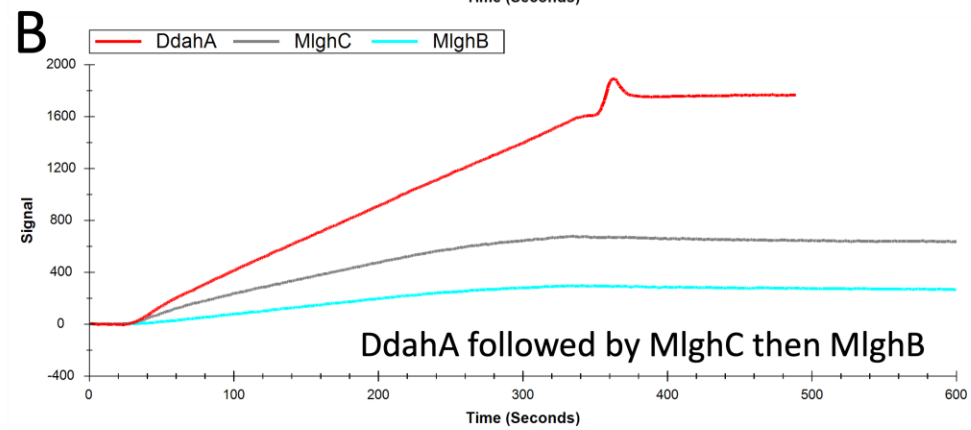
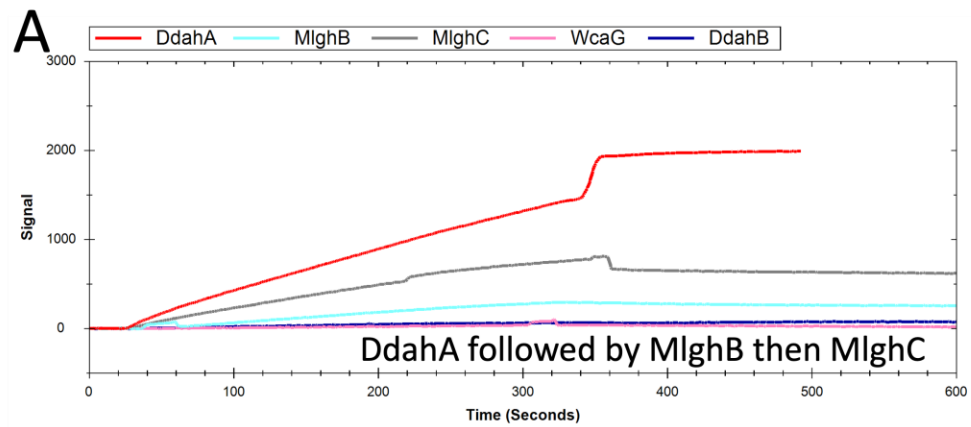
WcaG was eventually determined to be the 1st enzyme in the Mlgh pathway, thus studying the interactions of WcaG with MlghB/C represents the cognate pathway [57]. Also, McCallum et al. (2012) noted that the presence of WcaG was able to prevent normal heptose synthesis in the presence of DdahA, B, C, suggesting that WcaG might also interact with DdahB and C [96]. Here I used WcaG from strain 81-176 which expresses the Ddah enzymes, but it is 98% homologous to the WcaG found in NCTC 11168 which expresses the Mlgh enzymes and should therefore have very similar activity.

In figure 18, panel C, the first enzyme in the Mlgh pathway, WcaG, was immobilized. The immobilization of WcaG led to a higher signal than what was seen for DdahA. The cognate enzymes in the series (MlghB and MlghC) were injected as analytes before injecting DdahB and DdahC. Overall, smaller increases in signal were observed with WcaG compared with what was observed with immobilized DdahA. These injections revealed that the reductases (MlghC and DdahC) generally bound at higher levels than the epimerases (MlghB and DdahB) (figure 18C). This is clear for the Mlgh enzymes as MlghC lead to a higher increase in signal, despite being injected at a lower molarity (again MlghC is twice the size but injected at ~10x the concentration of MlghB). It is harder to draw definitive conclusions for the Ddah enzymes however, as DdahC both lead to a higher signal increase, was injected at a higher molarity, and is larger than MlghB. MlghC caused a higher increase in signal than DdahC though it was injected at only 1/6th of the DdahC concentration, and both proteins are of roughly the same size (Table 9). This may indicate that MlghC has a stronger interaction with WcaG, or that binding sites for DdahC were occupied by MlghC. MlghB only caused a small increase in signal although it was the first analyte and was injected at a high concentration. DdahB caused no discernible change in signal. Panel D in Figure 18 was essentially a repeat of panel C where WcaG was immobilized, with newly prepared MlghB (taken from the same expression stock, but glycerol was removed again). Though the rise in signal caused by analytes was generally quite low, the same trends seen in the previous run can be seen here: The reductases bound

with higher affinity than the epimerases (Figure 18C,D). Unlike the previous run, a small increase in DdahB signal was observed, at the same level as MlghB.

Kinetic analysis revealed the WcaG/MlghC complex had a K_D with an order of magnitude of 10^{-6} to 10^{-8} M, after the injection of MlghB (Figure 19C,D,F). As such, although MlghB had only bound minimally to WcaG, direct comparison cannot be made to the DdahA/MlghC complex, as MlghC was not the first analyte injected onto WcaG. It is however likely that the WcaG/MlghC complex is stronger than the WcaG/MlghB complex, with the latter having a K_D with an order of magnitude between 10^{-6} to 10^{-7} M (Figure 19C,D,F).

Figure 18, panel E detailed the immobilization of MlghB with MlghC and WcaG as analytes. MlghC led to an increased signal of about 300 units, while the subsequent WcaG injection caused no increase in signal. This indicates that MlghB is capable of interacting with MlghC, but does not interact very strongly with WcaG, as demonstrated in panel C. It also indicates that MlghC does not readily interact with WcaG once pre-engaged in interaction with MlghB. The MlghB/C complex had a K_D with a rough order of magnitude of 10^{-7} M, which was quite similar to the established DdahB/C complex, and these interactions seem stronger than the association of the WcaG/MlghB complex (K_D of 10^{-6} to 10^{-7} M) (Figure 19E,F).



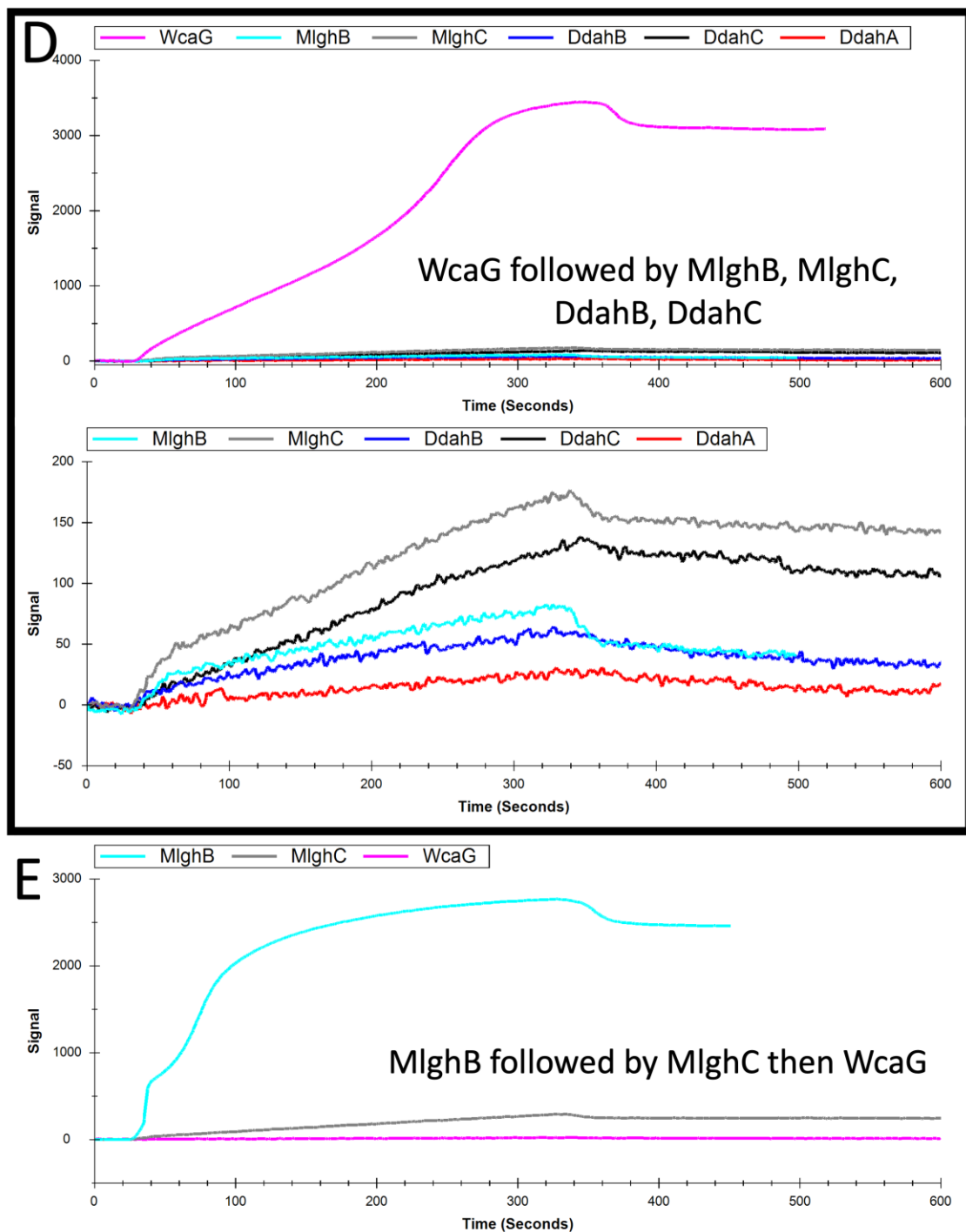
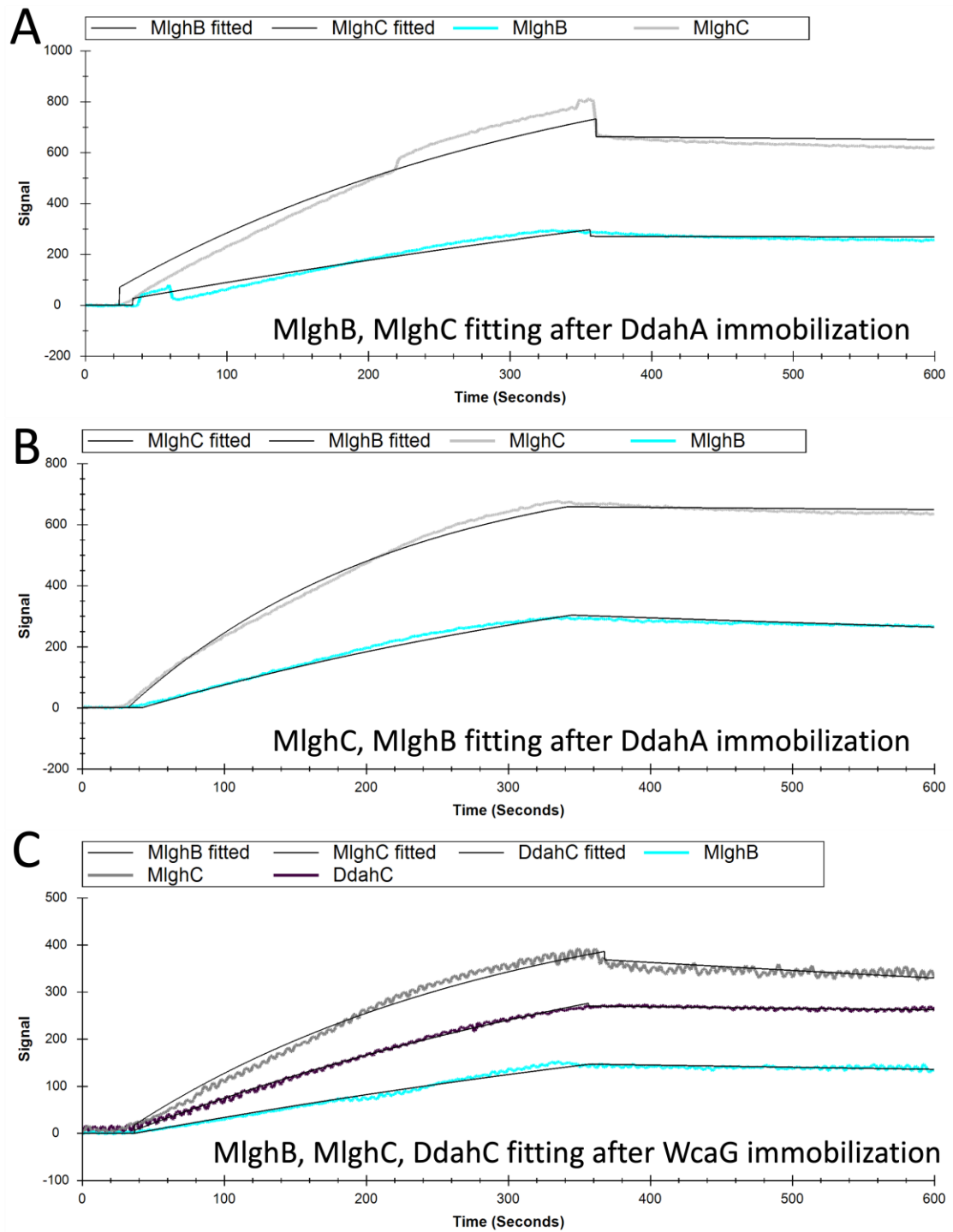


Figure 18: Tracedrawer outputs for SPR detailing interactions with MlghB and MlghC. (A) Injections of MlghB-1 and MlghC on immobilized DdahA. (B) Injections of MlghC and MlghB-1 on immobilized DdahA. (C) Injections of MlghB-1, MlghC, DdahB, and DdahC on immobilized WcaG. (D) Injections of MlghB-2, MlghC, DdahB, and DdahC on immobilized WcaG. (E) Injections of MlghC and WcaG on immobilized MlghB-2. All proteins had 200 μ L injected at a concentration presented in Table 9, with a 5-minute interaction time. All analytes were suspended in running buffer (1x PBS pH

7.4), while immobilized ligands were suspended in running buffer and then diluted $\frac{1}{2}$ in Nicoya activation buffer (to the concentrations presented in Table 9) immediately before injection. Immobilization and subsequent injection of analytes occurred in the same order as presented in the keys above the Tracedrawer outputs. The colours of the curves presented correspond to a specific protein and are consistent between panels



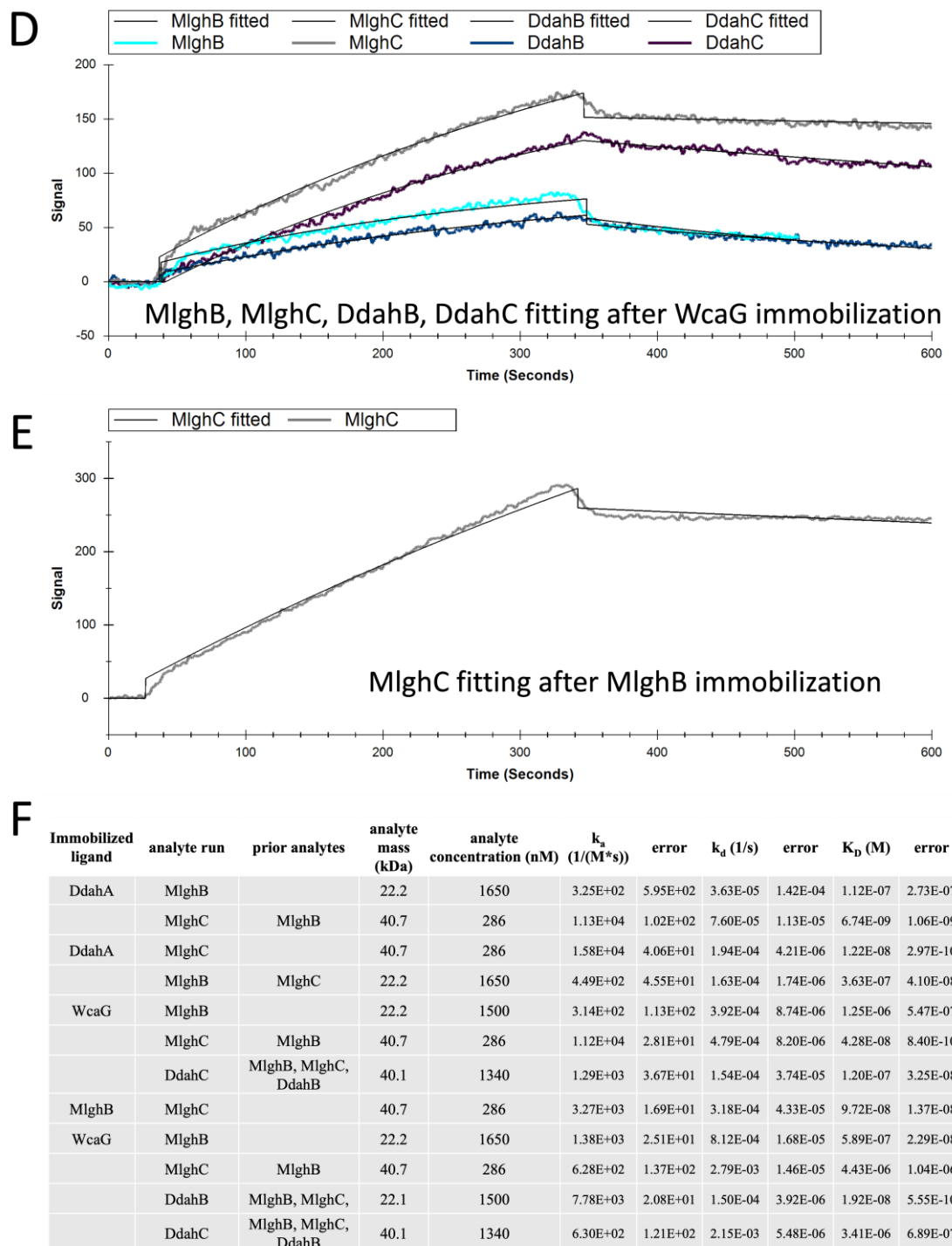


Figure 19: Attempted kinetic determination for the interaction of enzymes in the Mlgh and Ddah biosynthetic pathways.

(A) Injections of MlghB-1 and MlghC on immobilized DdahA. (B) Injections of MlghC and MlghB-1 on immobilized DdahA. (C) Injections of MlghB-1, MlghC, and DdahC on immobilized WcaG. (D) Injections of MlghB-2, MlghC, DdahB, DdahC, and DdahA on immobilized WcaG. (E) Injections of MlghC on immobilized MlghB-2. (F) Tracedrawer

output of kinetic constants based on curve fittings and defined analyte concentrations. Analyte concentrations seen in panels A-E can be found in panel F, with all analytes being injected at concentration according to Table 9. The buffer used in all experiments was 1x PBS pH 7.4, and all samples had 200 μ L injected with an interaction time of 5 minutes.

Taken as a whole, these data indicate that the reductase MlghC is able to interact with the first enzyme in the Mlgh or Ddah pathways more strongly than the epimerase MlghB (Figure 20A). This trend is also observed with immobilized WcaG for the Ddah homologs, with DdahC exhibiting greater binding than DdahB (though the higher concentration of DdahC may explain this). This is somewhat different from what was seen with the complete Ddah series where it was determined that interactions of any two enzymes hindered the interaction of the third. In Mlgh runs 1 and 2, MlghB and MlghC bound similarly to DdahA regardless of the order in which they were injected. As such, it is possible MlghB and MlghC bind to DdahA using different domains, allowing the formation of a multienzyme complex (Figure 20B). It is also possible they bound separately to unoccupied DdahA, without resulting in complete saturation (Figure 20D). Within the cognate Mlgh pathway, it appears that both MlghB and MlghC can bind to immobilized WcaG (or that WcaG was incompletely saturated by analyte), but WcaG is unable to displace preformed MlghB/C complex (Figure 18E, 20C,D,E). This may also be true for DdahA, but that injection order has not yet been tested.

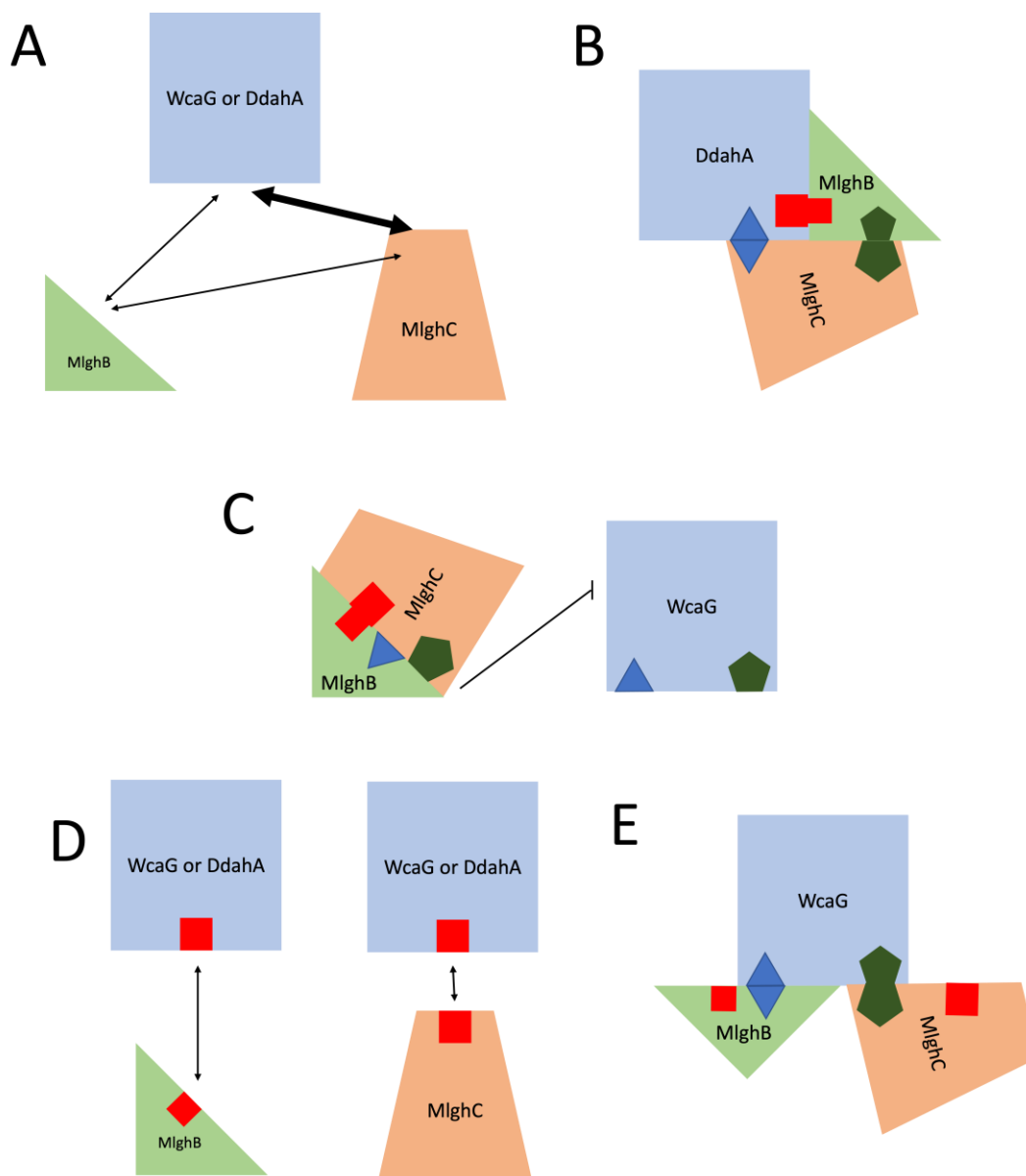


Figure 20: Proposed interactions between enzymes in the Mlgh pathway. (A) MlghC has been demonstrated to interact with WcaG, the cognate dehydratase in the Mlgh pathway, or DdahA, the initial oxidase in the Ddah pathway. MlghB, comparatively, interacts weakly with WcaG, DdahA, and DdahC. (B) MlghB and MlghC result in the same binding to DdahA regardless of injection order. As such, it is possible that all three interact in three enzyme complexes, binding using different domains. (C) WcaG is unable to effectively bind to MlghB or MlghC when these two enzymes are in complex. (D) MlghB and MlghC both interact with DdahA and WcaG, but it is possible that there was enough immobilized ligand to cause the first analyte to not saturate all possible binding sites. Thus, MlghB and MlghC may bind to multiple ligands instead of forming complexes with a single ligand, at the same time. (E) Theoretical configuration permitting MlghB and MlghC to interact with WcaG at the same time, while not permitting WcaG to bind to a preformed MlghB/C complex.

3.11 Microscale thermophoresis affirms formation of the DdahA/B complex

Like SPR, microscale thermophoresis (MST) is a technique that assesses binding between biomolecules. This technique works by placing fluorescently labelled, or intrinsically fluorescent, biomolecules in a temperature gradient, inducing thermophoresis. The movement of a protein across this gradient differs significantly from the movement of a protein–ligand complex, permitting the assessment of physical interactions [62]. This technique offers several benefits that complement my SPR work thus far. The first advantage is that MST studies interactions between molecules in solution and does not require the immobilization of a ligand as in SPR. This is beneficial as immobilization may alter the interaction characteristics, especially in cases using NTA chips, which will bind all proteins by the N-terminal His-tag. Additionally, because this work is conducted in capillaries and uses small volumes, I would be able to test the effect that the substrate has on modulating interactions efficiently, using much less than if it was added in an SPR experiment.

We have begun this work in collaboration with the Feuilloley group at the University of Rouen, Normandy (France). I have expressed and purified the capsular heptose biosynthesis enzymes, which have been sent to France for analysis. Work has been started to assess the interactions of DdahA and DdahB, as these were first shown to interact by SPR. In their experiments, DdahA was labelled with a fluorophore to allow detection by MST. Their work has affirmed the finding that these proteins interact, with initial runs using 25 nM DdahA and a starting concentration of 0.5 μ M DdahB, demonstrating an interaction with an estimated K_D of 623 nM (Figure 22A). Interestingly, when 0.1 mM of the substrate GDP-mannose was added, the K_D decreased over fivefold to 118 nM (Figure 22B). While GDP-*D-glycero-D-manno*-heptose is the preferred substrate of DdahA, it can catalyze GDP-mannose, indicating that the presence of substrate is important for stabilizing the interaction between these two enzymes. Since catalysis of this substrate is very slow, taking 3-5 hours under the conditions tested, and the MST experimental time frame is \sim 15 min, the simple binding of substrate affects the

interactions even in absence of significant catalysis. The reduction in K_D brought on by the presence of substrate gives more credence to the hypothesis of substrate channeling, as this process relies on binding between enzymes to allow for the transfer of pathway intermediates. Work is being continued to further characterize these interactions by MST, but protein aggregation within the capillaries must first be overcome.

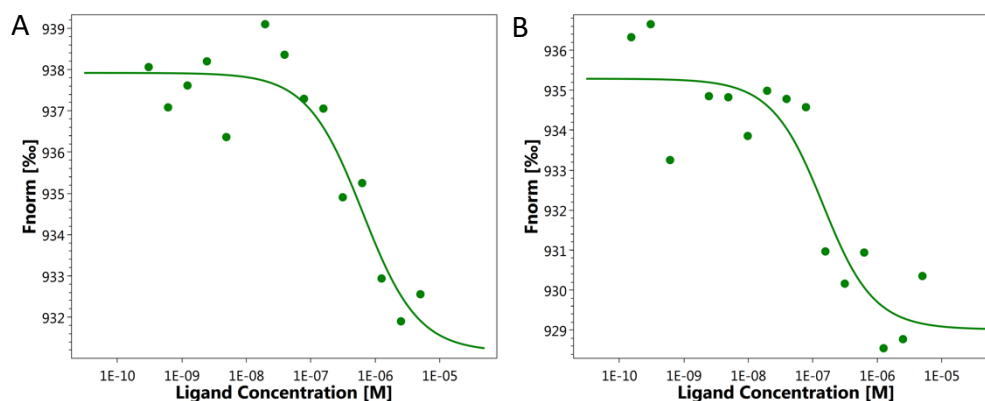


Figure 21: Microscale thermophoresis dose response curves assessing interactions between DdahA and DdahB. (A) In the absence of substrate or (B) in the presence of 0.1 mM GDP-mannose. The ligand concentration seen on the x axis refers to the concentration of DdahB present within a given capillary. A reduction in normalized fluorescence indicates an interaction between the analyte and ligand. DdahA was fluorescently labelled using the Monolith NT Protein Labeling Kit RED-NHS and was present in all capillaries at a concentration of 25 nM, suspended in 1x PBS pH 7.4. Graphs generated by Olivier Lesouhaitier and Florian Defontaine in the Feuilloley laboratory at the University of Rouen, Normandy.

Chapter 4

4 Discussion

4.1 *C. jejuni* NCTC 11168 capsular heptose in the activation of host macrophages

When looking at the activation by capsular heptose mutants, data indicate that the heptose is immunosuppressive to MQ-NCSU chicken macrophages, leading to significantly higher levels of nitrite induction when absent. Conversely, when the CPS was absent, lower levels of nitrites were seen, indicating that the CPS permits greater immunostimulation in this context. The heptose residue being slightly immunosuppressive aligns with the hypothesis of this study, which postulates that the heptose acts to diminish immune activation as a means to protect the bacteria. The CPS increasing immunostimulation was somewhat unexpected however, as capsules are structures often used by bacteria to evade the immune system, and structures that impair survival should be selected against. It is likely that the normal addition of this CPS has both beneficial and detrimental effects, and that these beneficial effects outweigh the detrimental ones, depending on the environment the bacterium is in. For example, expression of the *C. jejuni* CPS has been demonstrated to increase invasion of host epithelial cells, increase chicken gut colonization, and decrease sensitivity to serum killing in a strain specific manner [11,12,44,70,173]. These protective features are therefore selected for, at the cost of a slightly increased inflammatory response. Additionally, the CPS has been shown to be regulated by phase variation, indicating its expression can change based on the environment *C. jejuni* is in [46].

These trends in the nitrite induction were specific to live NCTC 11168, with heat-killed WT not resulting in detectable levels of nitrite. This is somewhat incongruent with current literature, which has shown that purified LOS, DNA, and outer membrane proteins from *C. jejuni* strain 81-176 induce nitric oxide in MQ-NCSU chicken macrophages [156]. These structures are however likely hidden, at least partially, by the CPS in both live and heat-killed bacteria. Currently, no studies have been conducted which implicate the *C. jejuni* CPS in nitrite induction, though the impact of the capsule

on other chicken macrophage effectors has been researched. An acapsular mutant of strain 11168H (a hypermotile derivative of *C. jejuni* NCTC 11168) demonstrated equivalent induction of IL-6 and IL-10 transcripts to WT in chicken bone marrow-derived macrophages, indicating that the CPS causes specific induction of NO, while not altering the expression of these cytokines [73]. Likewise, in the referenced study, a mutant lacking MeOPN backbone modifications demonstrated no difference in cytokine induction from WT. This indicates that differences in effector induction are either conferred by the modified heptose specifically, or that CPS modifications are specifically anti-inflammatory in the context of NO induction.

Unlike chicken macrophages, THP-1 macrophages showed little difference in effector induction between capsular heptose mutants. Several cytokines were tested by either in-house ELISA, or an external cytokine multiplex assay. These two assays gave quite similar results. The in-house ELISA looked at TNF α production and found no differences between WT and mutants, with the exception of the 12-hour time point. Here, the acapsular mutant exhibited lower levels of TNF α induction than WT, indicating that the CPS is immunostimulatory at this time, as with the MQ-NCSU cells at 5 hours. However, the cytokine multiplex did not show a difference between WT and mutants in the induction of the proinflammatory cytokines IL-1 α , IL-1 β , IL-6, IL-8, IL-12p40, IL-18, and TNF α or the anti-inflammatory cytokine IL-10. As this difference in TNF α induction caused by the acapsular mutant was only seen at one time point in the ELISA, and was not recapitulated in the multiplex, it is most likely that the capsular heptose and CPS do not greatly impact cytokine induction by *C. jejuni* NCTC 11168, in THP-1 human macrophages. This is not in line with the initial hypothesis, indicating that the capsular heptose does not play a protective role in the moderation of cytokine production within these cells. Similar results were found in the closely related strain 11168H where both an acapsular mutant and a mutant lacking MeOPN caused equivalent IL-6 and IL-10 expression to WT in human bone marrow-derived macrophages [73]. Conversely, the CPS does seem to be immunomodulatory with regards to strain 81-176, with an acapsular mutant resulting in greater TLR2 and TLR4 signaling in reporter THP-1 cells than WT [92]. This would indicate that, in this strain, the CPS is protective, lowering signaling that

leads to a proinflammatory response and as such the *C. jejuni* CPS is immunomodulatory, but in a strain specific manner. The *C. jejuni* strain 81-176 CPS is likely acting to protect against the presentation of other immunostimulatory surface components such as LOS, which has previously been demonstrated to induce TNF α in THP-1 cells [149].

It should be noted that control experiments were conducted to ensure the validity of the induction experiments. The MOI experiment was conducted to find an acceptable range of MOIs that could be used when analyzing effector induction, ensuring that slight variability in MOI between replicates did not greatly alter the data or confound the results. Likewise, the LDH release assay was conducted to assess macrophage cytotoxicity, which has the potential to impact effector induction. High death (denoted by a marked increase in LDH release) may result in low effector induction, due to killing before sufficient production, or higher effector induction caused by damaged cells releasing proinflammatory factors. Generally, WT *C. jejuni* and the capsular heptose mutants did not confer cytotoxicity when co-cultured with chicken macrophages. Human THP-1 macrophages also tolerated *C. jejuni* quite well, with no mutant or WT causing significantly greater LDH release than the macrophage only background, though LDH levels were slightly higher in all samples containing bacteria. Similar results were found by Bouwman et al. (2014), in which tested strains (not including strain NCTC 11168) of *C. jejuni* caused inflammasome formation but did not confer cytotoxicity in mouse J744.A1 macrophages [21].

One major limitation of the Griess assays and the ELISA/ cytokine multiplex is that they prohibit direct comparison between host cell lines. As stated, the Griess assay could not be used on THP-1 macrophages due to the fact that they are not potent producers of NO, and when tested, nearly all samples were below the threshold of detection [29,42,117]. Likewise, TNF α ELISAs could not feasibly be conducted on MQ-NCSU cells as these cells lack a functional TNF α gene, making it impossible to compare induction. While there are ELISA kits for the chicken homologues of other cytokines tested, they are prohibitively expensive. Therefore, to directly compare between human and chicken macrophages in their activation by *C. jejuni*, ROS induction was assessed using a fluorescence assay, and effector transcript induction was assessed by qRT-PCR.

The ROS induction assays demonstrated that *C. jejuni* NCTC 11168 diminishes intracellular ROS induction in both chicken and human macrophages in as little as 30 minutes, and that this activity was not impacted by the presence of the capsular heptose or the CPS. This trend was most notable in THP-1 macrophages, which had higher background levels of ROS, likely due to PMA differentiation. Mirroring my work, a 2022 preprint by Hong et al. indicates that *C. jejuni* moderates intracellular ROS induction in human intestinal epithelial cells [55]. They noted that co-cultured *C. jejuni* (strains 11168H, 81-176, and 488) resulted in a reduction of intracellular ROS after 3 and 24 hours. RT-qPCR data from the same study indicates that *C. jejuni* is causing a decrease in the transcription of NADPH oxidase Nox1, which acts to produce NO. Though initially thought to be caused by bacterial sequestration of active DCF, or a decrease in macrophage membrane permeability, a change in Nox1 production is likely the cause for the reduction in DCF found in macrophage supernatants after co-culture with NCTC 11168. It should be noted that while Hong et al. report a difference in intracellular ROS specifically, they are essentially conducting the same assay used in this thesis. In their assay, cells were co-cultured and then DCF was added, with a reading taken of the total well: cells + DCF containing supernatant. I however, read the supernatant and cell fractions separately and noted most of the signal observed was found in the supernatant. Again, it should be noted readings from the supernatant still represent a measure of intracellular ROS, as DCF-DA must be converted to DCF within the cell. As such, it appears that *C. jejuni* can downregulate intracellular ROS production in host cells (both human and chicken). Hong et al. did note strain specific differences in the measurement of extracellular H₂O₂, indicating that overall, the ability to moderate ROS production is likely strain specific. While the CPS did not impact the ability of *C. jejuni* to moderate host ROS induction, we are the first group to study the *C. jejuni* CPS in this context. Additionally, we are the first group to characterize a reduction of ROS induction by *C. jejuni* in host macrophages.

There is a clear difference between how *C. jejuni* deals with oxidative and nitrosative stress. As demonstrated, live NCTC 11168 causes NO induction in chicken macrophages, but decreases ROS levels relative to baseline in host macrophages. Induction of toxic

ROS compounds is reduced through the downregulation of Nox1, effectively protecting the bacteria before the active compound is produced [55]. This is likely because, as a microaerophile, *C. jejuni* is ill equipped to deal with oxidative stress after it arises. It is currently unknown how Nox1 transcriptional downregulation is mediated. When dealing with nitrosative stress however, it appears that *C. jejuni* uses a different tactic to protect itself, expressing proteins to combat NO, while still causing NO induction. These factors are CgB, a globin that is produced to efficiently neutralize NO that has entered the cytoplasm, and NrfA, a periplasmic reductase that acts on both nitrites and NO directly [39,119]. Interestingly, CgB is induced upon NO/nitrite stress specifically, and is not produced in response to superoxide [39]. NrfA conversely, is constitutively expressed and neutralizes its substrates by catalyzing reactions that produce ammonium ions and water [119].

Work assessing effector transcription by qRT-PCR, while quite preliminary, did generate interesting results. WT *C. jejuni* NCTC 11168 increased the transcription of IL-1 β , IL-6, IL-8, IL-10, and TNF α by a factor > 2 at nearly all time points tested between 0.5 and 3.5 hours in THP1 macrophages. Additionally, these early times of co-culture were chosen to determine when *C. jejuni* causes consistent transcript induction as literature indicates LPS significantly upregulates many transcripts within 1-4 hours of exposure to THP-1 cells [27,135]. The increase in transcription seen is consistent with literature, as bone marrow derived macrophages also displayed increased IL-6 and IL-10 transcription after 3 hours of co-culture with strain 11168H. At the effector level, co-culture of NCTC 11168 with THP-1 macrophages has been shown to upregulate secretion of IL-1 α , IL-1 β , IL-6, IL-8, and TNF α over 24 hours [63]. This indicates that increased transcription should have occurred, seen in as little as 30 minutes with my study. It should be noted that the data presented in Supplemental Figure 1 consists of only a single biological replicate, however. My data indicate that if qRT-PCR work is continued, it may be beneficial to compare transcript induction between capsular mutants at 2.5 hours of co-culture, due to all cytokines tested having increased transcription > 2 fold at this time point.

As noted in the results section, the transcription of effectors in MQ-NCSU macrophages was harder to assess due to issues with the qRT-PCR. Consistent Cts were unable to be

generated between equivalent samples, and often no Cts were given, not only for the cytokines tested in untreated samples, but also when looking at housekeeping genes and transcription within co-cultured macrophages. While a lack of Cts may indicate that there is little effector induction, several things point to this not being the case. The first is that if housekeeping gene expression is not seen or is inconsistent, there is more likely to be an issue with the PCR than a lack of appropriate transcript. Additionally, previous literature has demonstrated that MQ-NCSU cells upregulate the transcription of IL-6, IL-8, IL-10, IL-12, and iNOS within 8 hours of exposure to *C. jejuni* strain 81116 (109). These cells have also demonstrated increased transcription of IL-1 β , IL-10, IL-18, IFN γ , CXCLi2, and iNOS in response to campylobacter-derived ligands after 2-18 hours, dependent on the cytokine (110). It is apparent that these cells are likely to increase effector transcription in response to being challenged with *Campylobacter*. Several things were attempted to solve the issue of inconsistent Cts, including increasing the number of cells used, increasing the amount of RNA reverse transcribed, and increasing the amount of cDNA used in qPCR. My most recent work using this technique saw stabilization and consistency within Cts when cDNA was diluted by a factor of 3 or 9. These dilutions likely reduce the concentration of inhibitory contaminants in any reaction, permitting better replication. As such, if this work is continued, cDNA generated from both MQ-NCSU and THP-1 macrophages should be diluted before qPCR. These findings will help in comparing effector induction between mutants and between host cell lines. Additionally, if qRT-PCR studies are continued in the lab it may be interesting to also assess Nox1 expression to see if it correlates to the reduced supernatant fluorescence seen in the ROS assay.

Another way of assessing macrophage activation could be through looking at the activity of NF- κ B, a key pro-inflammatory transcription factor in macrophages. One way to measure NF- κ B indirectly is to assess the relative levels of its inhibitor I κ B α , which is degraded upon a proinflammatory signalling (such as TLR stimulation) to permit NF- κ B translocation to the nucleus. Therefore, decreases in I κ B α levels correspond to an increase in NF- κ B activity. This could be assessed in both human and chicken macrophages by conducting western blots on cell lysate. A loading control such as beta

actin would be required, and relative levels of I κ B α in macrophages alone, or those co-cultured with *C. jejuni*, could be assessed by densitometry.

One limitation of this study, beyond the lack of direct comparison between host responses, is the use of cell lines. Cell lines, while useful, are considered to be less translatable to *in vitro* infection than primary cells. Therefore, it may be interesting to attempt to recapitulate the findings of this study with bone-marrow derived macrophages or peripheral blood mononuclear cells. Particularly, what was seen with NO release, as this indicates that both CPS and heptose play a role in the nitrite induction from chicken cells. In addition to testing primary chicken macrophages, primary human macrophages may show differential NO release, which could not be studied in THP-1 cells due to their low NO production. While it could also be interesting to assess cytokine release in human primary cells, no notable phenotype was seen with THP-1 cells, making it unlikely to see a phenotype with primary cells. Still, THP-1 cells do express receptors differentially to primary cells, being known to be much less responsive to bacterial components such as LPS [20].

As a whole, this activation data indicates that the capsular heptose plays a protective role in the induction of NO from chicken macrophages, but does not impact human macrophage cytokine induction or host macrophage ROS induction, under the conditions tested.

4.2 *C. jejuni* NCTC 11168 capsular heptose in interactions with host macrophages.

Data presented indicate that the CPS and capsular heptose modify interactions of *C. jejuni* with host macrophages, though not according to the proposed hypothesis. I hypothesized that the capsular heptose would be protective, resulting in diminished adhesion to and uptake by the host macrophage, while increasing the intracellular survival of *C. jejuni* that were internalized.

Looking at the adhesion of *C. jejuni* to host macrophages and monocytes, it was observed that there were no statistically significant differences between WT and any mutant

lacking the heptose, indicating that the heptose does not significantly impact adhesion to host macrophages. The MlghB and MlghC knockout mutants did have decreased adhesion to THP-1 monocytes, indicating that normal expression of these genes may slightly increase bacterial adhesion to the host monocyte membrane. qPCR conducted by Wong et al. indicates that these two mutants upregulate the expression of *cj1429* by > 18-fold, which may be the cause of these phenotypes as the function of this unknown gene may alter other surface properties in these mutants [173]. Additionally, the presence of the CPS diminished adhesion to chicken, but not human, macrophages. Interestingly, when viewed with other presented data, the CPS diminishes adhesion but results in increased NO release from MQ-NCSU macrophages. In line with the behaviour of chicken macrophages, the absence of the CPS has been shown to increase adhesion to Caco-2 cells relative to WT [173]. The magnitude of this phenotype is much larger for Caco-2 cells than MQ-NCSU cells, with the KpsM mutant binding at roughly 600% and 400% compared to WT in each cell line, respectively. This work also demonstrates that the presence of the capsular heptose does not impact adhesion to either human Caco-2 intestinal epithelial cells or murine Raw 267.4 macrophages [173].

The increased binding of the acapsular KpsM mutant may occur for several reasons. The first reason is that the lack of the capsule increases exposure of other surface factors. These factors may bind scavenger receptors on the host macrophage cell surface, promoting adhesion. Many bacterial adhesins are also likely to have greater exposure to the environment, further permitting *C. jejuni* to bind to the host cell. Finally, the KpsM mutant has been demonstrated to have increased agglutination due to the exposure of adhesins, so it is possible that clusters of bacterial cells are binding to the host membrane, increasing the number of adherent bacteria enumerated [173].

It should be noted that many controls were used to ensure the validity of the phagocytosis assays. To ensure that the inoculum of each mutant was consistent with the inoculum of the WT, input suspensions were spot-plated and enumerated. Statistical analysis revealed that the inoculum of any mutant did not differ significantly from WT, in all assays conducted. Likewise, samples of co-culture supernatants were taken to examine if co-culture conditions (media alone or in the presence of macrophages/monocytes) impacted

bacterial viability. In no assay did any mutant differ between their initial inoculum and the CFU concentration found in the co-culture supernatants. This ultimately indicates that phenotypes observed are due to the functioning of the bacteria and not a difference in inoculum, or a change in bacterial viability. Macrophage cytotoxicity should also not be a confounding factor as seen with the LDH assays conducted when assessing activation.

One comment about this assay is that it may be beneficial to further limit internalization beyond what was done with the current methodology. Here, adherent bacteria were enumerated by co-culturing at 4°C, which should limit cytoskeletal rearrangement. This, however, is likely to be more effective in cells that are not professionally phagocytotic, as these cells have much lower phagocytic capacity than macrophages. As such, it may prove useful to further limit internalization using a chemical inhibitor such as dynasore. This inhibitor targets dynamin, a GTPase involved in clathrin mediated endocytosis, and internalization during phagocytosis [121]. While the addition of dynasore may be a refinement, no phenotype was observed in the presence or absence of the capsular heptose under the conditions tested in several cell lines, making the addition of dynasore unlikely to yield positive results. Additionally, similar methodologies to that used in this study are present in literature, demonstrating a great decrease in the internalization of bacteria by host macrophages and neutrophils at reduced temperatures [118,173].

Assessment of uptake by host macrophages revealed that the production of the CPS is protective to strain NCTC 11168, in that it decreases uptake by THP-1 macrophages. Conversely the addition of MeOPN is detrimental, causing higher uptake when produced in high quantities. The trend of elevated uptake for mutants with increased MeOPN addition, or diminished CPS, was also seen in the THP-1 monocytes and MQ-NCSU chicken macrophages, though significance was not achieved. Finally, the MlghB and MlghC mutants displayed roughly 1 log lower uptake by MQ-NCSU macrophages compared to WT after 3 hours, again indicating that the upregulation of *cj1429* may be protective in this context. While it was hypothesized that the capsular heptose is protective, decreasing uptake, it is now apparent that the CPS and addition of MeOPN that alter these interactions, specifically in human macrophages.

For Raw 267.4 murine macrophages, it was found that the acapsular KpsM knockout mutant was taken up at significantly higher levels than WT, indicating that the capsule generally decreases internalization by host macrophages [173]. No differences in Raw 267.4 uptake were seen for the other mutants tested, contrasting the finding that increased presentation of MeOPN augmented uptake by human macrophages. This, compounded by the difference in overall trends, indicates there is likely a degree of host specificity in how macrophages respond to *C. jejuni* expressing a modified capsule. Intriguingly, the MlghB and MlghC knockout mutants were unable to invade human intestinal epithelial cells, paralleling the 1 log reduction in uptake by chicken macrophages [173]. Uptake by these cells was also significantly increased in WcaG and WcaG Δ mutants, mirroring the phenotype exhibited by human macrophages. However, the acapsular mutant demonstrated the greatest uptake in human intestinal epithelial cells, while never surpassing uptake of WcaG Δ in human or chicken macrophages.

Data presented also affirm what was established with strain 11168H in human and chicken bone marrow derived macrophages. In this strain, when MeOPN synthesis is inhibited, both human and chicken macrophages exhibited decreased bacterial uptake [73]. This mirrors the increased uptake of the WcaG mutant by THP-1 macrophages, which produces a high abundance of MeOPN containing CPS, where WT does not. However, while the lack of the NCTC 11168 CPS resulted in a notable rise in uptake of all cells tested, the loss of the 11168H CPS did not alter uptake of this strain by host macrophages. This may be due to the fact that 11168H CPS contains MeOPN, while the NCTC 11168 CPS is devoid of it (though it possesses the machinery to produce and add MeOPN, as demonstrated in the capsular heptose mutants). The loss of the protective CPS may be balanced out by the loss of the detrimental MeOPN, creating WT-like output.

When looking at intracellular survival, data from the KpsM mutant indicates that the *C. jejuni* NCTC 11168 CPS decreases bacterial survival in both human and chicken macrophages, with this finding being specific to the earlier 1-hour time point for THP-1 cells. The increased survival of the WcaG Δ knockout mutant, which has lower CPS

expression than WT, mirrors this. The MlghB and MlghC mutants had diminished uptake by MQ-NCSU cells, but WT-like enumeration in the survival assay. This potentially indicates knockout of these genes (or the increased expression of *cj1429*) decreases both uptake and killing, causing this WT-like enumeration. THP-1 monocytes behaved similarly in the survival assay, with the MlghB and MlghC knockout mutants having a ~1 log reduction in survival at the later 3-hour time point.

As with the uptake assay, differences were seen from what was previously established with murine macrophages, pointing to host specificity in the clearance of *C. jejuni*. The CPS displayed no ability to modify bacterial survival within Raw 267.4 cells, but diminished survival in human and chicken macrophages [173]. Likewise, capsular modifications were shown not to impact survival in murine macrophages, while the expression of MlghB and MlghC insignificantly altered the survival within human monocytes. Strain NCTC 11168 was shown to survive somewhat differently compared to strain 11168H. The 11168H capsule does not affect survival within chicken bone marrow derived macrophages, but was shown to diminish survival in human bone marrow derived macrophages 3 hours after gentamicin treatment [73]. In line with my findings however, a lack of MeOPN did not notably impact survival of 11168H in human or chicken macrophages, and the highly MeOPN expressing WcaG mutant did not display altered survival compared to WT in tested human or chicken macrophages.

The overall trends of the acapsular KpsM mutant in chicken macrophages are interesting, as this mutant displayed significantly elevated levels of adhesion and survival, but only a trend of increased uptake. The elevated adhesion likely leads to increased uptake, which in turn leads to increased enumeration during the survival assay. The difference between the WT and KpsM mutant is most notable in the survival assay however, with the difference in CFU/mL output being roughly 2 logs at the 3-hour time point. This indicates that the lack of a CPS confers a significant advantage within these cells. While not expected, with capsules typically providing resistance to phagocytosis, there are reasons why this would occur. Increased survival may arise because the lack of a CPS increases aggregation of the KpsM mutant. These bacteria could then bind in higher numbers due to clumping but have higher survival due with aggregates being less

accessible to the cytotoxic components produced by the host macrophage. Data presented also demonstrate that MQ-NCSU cells produced less NO in response to the KpsM mutant than WT. As NO is an antimicrobial compound, logic holds that a significant reduction in NO production would confer an increase in intracellular survival. Additionally, the lack of NO production in THP-1 macrophages may indicate why increased survival of the KpsM mutant was not seen at the later time point tested.

One interesting future direction for this study would be the development of a *cj1429* knockout mutant. As demonstrated, the MlghB and MlghC knockout mutants lead to notable, though insignificant reductions, in adhesion to and intracellular survival in THP-1 monocytes, and uptake by MQ-NCSU macrophages. These mutants both upregulate *cj1429* transcription, a presently uncharacterized gene that is thought to be involved in capsular biosynthesis due to its placement within the NCTC 11168 genome [30].

Generating a knockout mutant of this gene, as well as potential double knockouts in the *mlghB/C* mutants that upregulate its transcription, may be beneficial for several reasons. Firstly, it may permit characterization of this gene, allowing study of how its expression alters the production and composition of the CPS. Secondly, it will allow for comparison both to WT and other mutants in the assays presented within this thesis. This would create an understanding of how altered *cj1429* transcription affects the virulence of NCTC 11168 and impacts the behaviour of the currently characterized mutants.

A limitation common to the phagocytosis assays is the lack of endogenous opsonins during co-culture. Opsonization is a process in which microbial surfaces are coated with host factors to better permit recognition and phagocytosis by immune cells [158].

Opsonization increases the sensitivity of host macrophages to pathogens, and as such greatly increases the rate of phagocytosis. Therefore, if opsonization is differential between WT *C. jejuni* and capsular heptose mutants, the phagocytosis of these bacteria may differ from non-opsonized conditions. Adding opsonins to the phagocytosis assays may not only display more notable or differential trends from what was observed, but could also convey how the CPS and capsular heptose impact resistance to opsonization. One technique to permit opsonization would be to incubate *C. jejuni* in media containing heat-inactivated autologous serum (human or chicken depending on the cell line) before

co-culturing with host macrophages [103]. Another method would be to coat *C. jejuni* with a nonspecific lectin and then use an anti-lectin antibody as an opsonin. This works as the Fc (fragment crystallizable) portion of a given antibody can be bound by Fc receptors on host macrophages, acting as an opsonin [158]. As such, opsonization may be an interesting next step in this study.

In addition to enumerating mutants to assess differences in phagocytosis, a potential future direction would entail tracking the phagocytosis of *C. jejuni* by host macrophages using fluorescence microscopy. Using labelled *C. jejuni*, as well as LysoTracker staining coupled with immunostaining of host cell lysosome-associated protein 1 (LAMP-1), the localization of bacteria within mature, acidic phagolysosomes can be determined [41]. Differences in compartmentalization would occur most likely with the acapsular mutant, being the one to display differential intracellular survival most notably. *C. jejuni* could be labelled with eFluor-670 dye to not only visualize the bacteria, but also to assess proliferation within the host macrophage. This dye is diluted as cells divide, providing an indication of proliferation. No significant differences in survival were seen between the 1- and 3-hour time points of the intracellular survival assay for any mutant, indicating little death between these time points. *C. jejuni* strain 81-176 has previously been shown to survive within human epithelial cells by avoiding trafficking to the lysosome, though human and chicken macrophages have demonstrated *C. jejuni* clearance within 24-48 hours [108,167,168].

Overall, significant differences between capsular heptose mutants and WT indicate that the NCTC 11168 CPS acts to diminish adhesion to and survival within chicken macrophages. The CPS also diminishes uptake by human macrophages, as well as survival early after internalization. Additionally, increased presentation of MeOPN to the CPS increases uptake by human macrophages.

4.3 Capsular heptose biosynthesis enzymes are able to interact physically

Data presented indicate that enzymes within, and between, the Ddah and Mlgh pathways are able to interact physically. SPR interactions between DdahA, B, and C indicate that these three enzymes can interact in a pairwise manner, but the binding of any two of these enzymes limits the binding of the third. The higher the signal obtained in the interactions between the DdahA/B complex, the less DdahC could bind when subsequently injected. Likewise, the formation of the DdahA/C or DdahB/C complex completely prevented a rise in signal when the third enzyme was injected. This was likely the result of much higher DdahC concentrations saturating the analyte, however, this still demonstrates the lack of displacement when the third cognate enzyme is injected. The DdahA/C complex seemed to be the most stable with an estimated K_D value at an order of magnitude of 10^{-9} M, compared to 10^{-8} M for the DdahA/B complex and 10^{-7} for the DdahB/C complex. This likely indicates that these three enzymes bind using a common domain, so that when two enzymes interact, their binding domains are hidden from the third enzyme.

Interactions within the Mlgh pathway again revealed that all three enzymes, WcaG, MlghB, and MlghC, can interact. Here it appeared that the initial oxidase WcaG was able to bind tighter to the final enzyme MlghC than to MlghB, with K_D values in the orders of 10^{-6} to 10^{-8} M and 10^{-6} to 10^{-7} M respectively. MlghB also bound to MlghC with an estimated K_D in the order of 10^{-7} M, with a WcaG injection not causing a rise in signal after the formation of the MlghB/C complex. Data provided also demonstrate binding between DdahA and MlghB or MlghC, with stronger interactions seen with MlghC (estimated K_D of 10^{-8} to 10^{-9} M compared to 10^{-7} M for MlghB), following the trends demonstrated with WcaG. DdahB and DdahC demonstrated interaction with WcaG, with DdahC exhibiting higher binding. This finding is harder to draw conclusions on however, as DdahC was injected at higher concentrations and has a greater mass, with both enzymes added after MlghB and MlghC already bound to the ligand. Overall, this work demonstrated that the epimerase MlghB interacts weakly with the initial enzyme in either series and with MlghC, relative to the interactions seen between DdahA or WcaG and the ultimate reductase MlghC. It appears likely that MlghB and MlghC are able to bind to DdahA at the same time. As such, it is possible that these three enzymes form a complex

together, in which each interacts using a unique set of binding domains (Figure 20B), or that MlghB and MlghC formed separate complexes (Figure 20D). This is also possible for the oxidase WcaG, either binding MlghB and MlghC at the same time, or forming separate pairwise complexes. It was demonstrated that WcaG cannot effectively displace the MlghB/C complex at the concentrations tested (Figure 20C), and thus if a tripartite complex forms on WcaG, it would have to be in an orientation that does not permit the direct interaction between MlghB and MlghC, as seen in Figure 20E.

Data from the Ddah pathway may seem to conflict with the proposed hypothesis that these enzymes interact in order to engage in substrate channeling, thereby protecting pathway intermediates. In this pathway, there was not a trend in tighter interactions, or decreasing K_D values following the sequential order in which these enzymes modify the precursor heptose. The DdahA/B and DdahA/C complexes were stronger than the DdahB/C complex. Additionally, data demonstrates that, under the conditions tested, the addition of the third enzyme to the pairwise complex of any two other enzymes does not cause great displacement. However, it should be noted that the substrate was not present in these analyses, which may greatly impact the flow of product between enzymes. For example, the DdahA/B complex may have high affinity in the presence of the DdahA product GDP-6-deoxy-4-keto-D-*lyxo*-heptose, but when acted on by DdahB to form GDP-6-deoxy-4-keto-D-*arabino*-heptose, affinity may decrease, permitting the formation of the DdahB/C complex. This may also be the case in the Mlgh series, with the WcaG/MlghB and MlghB/C complexes having K_D values with the same order of magnitude, in the absence of substrate. As such, it will be beneficial to study interactions in the presence of substrate. Masters' student Brian Yang has been working diligently to produce the precursor sugar GDP-D-*glycero*-D-*manno*-heptose, though a high yield stock has not been generated as of writing this section. Until then, a surrogate sugar GDP-mannose can be used in interactions, though it is not the preferred substrate and is catalyzed much slower than GDP-D-*glycero*-D-*manno*-heptose. This could however provide the opportunity to preload the substrate onto the ligand prior to immobilization, allowing assessment of how its presence (with limited catalysis) impacts interactions between enzymes.

The finding that the reductases (DdahC and MlghC) can interact with WcaG gives credence to a thought proposed in the article where these enzymes were first characterized. Here it was hypothesized that WcaG and DdahC are able to interact in some way, as the addition of DdahC to a reaction mixture greatly increased the activity of WcaG, independent of the amount of product produced by DdahC [96]. As such, it is possible that even though the reductases are not sequential to the WcaG oxidase in the reaction pathway, the presence of DdahC or MlghC increases flux through the oxidase. This may result from an interaction between enzymes causing some conformational change, or stabilizing interactions between WcaG and the epimerases, further permitting channeling. This would be beneficial in strain NCTC 11168 as it would result in greater 6-O-Me-L-*gluco*-heptose production. In strain 81-176, increased flux through WcaG would result in a higher production of heptose with a 6-hydroxy moiety, the proportions of which have not been quantified relative to 6-deoxy-D-*altro*-heptose.

There were some limitations to this study that caused analysis to be mostly qualitative. As noted in the results section, many solutions were used in an attempt to regenerate, stripping analyte from ligand. Because of incomplete ligand regeneration or loss of analyte activity, separate chips were used in an attempt to derive kinetic data. At most, three dilutions of the analyte resolved proper signals, meaning accurate determination could not be completed. While more runs can be conducted with carboxyl chips, which covalently immobilize the ligand, they are not ideal as the ligand cannot be uncoupled, meaning the chip can only be used once. As such, many chips are needed to attain adequate data, especially noting that ligand immobilization is not always consistent between experimental runs, despite proteins coming from the same stock.

One way to get more use out of the sensor chips, thereby decreasing costs and increasing feasibility, is switching to the nickel affinity chips (NTA chips). These chips permit the non-covalent immobilization of His-tagged proteins via the interaction of the His-tag and nickel bound to the chip. Nickel can be stripped by chelation with EDTA and thus these chips can potentially be reused. As noted, however, all of the enzymes purified and tested by SPR have been His-tagged, meaning they cannot be used as analytes, because they

would compete for binding to the chip with any ligand. One way to deal with this is by developing constructs with TEV-cleavable His-tags, permitting non-tagged analytes to be used. Currently, the Creuzenet lab possesses TEV-cleavable DdahB and MlghB (previously generated by Heba Barnawi [15]), meaning that an SPR experimental next step will be the immobilization of HIS-tagged DdahA or DdahC, flowing over cleaved DdahB. These three enzymes showed strong, clear interactions, and as such will be the first targets from proper kinetic determination. The TEV cleavable DdahB construct has an extra methionine and serine residue on its N-terminus compared to native DdahB, but this should have little impact on the interactions seen due to the relatively small addition at the end of the protein. Additionally, the His-tags, which are much larger than the MS sequence, still permit the interactions seen by SPR. A similar experiment can be performed using the immobilization of HIS-tagged DdahA or DdahC, flowing over cleaved MlghB. I have also begun work to insert TEV cleavage sequences into the other Ddah and Mlgh series enzymes, as well as remove the DdahB-TEV MS residues. No success was obtained despite repeated attempts using primers and methods previously reported [15,86]. To move forward, complementary primers were designed following instructions for Aligent QuikChange II Site-Directed Mutagenesis [3], and PCR is currently underway by Honours thesis student Mahmoud Mahmoudpour.

In addition to attempting further analysis by SPR, it will be beneficial to confirm interactions using other biochemical techniques such as gel filtration chromatography, and analytical ultracentrifugation. In gel filtration chromatography, enzymes are passed through a gel filtration column by FPLC, both individually and combined in solution. If enzymes form complexes, fractions corresponding to the combined mass of several enzymes will be eluted [112]. Analytical ultracentrifugation characterizes interactions by assessing sedimentation velocity or sedimentation equilibrium of proteins in solution. Put simply, this technique uses optics to assess the behaviour of macromolecules as they are centrifuged, with the behaviour of these molecules being dependent on the degree to which they interact [33]. Techniques like these require an estimation of binding affinity however, as this is needed to determine what concentration of proteins will resolve complexes. As such, the SPR work presented here can permit further characterization of

the capsular heptose biosynthesis enzymes. One additional biochemical technique that the Creuzenet lab has been pursuing is MST, which affirmed that DdahA and DdahB can interact. Use of this technique also demonstrated the importance of substrate, with the K_D lowering 5-fold upon the addition of GDP-mannose. This work gives more credence to the hypothesis of substrate channeling, as this process depends on physical interactions between enzymes to allow for the transfer of pathway intermediates.

We hypothesized that the *C. jejuni* capsular biosynthesis enzymes engage in substrate channeling to limit substrate degradation in the cytosol. Though interactions between the enzymes of the capsular heptose biosynthesis pathways have been established, and data affirms the possibility of substrate channelling, work has not been completed to say that substrate channelling is occurring definitively. It is important to characterize interactions however, as physical interactions between subsequent enzymes in a biosynthetic pathway is required for substrate channelling to occur. Beyond this, these interactions must permit the passing of pathway intermediates from one enzyme to the next. Therefore, to determine if physical interactions between enzymes are important for pathway efficiency, Creuzenet lab plans to create binding mutants for partners identified by SPR. The crystal structure of the capsular heptose biosynthesis enzymes has recently been elucidated through collaboration with the Naismith group [15]. *In silico* docking studies can be conducted to determine which residues are important for interfacing between binding partners. Additionally, this analysis will help determine the probability of electrostatic guidance and intramolecular tunnel formation [37,137,169]. Once the residues that impact binding are determined, mutants can be generated, and their binding capacity can be assessed using biochemical techniques such as SPR or MST.

To assess if altered protein-protein interactions affect pathway efficiency, reaction mixtures containing groups of wild-type enzymes, or binding mutants, will be created and product quantity can be assessed via capillary electrophoresis. I expect that reaction mixtures containing binding mutants will have lower heptose output than mixtures containing the wild-type enzymes, due to the increased degradation of pathway intermediates. Another means of studying the importance of physical interactions in

product formation would be to physically immobilize the enzymes in a reaction mixture, forcing intermediates to diffuse between active sites [152].

Overall, data presented in this thesis indicates that the enzymes of the Mlgh and Ddah capsular heptose biosynthesis pathways are able to interact physically, with subsequent testing needed to further characterize these interactions, both in terms of how strong binding is, and how interactions impact heptose production.

4.4 Overall significance and conclusions

Campylobacter jejuni is one of the leading causes of gastrointestinal disease worldwide, and with growing concerns of antibiotic resistance, it is likely that this pathogen will only pose a growing threat in the future. As such, it is imperative to characterize bacterial virulence factors, as even a mechanistic understanding of virulence factor production, or the impact of virulence factors on the interface with host cells, has the potential to shape treatment and prophylaxis. As stated in the introduction, the ultimate goal of this research would be to perturb the production of virulence factors in *C. jejuni* residing commensally in chickens, such that transmission to humans is reduced. While research is not at that stage, inquiry has revealed how modifications to the NCTC 11168 capsule impacts the behaviour of host macrophages, and provides further insights into capsular heptose production.

Overall, in this thesis I have characterized interactions between capsular heptose biosynthesis enzymes, and have assessed how the NCTC 11168 CPS and capsular heptose impact the interaction between *C. jejuni* and host macrophages. I provide evidence that enzymes within, and between, the Ddah and Mlgh capsular heptose biosynthesis pathways can interact physically, and that these interactions are likely modified by the presence of substrate. I also saw that live WT induced NO in chicken macrophages, while lowering the induction of intracellular ROS from human and chicken macrophages. The capsular heptose decreased nitrite induction, while the presence of the CPS increased nitrite induction, though neither impacted ROS levels. WT induced the transcription of IL-1 β , IL-6, IL-8, IL-10, and TNF α , and caused notable increases in the

secretion of proinflammatory cytokines IL-1 α , IL-1 β , IL-6, IL-8, IL-18, TNF α , and the anti-inflammatory cytokine IL-10, from THP-1 macrophages. Analysis revealed that the presence of the CPS or capsular heptose did not affect the induction of any tested cytokine. Looking at interactions between *C. jejuni* and host cells revealed that the NCTC 11168 CPS acts to diminish adhesion to, and survival within, chicken macrophages. The CPS also diminishes uptake by human macrophages, as well as survival early after internalization. Additionally, high levels of MeOPN presentation on the CPS impairs uptake by human macrophages.

Overall, this work presents novel data regarding the behaviour of *C. jejuni* NCTC 11168 and how its uniquely modified capsule impacts interactions with host macrophages. This furthers knowledge in the study of this pathogen and provides a scaffold for further investigation at the intersection of strain-specific virulence, host-specific immune responses, and mechanistically targeted treatment.

References

- [1] A. Agunos, D. Léger, B. Avery, E. Parmley, A. Deckert, C. Carson, R. Reid-Smith, R. Irwin, Ciprofloxacin-resistant *Campylobacter* in broiler chicken in Canada, *CCDR*. 40 (2014) 36–41.
- [2] A. Alemka, H. Nothaft, J. Zheng, C.M. Szymanski, N-glycosylation of *Campylobacter jejuni* surface proteins promotes bacterial fitness, *Infect Immun*. 81 (2013) 1674–1682.
- [3] Aligent Technologies, Inc., Quikchange II site-directed mutagenesis kit, (n.d.).
- [4] Allied Health Department, Public Health Program, College of Health Sciences, University of Bahrain, Manama, Bahrain, G. Asokan, T. Ramadhan, Nursing, College of Health Sciences, WHO Collaborating Centre for Nursing Development University of Bahrain, Manama, Bahrain, E. Ahmed, Nursing, College of Health Sciences, WHO Collaborating Centre for Nursing Development University of Bahrain, Manama, Bahrain, H. Sanad, Nursing, College of Health Sciences, WHO Collaborating Centre for Nursing Development University of Bahrain, Manama, Bahrain, WHO global priority pathogens list: a bibliometric analysis of medline-pubmed for knowledge mobilization to infection prevention and control practices in Bahrain, *OMJ*. 34 (2019) 184–193.
- [5] L.B. van Alphen, C.Q. Wenzel, M.R. Richards, C. Fodor, R.A. Ashmus, M. Stahl, A.V. Karlyshev, B.W. Wren, A. Stintzi, W.G. Miller, T.L. Lowary, C.M. Szymanski, Biological roles of the O-methyl phosphoramidate capsule modification in *Campylobacter jejuni*, *PLoS ONE*. 9 (2014) e87051.
- [6] C.W. Ang, M.A. De Klerk, H.P. Endtz, B.C. Jacobs, J.D. Laman, F.G. van der Meché, P.A. van Doorn, Guillain-Barré syndrome- and Miller Fisher syndrome-associated *Campylobacter jejuni* lipopolysaccharides induce anti-GM1 and anti-GQ1b Antibodies in rabbits, *Infect Immun*. 69 (2001) 2462–2469.
- [7] G. Arango Duque, A. Descoteaux, Macrophage cytokines: involvement in immunity and infectious diseases, *Front Immunol*. 5 (2014) 491.
- [8] H. Asakura, M. Yamasaki, S. Yamamoto, S. Igimi, Deletion of *peb4* gene impairs cell adhesion and biofilm formation in *Campylobacter jejuni*, *FEMS Microbiology Letters*. 275 (2007) 278–285.
- [9] S.S.A. Ashgar, N.J. Oldfield, K.G. Wooldridge, M.A. Jones, G.J. Irving, D.P.J. Turner, D.A.A. Ala'Aldeen, Capa, an autotransporter protein of *Campylobacter jejuni*, mediates association with human epithelial cells and colonization of the chicken gut, *J Bacteriol*. 189 (2007) 1856–1865.
- [10] H. Auld, D. MacIver, J. Klaassen, Heavy rainfall and waterborne disease outbreaks: the Walkerton example, *Journal of Toxicology and Environmental Health, Part A*. 67 (2004) 1879–1887.
- [11] B.M. Bachtiar, P.J. Coloe, B.N. Fry, Knockout mutagenesis of the *kpsE* gene of *Campylobacter jejuni* 81116 and its involvement in bacterium–host interactions, *FEMS Immunol Med Microbiol*. 49 (2007) 149–154.
- [12] D.J. Bacon, C.M. Szymanski, D.H. Burr, R.P. Silver, R.A. Alm, P. Guerry, A phase-variable capsule is involved in virulence of *Campylobacter jejuni* 81-176: *C. jejuni* capsular phase variation, *Molecular Microbiology*. 40 (2001) 769–777.

- [13] C.C. Bain, A. Schridde, Origin, Differentiation, and Function of Intestinal Macrophages, *Front. Immunol.* 9 (2018) 2733.
- [14] N. Barjesteh, S. Behboudi, J.T. Brisbin, A.I. Villanueva, É. Nagy, S. Sharif, TLR Ligands Induce Antiviral Responses in Chicken Macrophages, *PLoS ONE.* 9 (2014) e105713.
- [15] H. Barnawi, L. Woodward, N. Fava, M. Roubakha, S.D. Shaw, C. Kubinec, J.H. Naismith, C. Creuzenet, Structure-function studies of the C3/C5 epimerases and C4 reductases of the *Campylobacter jejuni* capsular heptose modification pathways, *J Biol Chem.* (2021) 100352.
- [16] D. Bernardo, A.C. Marin, S. Fernández-Tomé, A. Montalban-Arques, A. Carrasco, E. Tristán, L. Ortega-Moreno, I. Mora-Gutiérrez, A. Díaz-Guerra, R. Caminero-Fernández, P. Miranda, F. Casals, M. Caldas, M. Jiménez, S. Casabona, F. De la Morena, M. Esteve, C. Santander, M. Chaparro, J.P. Gisbert, Human intestinal pro-inflammatory CD11c^{high}CCR2⁺CX3CR1⁺ macrophages, but not their tolerogenic CD11c⁻CCR2⁻CX3CR1⁻ counterparts, are expanded in inflammatory bowel disease, *Mucosal Immunol.* 11 (2018) 1114–1126.
- [17] E. Beshearse, B.B. Bruce, G.F. Nane, R.M. Cooke, W. Aspinall, T. Hald, S.M. Crim, P.M. Griffin, K.E. Fullerton, S.A. Collier, K.M. Benedict, M.J. Beach, A.J. Hall, A.H. Havelaar, Attribution of illnesses transmitted by food and water to comprehensive transmission pathways using structured expert judgment, *United States, Emerg. Infect. Dis.* 27 (2021) 182–195.
- [18] A. Bhalla, S. Prabhakar, R. Rajan, R. Kaushik, P. Kharbanda, Acute flaccid paralysis in adults: our experience, *J Emerg Trauma Shock.* 7 (2014) 149.
- [19] R.E. Black, M.M. Levine, M.L. Clements, T.P. Hughes, M.J. Blaser, Experimental *Campylobacter jejuni* infection in humans, *Journal of Infectious Diseases.* 157 (1988) 472–479.
- [20] H. Bosshart, M. Heinzelmann, THP-1 cells as a model for human monocytes, *Ann. Transl. Med.* 4 (2016) 438–438.
- [21] L.I. Bouwman, M.R. de Zoete, N.M.C. Bleumink-Pluym, R.A. Flavell, J.P.M. van Putten, Inflammasome activation by *Campylobacter jejuni*, *J.I.* 193 (2014) 4548–4557.
- [22] B. Bulutoglu, K.E. Garcia, F. Wu, S.D. Minter, S. Banta, Direct evidence for metabolon formation and substrate channeling in recombinant TCA cycle enzymes, *ACS Chem. Biol.* 11 (2016) 2847–2853.
- [23] P.M. Burnham, D.R. Hendrixson, *Campylobacter jejuni*: collective components promoting a successful enteric lifestyle, *Nat Rev Microbiol.* 16 (2018) 551–565.
- [24] Centers for Disease Control and Prevention, Antibiotic resistance threats in the United States, (2019).
- [25] Centers for Disease Control and Prevention, Chicken and food poisoning, (2020).
- [26] Centers for Disease Control and Prevention, Outbreak of multidrug-resistant *Campylobacter* infections linked to contact with pet store puppies, (2021).
- [27] W. Chanput, J. Mes, R.A.M. Vreeburg, H.F.J. Savelkoul, H.J. Wichers, Transcription profiles of LPS-stimulated THP-1 monocytes and macrophages: a tool to study inflammation modulating effects of food-derived compounds, *Food Funct.* 1 (2010) 254.

- [28] J.E. Christensen, S.A. Pacheco, M.E. Konkel, Identification of a *Campylobacter jejuni*-secreted protein required for maximal invasion of host cells, *Molecular Microbiology*. 73 (2009) 650–662.
- [29] M.A. Cinelli, H.T. Do, G.P. Miley, R.B. Silverman, Inducible nitric oxide synthase: regulation, structure, and inhibition, *Med Res Rev*. 40 (2020) 158–189.
- [30] C.G. Clark, P.M. Chong, S.J. McCorrister, P. Simon, M. Walker, D.M. Lee, K. Nguy, K. Cheng, M.W. Gilmour, G.R. Westmacott, The CJIE1 prophage of *Campylobacter jejuni* affects protein expression in growth media with and without bile salts, *BMC Microbiol*. 14 (2014) 70.
- [31] C.G. Clark, L. Price, R. Ahmed, D.L. Woodward, P.L. Melito, F.G. Rodgers, F. Jamieson, B. Ciebin, A. Li, A. Ellis, Characterization of waterborne outbreak-associated *Campylobacter jejuni*, Walkerton, Ontario, *Emerg. Infect. Dis*. 9 (2003) 1232–1241.
- [32] T.N. Clarke, M.A. Schilling, L.A. Melendez, S.D. Isidean, C.K. Porter, F.M. Poly, A systematic review and meta-analysis of Penner serotype prevalence of *Campylobacter jejuni* in low- and middle-income countries, *PLoS ONE*. 16 (2021) e0251039.
- [33] J.L. Cole, J.W. Lary, T. P. Moody, T.M. Laue, Analytical ultracentrifugation: sedimentation velocity and sedimentation equilibrium, in: *Methods in Cell Biology*, Elsevier, 2008: pp. 143–179.
- [34] A.T. Corcoran, H. Annuk, A.P. Moran, The structure of the lipid anchor of *Campylobacter jejuni* polysaccharide, *FEMS Microbiology Letters*. 257 (2006) 228–235.
- [35] A. Dillon, D.D. Lo, *M Cells: Intelligent Engineering of Mucosal Immune Surveillance*, *Front. Immunol*. 10 (2019) 1499.
- [36] D. Domman, C. Ruis, M.J. Dorman, M. Shakya, P.S.G. Chain, Novel insights into the spread of enteric pathogens using genomics, *The Journal of Infectious Diseases*. (2019) jiz220.
- [37] N.C. Dubey, B.P. Tripathi, Nature inspired multienzyme immobilization: strategies and concepts, *ACS Appl. Bio Mater*. 4 (2021) 1077–1114.
- [38] J.N.S. Eisenberg, G. Trueba, W. Cevallos, J.E. Goldstick, D. Bhavnani, Impact of rainfall on diarrheal disease risk associated with unimproved water and sanitation, *The American Journal of Tropical Medicine and Hygiene*. 90 (2014) 705–711.
- [39] K.T. Elvers, G. Wu, N.J. Gilberthorpe, R.K. Poole, S.F. Park, Role of an inducible single-domain hemoglobin in mediating resistance to nitric oxide and nitrosative stress in *Campylobacter jejuni* and *Campylobacter coli*, *J Bacteriol*. 186 (2004) 5332–5341.
- [40] R.C. Flanagan, J.M. Neal-McKinney, A.S. Dhillon, W.G. Miller, M.E. Konkel, Examination of *Campylobacter jejuni* putative adhesins leads to the identification of a new protein, designated flpa, required for chicken colonization, *Infect Immun*. 77 (2009) 2399–2407.
- [41] R.S. Flanagan, D.E. Heinrichs, A fluorescence based-proliferation assay for the identification of replicating bacteria within host cells, *Front. Microbiol*. 9 (2018) 3084.

- [42] P. Fontán, V. Aris, S. Ghanny, P. Soteropoulos, I. Smith, Global transcriptional profile of *Mycobacterium tuberculosis* during THP-1 human macrophage infection, *IAI*. 76 (2008) 717–725.
- [43] S. Goon, J.F. Kelly, S.M. Logan, C.P. Ewing, P. Guerry, Pseudaminic acid, the major modification on *Campylobacter* flagellin, is synthesized via the Cj1293 gene: *Campylobacter* flagellin glycosylation, *Molecular Microbiology*. 50 (2003) 659–671.
- [44] A.J. Grant, C. Coward, M.A. Jones, C.A. Woodall, P.A. Barrow, D.J. Maskell, Signature-Tagged Transposon Mutagenesis Studies Demonstrate the Dynamic Nature of Cecal Colonization of 2-Week-Old Chickens by *Campylobacter jejuni*, *AEM*. 71 (2005) 8031–8041.
- [45] P. Guerry, C.P. Ewing, M. Schirm, M. Lorenzo, J. Kelly, D. Pattarini, G. Majam, P. Thibault, S. Logan, Changes in flagellin glycosylation affect *Campylobacter* autoagglutination and virulence, *Mol Microbiol*. 60 (2006) 299–311.
- [46] P. Guerry, F. Poly, M. Riddle, A.C. Maue, Y.-H. Chen, M.A. Monteiro, *Campylobacter* polysaccharide capsules: virulence and vaccines, *Front. Cell. Inf. Microbio*. 2 (2012).
- [47] P. Guerry, C.M. Szymanski, *Campylobacter* sugars sticking out, *Trends in Microbiology*. 16 (2008) 428–435.
- [48] P. Guerry, C.M. Szymanski, M.M. Prendergast, T.E. Hickey, C.P. Ewing, D.L. Pattarini, A.P. Moran, Phase variation of *Campylobacter jejuni* 81-176 lipooligosaccharide affects ganglioside mimicry and invasiveness in vitro, *Infect Immun*. 70 (2002) 787–793.
- [49] T. Hannu, L. Mattila, H. Rautelin, P. Pelkonen, P. Lahdenne, A. Siitonen, M. Leirisalo-Repo, *Campylobacter*-triggered reactive arthritis: a population-based study, *Rheumatology*. 41 (2002) 312–318.
- [50] S.L. Harper, V.L. Edge, J. Ford, M.K. Thomas, D.L. Pearl, J. Shirley, IHACC, RICG, S.A. McEWEN, Acute gastrointestinal illness in two Inuit communities: burden of illness in Rigolet and Iqaluit, Canada, *Epidemiol. Infect*. 143 (2015) 3048–3063.
- [51] L.M. Harrison, C. van den Hoogen, W.C.E. van Haaften, V.L. Tesh, Chemokine Expression in the Monocytic Cell Line THP-1 in Response to Purified Shiga Toxin 1 and/or Lipopolysaccharides, *IAI*. 73 (2005) 403–412.
- [52] W.C. Hazeleger, J.D. Janse, P.M. Koenraad, R.R. Beumer, F.M. Rombouts, T. Abee, Temperature-dependent membrane fatty acid and cell physiology changes in coccoid forms of *Campylobacter jejuni*, *Appl Environ Microbiol*. 61 (1995) 2713–2719.
- [53] D.R. Hendrixson, V.J. DiRita, Identification of *Campylobacter jejuni* genes involved in commensal colonization of the chick gastrointestinal tract: *C. jejuni* commensal colonization, *Molecular Microbiology*. 52 (2004) 471–484.
- [54] N. Ho, A.N. Kondakova, Y.A. Knirel, C. Creuzenet, The biosynthesis and biological role of 6-deoxyheptose in the lipopolysaccharide O-antigen of *Yersinia pseudotuberculosis*: 6-Deoxyheptose: biosynthesis and role in virulence, *Molecular Microbiology*. 68 (2008) 424–447.
- [55] G. Hong, C. Davies, Z. Omole, J. Liaw, A.D. Grabowska, B. Canonico, N. Corcionivoschi, B. Wren, N. Dorrell, A. Elmi, O. Gundogdu, *Campylobacter jejuni*

- modulates reactive oxygen species production and NADPH oxidase 1 expression in human intestinal epithelial cells, *Microbiology*, 2022.
- [56] L. Hu, D.J. Kopecko, *Campylobacter jejuni* 81-176 associates with microtubules and dynein during invasion of human intestinal cells, *Infect Immun.* 67 (1999) 4171–4182.
- [57] J.P. Huddleston, T.K. Anderson, K.D. Spencer, J.B. Thoden, F.M. Raushel, H.M. Holden, Structural analysis of Cj1427, an essential NAD-dependent dehydrogenase for the biosynthesis of the heptose residues in the capsular polysaccharides of *Campylobacter jejuni*, *Biochemistry.* 59 (2020) 1314–1327.
- [58] J.P. Huddleston, F.M. Raushel, Functional characterization of Cj1427, a unique ping-pong dehydrogenase responsible for the oxidation of gdp-D-*glycero- α -D-manno*-heptose in *Campylobacter jejuni*, *Biochemistry.* 59 (2020) 1328–1337.
- [59] R.A.C. Hughes, J.H. Rees, Clinical and epidemiologic features of Guillain-Barré syndrome, *J INFECT DIS.* 176 (1997) S92–S98.
- [60] T. Iacob, D. Țățulescu, M. Lupșe, D. Dumitrașcu, Post-infectious irritable bowel syndrome after a laboratory-proven enteritis, *Exp Ther Med.* (2020).
- [61] N. Ikeda, A.V. Karlyshev, Putative mechanisms and biological role of coccoid form formation in *Campylobacter jejuni*, *European Journal of Microbiology and Immunology.* 2 (2012) 41–49.
- [62] M. Jerabek-Willemsen, T. André, R. Wanner, H.M. Roth, S. Duhr, P. Baaske, D. Breitsprecher, Microscale thermophoresis: interaction analysis and beyond, *Journal of Molecular Structure.* 1077 (2014) 101–113.
- [63] M.A. Jones, S. Töttemeyer, D.J. Maskell, C.E. Bryant, P.A. Barrow, Induction of proinflammatory responses in the human monocytic cell line THP-1 by *Campylobacter jejuni*, *IAI.* 71 (2003) 2626–2633.
- [64] F. Jorgensen, J. Ellis-Iversen, S. Rushton, S.A. Bull, S.A. Harris, S.J. Bryan, A. Gonzalez, T.J. Humphrey, Influence of season and geography on *Campylobacter jejuni* and *C. coli* subtypes in housed broiler flocks reared in Great Britain, *Appl. Environ. Microbiol.* 77 (2011) 3741–3748.
- [65] C. Jung, J.-P. Hugot, F. Barreau, Peyer's Patches: The Immune Sensors of the Intestine, *International Journal of Inflammation.* 2010 (2010) 1–12.
- [66] J. Jung, K. Skinner, Foodborne and waterborne illness among Canadian Indigenous populations: A scoping review, *Canada Communicable Disease Report.* 43 (2017) 7–13.
- [67] N.O. Kaakoush, N. Castaño-Rodríguez, H.M. Mitchell, S.M. Man, Global epidemiology of *Campylobacter* infection, *Clin. Microbiol. Rev.* 28 (2015) 687–720.
- [68] M.I. Kanipes, E. Papp-Szabo, P. Guerry, M.A. Monteiro, Mutation of waaC, encoding heptosyltransferase I in *Campylobacter jejuni* 81-176, affects the structure of both lipooligosaccharide and capsular carbohydrate, *JB.* 188 (2006) 3273–3279.
- [69] A.V. Karlyshev, P. Everest, D. Linton, S. Cawthraw, D.G. Newell, B.W. Wren, The *Campylobacter jejuni* general glycosylation system is important for attachment to human epithelial cells and in the colonization of chicks, *Microbiology.* 150 (2004) 1957–1964.

- [70] T. Keo, J. Collins, P. Kunwar, M.J. Blaser, N.M. Iovine, Campylobacter capsule and lipooligosaccharide confer resistance to serum and cationic antimicrobials, *Virulence*. 2 (2011) 30–40.
- [71] A.A. Kermani, R. Roy, C. Gopalasingam, K.I. Kocurek, T.R. Patel, L.J. Alderwick, G.S. Besra, K. Fütterer, Crystal structure of the TreS:Pep2 complex, initiating α -glucan synthesis in the GlgE pathway of mycobacteria, *J. Biol. Chem.* 294 (2019) 7348–7359.
- [72] M. Kervella, J.M. Pagès, Z. Pei, G. Grollier, M.J. Blaser, J.L. Fauchère, Isolation and characterization of two Campylobacter glycine-extracted proteins that bind to HeLa cell membranes, *Infect Immun.* 61 (1993) 3440–3448.
- [73] S. Kim, A. Vela, S.M. Clohisey, S. Athanasiadou, P. Kaiser, M.P. Stevens, L. Vervelde, Host-specific differences in the response of cultured macrophages to *Campylobacter jejuni* capsule and O-methyl phosphoramidate mutants, *Vet Res.* 49 (2018) 3.
- [74] D. Knorr, M.A. Augustin, Preserving the food preservation legacy, *Critical Reviews in Food Science and Nutrition*. (2022) 1–20.
- [75] M.E. Konkel, J.D. Klena, V. Rivera-Amill, M.R. Monteville, D. Biswas, B. Raphael, J. Mickelson, Secretion of virulence proteins from *Campylobacter jejuni* is dependent on a functional flagellar export apparatus, *J Bacteriol.* 186 (2004) 3296–3303.
- [76] M.E. Konkel, C.L. Larson, R.C. Flanagan, *Campylobacter jejuni* FlpA binds fibronectin and is required for maximal host cell adherence, *J Bacteriol.* 192 (2010) 68–76.
- [77] M.E. Konkel, P.K. Talukdar, N.M. Negretti, C.M. Klappenbach, Taking control: *Campylobacter jejuni* binding to fibronectin sets the stage for cellular adherence and invasion, *Front. Microbiol.* 11 (2020) 564.
- [78] J.K. Kovács, A. Cox, B. Schweitzer, G. Maróti, T. Kovács, H. Fenyvesi, L. Emödy, G. Schneider, Virulence traits of inpatient *Campylobacter jejuni* isolates, and a transcriptomic approach to identify potential genes maintaining intracellular survival, *Microorganisms*. 8 (2020) 531.
- [79] M. Kowarik, N.M. Young, S. Numao, B.L. Schulz, I. Hug, N. Callewaert, D.C. Mills, D.C. Watson, M. Hernandez, J.F. Kelly, M. Wacker, M. Aebi, Definition of the bacterial N-glycosylation site consensus sequence, *EMBO J.* 25 (2006) 1957–1966.
- [80] J.C. Larsen, C. Szymanski, P. Guerry, N-linked protein glycosylation is required for full competence in *Campylobacter jejuni* 81-176, *J Bacteriol.* 186 (2004) 6508–6514.
- [81] C.L. Larson, D.R. Samuelson, T.P. Eucker, J.L. O’Loughlin, M.E. Konkel, The fibronectin-binding motif within FlpA facilitates *Campylobacter jejuni* adherence to host cell and activation of host cell signaling, *Emerging Microbes & Infections*. 2 (2013) 1–12.
- [82] J. Lee, N.D. Ridgway, Substrate channeling in the glycerol-3-phosphate pathway regulates the synthesis, storage and secretion of glycerolipids, *Biochimica et Biophysica Acta (BBA) - Molecular and Cell Biology of Lipids*. 1865 (2020) 158438.

- [83] S. Lee, D.K. Lee, What is the proper way to apply the multiple comparison test?, *Korean J Anesthesiol.* 71 (2018) 353–360.
- [84] R.E. Levin, *Campylobacter jejuni*: a review of its characteristics, pathogenicity, ecology, distribution, subspecies characterization and molecular methods of detection, *Food Biotechnology.* 21 (2007) 271–347.
- [85] X. Liao, Y. Shen, R. Zhang, K. Sugi, N.T. Vasudevan, M.A. Alaiti, D.R. Sweet, L. Zhou, Y. Qing, S.L. Gerson, C. Fu, A. Wynshaw-Boris, R. Hu, M.A. Schwartz, H. Fujioka, B. Richardson, M.J. Cameron, H. Hayashi, J.S. Stamler, M.K. Jain, Distinct roles of resident and nonresident macrophages in nonischemic cardiomyopathy, *Proc. Natl. Acad. Sci. U.S.A.* 115 (2018).
- [86] H. Liu, J.H. Naismith, An efficient one-step site-directed deletion, insertion, single and multiple-site plasmid mutagenesis protocol, *BMC Biotechnol.* 8 (2008) 91.
- [87] R. Lv, K. Wang, J. Feng, D.D. Heeney, D. Liu, X. Lu, Detection and quantification of viable but non-culturable *Campylobacter jejuni*, *Front. Microbiol.* 10 (2020) 2920.
- [88] N. Macesic, V. Hall, A. Mahony, L. Hueston, G. Ng, R. Macdonell, A. Hughes, G. Fitt, M.L. Grayson, Acute flaccid paralysis: the new, the old, and the preventable, *Open Forum Infectious Diseases.* 3 (2016) ofv190.
- [89] M.B. Maeß, S. Sendelbach, S. Lorkowski, Selection of reliable reference genes during THP-1 monocyte differentiation into macrophages, *BMC Molecular Biol.* 11 (2010) 90.
- [90] W.M. Manetu, S. M'masi, C.W. Recha, Diarrhea disease among children under 5 years of age: a global systematic review, *OJEpi.* 11 (2021) 207–221.
- [91] E.P. Marder, P.R. Cieslak, A.B. Cronquist, J. Dunn, S. Lathrop, T. Rabatsky-Ehr, P. Ryan, K. Smith, M. Tobin-D'Angelo, D.J. Vugia, S. Zansky, K.G. Holt, B.J. Wolpert, M. Lynch, R. Tauxe, A.L. Geissler, Incidence and trends of infections with pathogens transmitted commonly through food and the effect of increasing use of culture-independent diagnostic tests on surveillance — foodborne diseases active surveillance network, 10 U.S. sites, 2013–2016, *MMWR Morb. Mortal. Wkly. Rep.* 66 (2017) 397–403.
- [92] A.C. Maue, K.L. Mohawk, D.K. Giles, F. Poly, C.P. Ewing, Y. Jiao, G. Lee, Z. Ma, M.A. Monteiro, C.L. Hill, J.S. Ferderber, C.K. Porter, M.S. Trent, P. Guerry, The polysaccharide capsule of *Campylobacter jejuni* modulates the host immune response, *Infect. Immun.* 81 (2013) 665–672.
- [93] A.C. Maue, F. Poly, P. Guerry, A capsule conjugate vaccine approach to prevent diarrheal disease caused by *Campylobacter jejuni*, *Human Vaccines & Immunotherapeutics.* 10 (2014) 1499–1504.
- [94] M. McCallum, G.S. Shaw, C. Creuzenet, Characterization of the dehydratase WcbK and the reductase WcaG involved in GDP-6-deoxy-manno-heptose biosynthesis in *Campylobacter jejuni*, *Biochemical Journal.* 439 (2011) 235–248.
- [95] M. McCallum, G.S. Shaw, C. Creuzenet, Comparison of predicted epimerases and reductases of the *Campylobacter jejuni* D-*altro*- and L-*gluco*-heptose synthesis pathways, *J. Biol. Chem.* 288 (2013) 19569–19580.
- [96] M. McCallum, S.D. Shaw, G.S. Shaw, C. Creuzenet, Complete 6-deoxy-D-*altro*-heptose biosynthesis pathway from *Campylobacter jejuni*: more complex than anticipated, *J. Biol. Chem.* 287 (2012) 29776–29788.

- [97] D.J. McNally, A.J. Aubry, J.P.M. Hui, N.H. Khieu, D. Whitfield, C.P. Ewing, P. Guerry, J.-R. Brisson, S.M. Logan, E.C. Soo, Targeted metabolomics analysis of *Campylobacter coli* vc167 reveals legionaminic acid derivatives as novel flagellar glycans, *Journal of Biological Chemistry*. 282 (2007) 14463–14475.
- [98] D.J. McNally, J.P.M. Hui, A.J. Aubry, K.K.K. Mui, P. Guerry, J.-R. Brisson, S.M. Logan, E.C. Soo, Functional characterization of the flagellar glycosylation locus in *Campylobacter jejuni* 81–176 using a focused metabolomics approach, *Journal of Biological Chemistry*. 281 (2006) 18489–18498.
- [99] F.M. Meyer, J. Gerwig, E. Hammer, C. Herzberg, F.M. Commichau, U. Völker, J. Stülke, Physical interactions between tricarboxylic acid cycle enzymes in *Bacillus subtilis*: Evidence for a metabolon, *Metabolic Engineering*. 13 (2011) 18–27.
- [100] E.W. Miles, S. Rhee, D.R. Davies, The molecular basis of substrate channeling, *J. Biol. Chem.* 274 (1999) 12193–12196.
- [101] P.F. Mixter, J.D. Klena, G.A. Flom, A.M. Siegesmund, M.E. Konkel, In vivo tracking of *Campylobacter jejuni* by using a novel recombinant expressing green fluorescent protein, *Appl Environ Microbiol.* 69 (2003) 2864–2874.
- [102] M.A. Monteiro, A. Noll, R.M. Laird, B. Pequegnat, Z. Ma, L. Bertolo, C. DePass, E. Omari, P. Gabryelski, O. Redkyna, Y. Jiao, S. Borrelli, F. Poly, P. Guerry, *Campylobacter jejuni* capsule polysaccharide conjugate vaccine, in: A.K. Prasad (Ed.), ACS Symposium Series, American Chemical Society, Washington, DC, 2018: pp. 249–271.
- [103] M.A. Moore, Z.W. Hakki, R.L. Gregory, L.E. Gfell, W.K. Kim-Park, M.J. Kowolik, Influence of heat inactivation of human serum on the opsonization of *Streptococcus mutans*, *Ann NY Acad Sci.* 832 (1997) 383–393.
- [104] A.P. Moran, Structure and conserved characteristics of *Campylobacter jejuni* lipopolysaccharides, *J INFECT DIS.* 176 (1997) S115–S121.
- [105] I. Morgunov, P.A. Srere, Interaction between citrate synthase and malate dehydrogenase: substrate channeling of oxaloacetate, *J. Biol. Chem.* 273 (1998) 29540–29544.
- [106] R.J. Mostowy, K.E. Holt, Diversity-generating machines: genetics of bacterial sugar-coating, *Trends in Microbiology*. 26 (2018) 1008–1021.
- [107] A. Mukabutera, D. Thomson, M. Murray, P. Basinga, L. Nyirazinyoye, S. Atwood, K.P. Savage, A. Ngirimana, B.L. Hedt-Gauthier, Rainfall variation and child health: effect of rainfall on diarrhea among under 5 children in Rwanda, 2010, *BMC Public Health*. 16 (2016) 731.
- [108] M.A. Myszewski, N.J. Stern, Phagocytosis and intracellular killing of *Campylobacter jejuni* by elicited chicken peritoneal macrophages, *Avian Diseases*. 35 (1991) 750.
- [109] J.S. Nanra, S.M. Buitrago, S. Crawford, J. Ng, P.S. Fink, J. Hawkins, I.L. Scully, L.K. McNeil, J.M. Aste-Amézaga, D. Cooper, K.U. Jansen, A.S. Anderson, Capsular polysaccharides are an important immune evasion mechanism for *Staphylococcus aureus*, *Hum Vaccin Immunother.* 9 (2013) 480–487.
- [110] N.M. Negretti, C.R. Gourley, P.K. Talukdar, G. Clair, C.M. Klappenbach, C.J. Lauritsen, J.N. Adkins, M.E. Konkel, The *Campylobacter jejuni* CiaD effector co-opts the host cell protein IQGAP1 to promote cell entry, *Nat Commun.* 12 (2021) 1339.

- [111] D.G. Newell, M. Koopmans, L. Verhoef, E. Duizer, A. Aidara-Kane, H. Sprong, M. Opsteegh, M. Langelaar, J. Threlfall, F. Scheutz, J. van der Giessen, H. Kruse, Food-borne diseases — The challenges of 20 years ago still persist while new ones continue to emerge, *International Journal of Food Microbiology*. 139 (2010) S3–S15.
- [112] C. Ó’Fágáin, P.M. Cummins, B.F. O’Connor, Gel-filtration chromatography, in: D. Walls, S.T. Loughran (Eds.), *Protein Chromatography*, Springer New York, New York, NY, 2017: pp. 15–25.
- [113] S.L.W. On, C.S. Harrington, Evaluation of numerical analysis of PFGE-DNA profiles for differentiating *Campylobacter fetus* subspecies by comparison with phenotypic, PCR and 16S rDNA sequencing methods, *J Appl Microbiol*. 90 (2001) 285–293.
- [114] Z. Pei, C. Burucoa, B. Grignon, S. Baqar, X.-Z. Huang, D.J. Kopecko, A.L. Bourgeois, J.-L. Fauchere, M.J. Blaser, Mutation in the *peb1A* locus of *Campylobacter jejuni* reduces interactions with epithelial cells and intestinal colonization of mice, *Infect Immun*. 66 (1998) 938–943.
- [115] B. Pequegnat, R.M. Laird, C.P. Ewing, C.L. Hill, E. Omari, F. Poly, M.A. Monteiro, P. Guerry, Phase-variable changes in the position of O-methyl phosphoramidate modifications on the polysaccharide capsule of *Campylobacter jejuni* modulate serum resistance, *J Bacteriol*. 199 (2017).
- [116] M.P. Pereira, E.D. Brown, Bifunctional catalysis by CDP-ribitol synthase: convergent recruitment of reductase and cytidylyltransferase activities in *Haemophilus influenzae* and *staphylococcus aureus*, *Biochemistry*. 43 (2004) 11802–11812.
- [117] G.I. Pérez-Pérez, V.L. Shepherd, J.D. Morrow, M.J. Blaser, Activation of human THP-1 cells and rat bone marrow-derived macrophages by *Helicobacter pylori* lipopolysaccharide., *Infection and Immunity*. 63 (1995) 1183–1187.
- [118] P.K. Peterson, J. Verhoef, P.G. Quie, Influence of temperature on opsonization and phagocytosis of Staphylococci, *Infect Immun*. 15 (1977) 175–179.
- [119] M.S. Pittman, K.T. Elvers, L. Lee, M.A. Jones, R.K. Poole, S.F. Park, D.J. Kelly, Growth of *Campylobacter jejuni* on nitrate and nitrite: electron transport to NapA and NrfA via NrfH and distinct roles for NrfA and the globin Cgb in protection against nitrosative stress: Roles of Nap and Nrf systems in *C. jejuni*, *Molecular Microbiology*. 63 (2007) 575–590.
- [120] G.L. Popa, M.I. Popa, *Salmonella spp.* infection – a continuous threat worldwide, *Germes*. 11 (2021) 88–96.
- [121] G. Preta, J.G. Cronin, I.M. Sheldon, Dynasore - not just a dynamin inhibitor, *Cell Commun Signal*. 13 (2015) 24.
- [122] Public Health Agency of Canada, Reported cases from 1924 to 2018 in Canada - Notifiable diseases on-line, (2018).
- [123] W.M. Quinteiro-Filho, J.T. Brisbin, D.C. Hodgins, S. Sharif, Lactobacillus and Lactobacillus cell-free culture supernatants modulate chicken macrophage activities, *Research in Veterinary Science*. 103 (2015) 170–175.
- [124] M.A. Qureshi, L. Miller, H.S. Lillehoj, M.D. Ficken, Establishment and characterization of a chicken mononuclear cell line, *Veterinary Immunology and Immunopathology*. 26 (1990) 237–250.

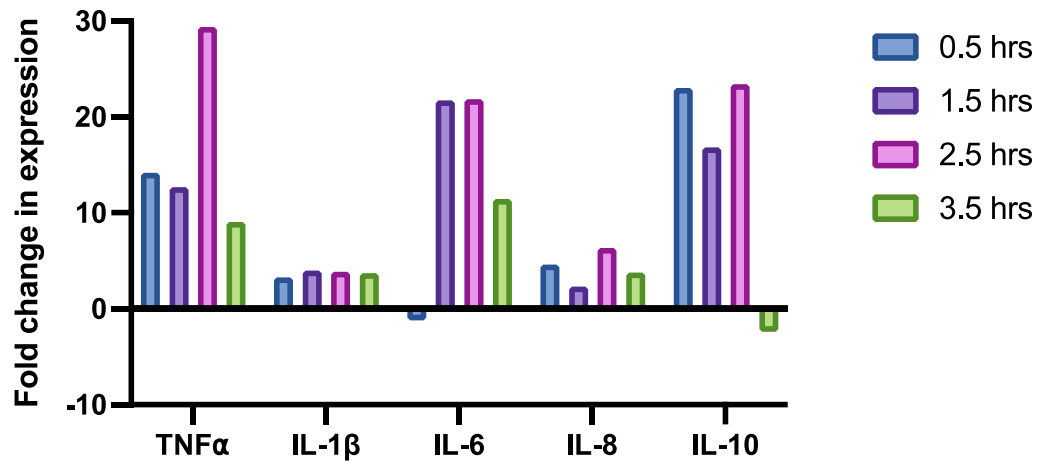
- [125] A. Ramakrishnan, N.M. Schumack, C.L. Gariepy, H. Eggleston, G. Nunez, N. Espinoza, M. Nieto, R. Castillo, J. Rojas, A.J. McCoy, Z. Beck, G.R. Matyas, C.R. Alving, P. Guerry, F. Poly, R.M. Laird, Enhanced immunogenicity and protective efficacy of a *Campylobacter jejuni* conjugate vaccine coadministered with liposomes containing monophosphoryl lipid a and QS-21, *MSphere*. 4 (2019) e00101-19, /msphere/4/3/mSphere101-19.atom.
- [126] G. Rasschaert, L. De Zutter, L. Herman, M. Heyndrickx, *Campylobacter* contamination of broilers: the role of transport and slaughterhouse, *International Journal of Food Microbiology*. 322 (2020) 108564.
- [127] G. Reddy, R.M. van Dam, Food, culture, and identity in multicultural societies: Insights from Singapore, *Appetite*. 149 (2020) 104633.
- [128] Roche, Cytotoxicity detection kit (LDH), (2016).
- [129] F. Rohde, B. Schusser, T. Hron, H. Farkašová, J. Plachý, S. Härtle, J. Hejnar, D. Elleder, B. Kaspers, Characterization of chicken tumor necrosis factor- α , a long missed cytokine in birds, *Front. Immunol.* 9 (2018) 605.
- [130] A. Rose, E. Kay, B.W. Wren, M.J. Dallman, The *Campylobacter jejuni* NCTC11168 capsule prevents excessive cytokine production by dendritic cells, *Med Microbiol Immunol.* 201 (2012) 137–144.
- [131] N. Sanyal, B.W. Arentson, M. Luo, J.J. Tanner, D.F. Becker, First evidence for substrate channeling between proline catabolic enzymes: a validation of domain fusion analysis for predicting protein-protein interactions, *J. Biol. Chem.* 290 (2015) 2225–2234.
- [132] E. Scallan, R.M. Hoekstra, B.E. Mahon, T.F. Jones, P.M. Griffin, An assessment of the human health impact of seven leading foodborne pathogens in the United States using disability adjusted life years, *Epidemiol. Infect.* 143 (2015) 2795–2804.
- [133] R.L. Scharff, Food attribution and economic cost estimates for meat- and poultry-related illnesses, *Journal of Food Protection*. 83 (2020) 959–967.
- [134] M. Sebald, M. Veron, Base DNA content and classification of Vibrios, *Ann Inst Pasteur (Paris)*. 105 (1963) 897–910.
- [135] O. Sharif, V.N. Bolshakov, S. Raines, P. Newham, N.D. Perkins, Transcriptional profiling of the LPS induced NF-kappaB response in macrophages, *BMC Immunol.* 8 (2007) 1.
- [136] S.K. Sheppard, M.C.J. Maiden, The evolution of *Campylobacter jejuni* and *Campylobacter coli*, *Cold Spring Harb Perspect Biol.* 7 (2015) a018119.
- [137] J. Shi, Y. Wu, S. Zhang, Y. Tian, D. Yang, Z. Jiang, Bioinspired construction of multi-enzyme catalytic systems, *Chem. Soc. Rev.* 47 (2018) 4295–4313.
- [138] M. Shigematsu, A. Umeda, S. Fujimoto, K. Amako, Spirochaete-like swimming mode of *Campylobacter jejuni* in a viscous environment, *Journal of Medical Microbiology*. 47 (1998) 521–526.
- [139] A.M. Siegesmund, M.E. Konkel, J.D. Klena, P.F. Mixter, *Campylobacter jejuni* infection of differentiated THP-1 macrophages results in interleukin 1 β release and caspase-1-independent apoptosis, *Microbiology*. 150 (2004) 561–569.
- [140] J. Silva, D. Leite, M. Fernandes, C. Mena, P.A. Gibbs, P. Teixeira, *Campylobacter spp.* as a Foodborne Pathogen: A Review, *Front. Microbio.* 2 (2011).

- [141] R.P. Silver, K. Prior, C. Nsahlai, L.F. Wright, ABC transporters and the export of capsular polysaccharides from Gram-negative bacteria, *Research in Microbiology*. 152 (2001) 357–364.
- [142] C.P.A. Skarp, M.-L. Hänninen, H.I.K. Rautelin, Campylobacteriosis: the role of poultry meat, *Clinical Microbiology and Infection*. 22 (2016) 103–109.
- [143] C.K. Smith, M. AbuOun, S.A. Cawthraw, T.J. Humphrey, L. Rothwell, P. Kaiser, P.A. Barrow, M.A. Jones, Campylobacter colonization of the chicken induces a proinflammatory response in mucosal tissues, *FEMS Immunology & Medical Microbiology*. 54 (2008) 114–121.
- [144] M.C.H. Sørensen, L.B. van Alphen, C. Fodor, S.M. Crowley, B.B. Christensen, C.M. Szymanski, L. Brøndsted, Phase variable expression of capsular polysaccharide modifications allows *Campylobacter jejuni* to avoid bacteriophage infection in chickens, *Front. Cell. Inf. Microbio.* 2 (2012).
- [145] N.M. van Sorge, N.M.C. Bleumink, S.J. van Vliet, E. Saeland, W.-L. van der Pol, Y. van Kooyk, J.P.M. van Putten, *N*-glycosylated proteins and distinct lipooligosaccharide glycoforms of *Campylobacter jejuni* target the human C-type lectin receptor MGL, *Cellular Microbiology*. 11 (2009) 1768–1781.
- [146] P.A. Srere, B. Mattiasson, K. Mosbach, An immobilized three-enzyme system: a model for microenvironmental compartmentation in mitochondria, *Proceedings of the National Academy of Sciences*. 70 (1973) 2534–2538.
- [147] J.D. Stanaway, A. Parisi, K. Sarkar, B.F. Blacker, R.C. Reiner, S.I. Hay, M.R. Nixon, C. Dolecek, S.L. James, A.H. Mokdad, G. Abebe, E. Ahmadian, F. Alahdab, B.T.T. Alemnew, V. Alipour, F. Allah Bakeshei, M.D. Animut, F. Ansari, J. Arabloo, E.T. Asfaw, M. Bagherzadeh, Q. Bassat, Y.M.M. Belayneh, F. Carvalho, A. Daryani, F.M. Demeke, A.B.B. Demis, M. Dubey, E.E. Duken, S.J. Dunachie, A. Eftekhari, E. Fernandes, R. Fouladi Fard, G.A. Gedefaw, B. Geta, K.B. Gibney, A. Hasanzadeh, C.L. Hoang, A. Kasaeian, A. Khater, Z.T. Kidanemariam, A.M. Lakew, R. Malekzadeh, A. Melese, D.T. Mengistu, T. Mestrovic, B. Miazgowski, K.A. Mohammad, M. Mohammadian, A. Mohammadian-Hafshejani, C.T. Nguyen, L.H. Nguyen, S.H. Nguyen, Y.L. Nirayo, A.T. Olagunju, T.O. Olagunju, H. Pourjafar, M. Qorbani, M. Rabiee, N. Rabiee, A. Rafay, A. Rezapour, A.M. Samy, S.G. Sepanlou, M.A. Shaikh, M. Sharif, M. Shigematsu, B. Tessema, B.X. Tran, I. Ullah, E.M. Yimer, Z. Zaidi, C.J.L. Murray, J.A. Crump, The global burden of non-typhoidal salmonella invasive disease: a systematic analysis for the Global Burden of Disease Study 2017, *The Lancet Infectious Diseases*. 19 (2019) 1312–1324.
- [148] B. Steinbrueckner, G. Haerter, K. Pelz, M. Kist, Routine identification of *Campylobacter jejuni* and *Campylobacter coli* from human stool samples, *FEMS Microbiology Letters*. 179 (1999) 227–232.
- [149] H.N. Stephenson, C.M. John, N. Naz, O. Gundogdu, N. Dorrell, B.W. Wren, G.A. Jarvis, M. Bajaj-Elliott, *Campylobacter jejuni* Lipooligosaccharide Sialylation, Phosphorylation, and Amide/Ester Linkage Modifications Fine-tune Human Toll-like Receptor 4 Activation, *J. Biol. Chem.* 288 (2013) 19661–19672.
- [150] H.-N. Su, Z.-H. Chen, S.-B. Liu, L.-P. Qiao, X.-L. Chen, H.-L. He, X. Zhao, B.-C. Zhou, Y.-Z. Zhang, Characterization of bacterial polysaccharide capsules and

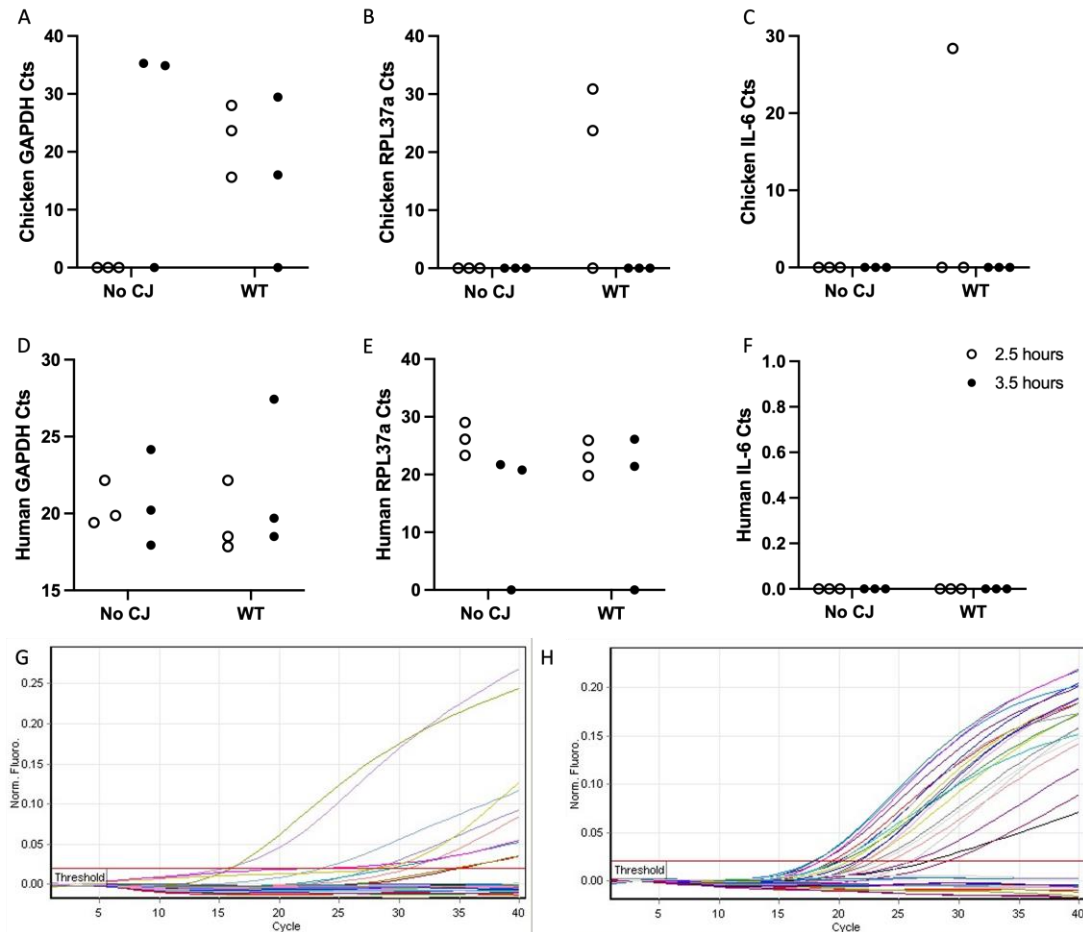
- detection in the presence of deliquescent water by atomic force microscopy, *Appl. Environ. Microbiol.* 78 (2012) 3476–3479.
- [151] B. Sumegi, A.D. Sherry, C.R. Malloy, Channeling of TCA cycle intermediates in cultured *Saccharomyces cerevisiae*, *Biochemistry.* 29 (1990) 9106–9110.
- [152] L.J. Sweetlove, A.R. Fernie, The role of dynamic enzyme assemblies and substrate channelling in metabolic regulation, *Nat Commun.* 9 (2018) 2136.
- [153] C.M. Szymanski, D.H. Burr, P. Guerry, *Campylobacter* protein glycosylation affects host cell interactions, *Infect Immun.* 70 (2002) 2242–2244.
- [154] C.M. Szymanski, M. King, M. Haardt, G.D. Armstrong, *Campylobacter jejuni* motility and invasion of Caco-2 cells, *Infect Immun.* 63 (1995) 4295–4300.
- [155] C.M. Szymanski, F.St. Michael, H.C. Jarrell, J. Li, M. Gilbert, S. Larocque, E. Vinogradov, J.-R. Brisson, Detection of conserved N-linked glycans and phase-variable lipooligosaccharides and capsules from *Campylobacter* cells by mass spectrometry and high resolution magic angle spinning nmr spectroscopy, *Journal of Biological Chemistry.* 278 (2003) 24509–24520.
- [156] K. Taha-Abdelaziz, J. Astill, B. Shojadoost, S. Borrelli, M. A Monteiro, S. Sharif, *Campylobacter*-derived ligands induce cytokine and chemokine expression in chicken macrophages and cecal tonsil mononuclear cells, *Veterinary Microbiology.* 246 (2020) 108732.
- [157] S. Tedesco, F. De Majo, J. Kim, A. Trenti, L. Trevisi, G.P. Fadini, C. Bolego, P.W. Zandstra, A. Cignarella, L. Vitiello, Convenience versus Biological Significance: Are PMA-Differentiated THP-1 Cells a Reliable Substitute for Blood-Derived Macrophages When Studying in Vitro Polarization?, *Front. Pharmacol.* 9 (2018) 71.
- [158] L. Thau, E. Asuka, K. Mahajan, Physiology, opsonization, in: StatPearls, StatPearls Publishing, Treasure Island (FL), 2020.
- [159] S. Tsuchiya, M. Yamabe, Y. Yamaguchi, Y. Kobayashi, T. Konno, K. Tada, Establishment and characterization of a human acute monocytic leukemia cell line (THP-1), *Int. J. Cancer.* 26 (1980) 171–176.
- [160] W.H.O. Unicef, Progress on drinking water, sanitation and hygiene in schools: special focus on COVID19, 2020.
- [161] M.M. Vaezirad, *Campylobacter jejuni* strategies to evade hostile environments, Utrecht University, 2017.
- [162] E.R. Vimr, S.M. Steenbergen, Early molecular-recognition events in the synthesis and export of group 2 capsular polysaccharides, *Microbiology.* 155 (2009) 9–15.
- [163] A.H.M. van Vliet, J.M. Ketley, Pathogenesis of enteric *Campylobacter* infection, *J Appl Microbiol.* 90 (2001) 45S-56S.
- [164] A. Vojdani, E. Vojdani, Reaction of antibodies to *Campylobacter jejuni* and cytolethal distending toxin B with tissues and food antigens, *WJG.* 25 (2019) 1050–1066.
- [165] C. Wagner, J. Bonnardel, C. Da Silva, L. Martens, J.-P. Gorvel, H. Lelouard, Some news from the unknown soldier, the Peyer’s patch macrophage, *Cellular Immunology.* 330 (2018) 159–167.
- [166] R. Walker, R.W. Kaminski, C. Porter, R.K.M. Choy, J.A. White, J.M. Fleckenstein, F. Cassels, L. Bourgeois, Vaccines for protecting infants from bacterial causes of diarrheal disease, *Microorganisms.* 9 (2021) 1382.

- [167] T.M. Wassenaar, M. Engelskirchen, S. Park, A. Lastovica, Differential uptake and killing potential of *Campylobacter jejuni* by human peripheral monocytes/macrophages, *Medical Microbiology and Immunology*. 186 (1997) 139–144.
- [168] R.O. Watson, J.E. Galán, *Campylobacter jejuni* survives within epithelial cells by avoiding delivery to lysosomes, *PLoS Pathog.* 4 (2008) e14.
- [169] I. Wheeldon, S.D. Minter, S. Banta, S.C. Barton, P. Atanassov, M. Sigman, Substrate channelling as an approach to cascade reactions, *Nature Chem.* 8 (2016) 299–309.
- [170] C. Whitfield, Biosynthesis and assembly of capsular polysaccharides in *Escherichia coli*, *Annu. Rev. Biochem.* 75 (2006) 39–68.
- [171] M.S. Williams, N.J. Golden, E.D. Ebel, E.T. Crarey, H.P. Tate, Temporal patterns of *Campylobacter* contamination on chicken and their relationship to campylobacteriosis cases in the United States, *International Journal of Food Microbiology*. 208 (2015) 114–121.
- [172] G.S.K. Withanage, P. Mastroeni, H.J. Brooks, D.J. Maskell, I. McConnell, Oxidative and nitrosative responses of the chicken macrophage cell line MQ-NCSU to experimental *Salmonella* infection, *British Poultry Science*. 46 (2005) 261–267.
- [173] A. Wong, D. Lange, S. Houle, N.P. Arbatsky, M.A. Valvano, Y.A. Knirel, C.M. Dozois, C. Creuzenet, Role of capsular modified heptose in the virulence of *Campylobacter jejuni*, *Molecular Microbiology*. 96 (2015) 1136–1158.
- [174] M.M.S.M. Wösten, J.A. Wagenaar, J.P.M. van Putten, The FlgS/FlgR two-component signal transduction system regulates the fla regulon in *Campylobacter jejuni*, *Journal of Biological Chemistry*. 279 (2004) 16214–16222.
- [175] F. Wu, S. Minter, Krebs cycle metabolon: structural evidence of substrate channeling revealed by cross-linking and mass spectrometry, *Angew. Chem. Int. Ed.* 54 (2015) 1851–1854.
- [176] L. Yang, H. Guo, Y. Li, X. Meng, L. Yan, Dan Zhang, S. Wu, H. Zhou, L. Peng, Q. Xie, X. Jin, Oleoylethanolamide exerts anti-inflammatory effects on LPS-induced THP-1 cells by enhancing PPAR α signaling and inhibiting the NF- κ B and ERK1/2/AP-1/STAT3 pathways, *Sci Rep.* 6 (2016) 34611.
- [177] K.T. Young, L.M. Davis, V.J. DiRita, *Campylobacter jejuni*: molecular biology and pathogenesis, *Nat Rev Microbiol.* 5 (2007) 665–679.
- [178] N. Zebian, A. Merckx-Jacques, P.P. Pittock, S. Houle, C.M. Dozois, G.A. Lajoie, C. Creuzenet, Comprehensive analysis of flagellin glycosylation in *Campylobacter jejuni* NCTC 11168 reveals incorporation of legionaminic acid and its importance for host colonization, *Glycobiology*. 26 (2016) 386–397.
- [179] M. Zolli, D.J. Kobric, E.D. Brown, Reduction precedes cytidylyl transfer without substrate channeling in distinct active sites of the bifunctional CDP-ribitol synthase from *Haemophilus influenzae*, *Biochemistry*. 40 (2001) 5041–5048.
- [180] The European Union summary report on trends and sources of zoonoses, zoonotic agents and food-borne outbreaks in 2013, *EFSA Journal*. (n.d.).

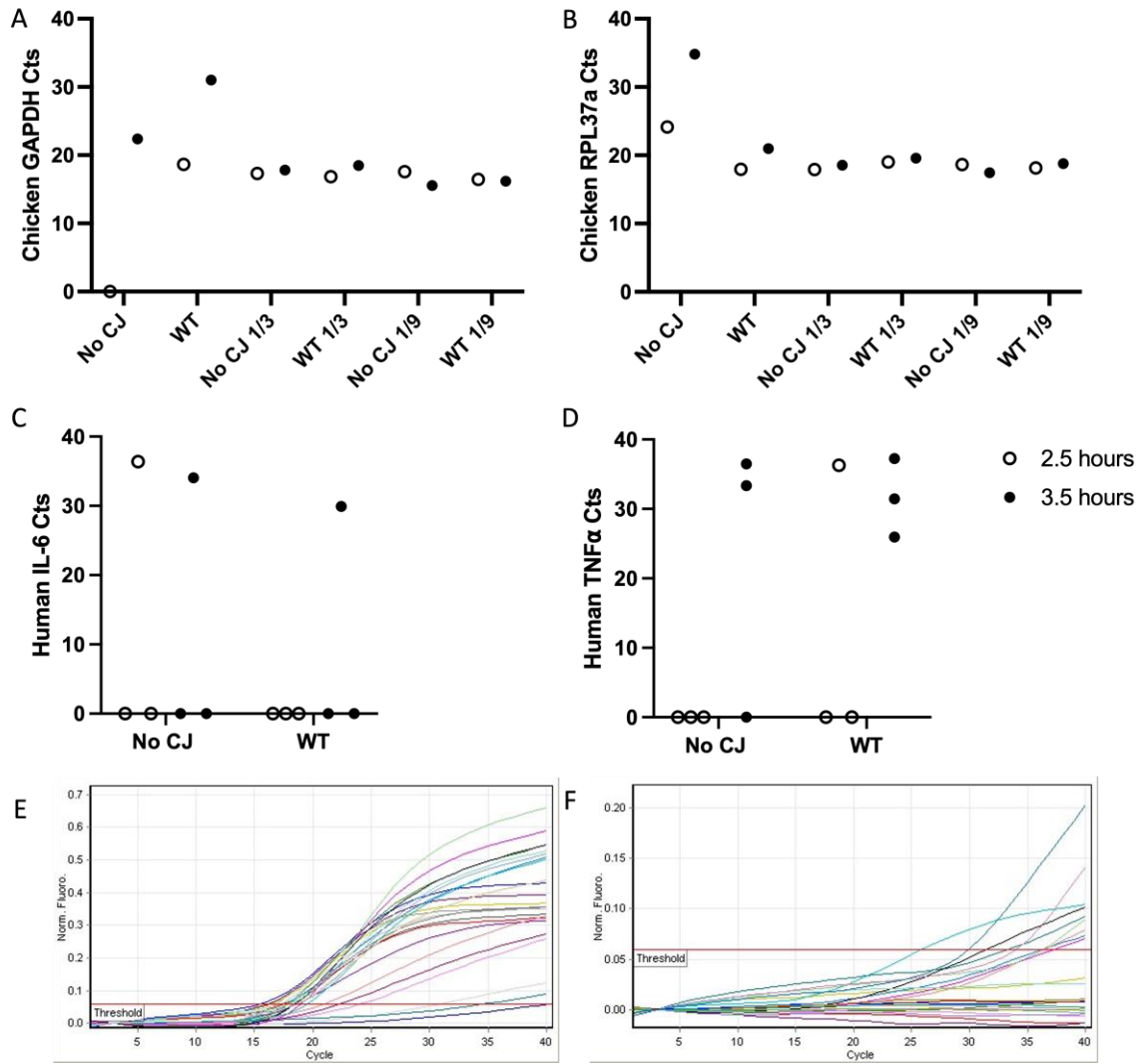
Appendix 1: qRT-PCR figures



Supplemental Figure 1: Fold change in the expression of THP-1 macrophage cytokine mRNA upon challenge with WT *C. jejuni*. Data consists of a single biological replicate (n=1), run with technical triplicates. 1×10^6 cells were co-cultured at an MOI of 200 (37°C, 5% CO₂) for 0.5 to 3.5 hours before being lysed with Trizol reagent. RNA was subsequently extracted and quantitated by nanodrop. One μ g of RNA was reverse transcribed using Superscript II reverse transcriptase. One μ L of the cDNA preparation was added to PowerUp SYBR Green master mix for qPCR analysis. The fold change is expressed relatively to samples from non-exposed macrophages.



Supplemental Figure 2: Cycling threshold values for cDNA generated from the co-culture of wild-type *C. jejuni* with host macrophages. 1×10^6 THP-1 (hu) or 3×10^6 MQ-NCSU (ch) macrophages were co-cultured at an MOI of 200 (37°C , $5\% \text{CO}_2$) for 2.5 or 3.5 hours before being lysed with Trizol reagent. RNA was subsequently extracted and quantitated by nanodrop. One μg of THP-1 or $3 \mu\text{g}$ of MQ-NCSU derived RNA was reverse transcribed using SuperScript II reverse transcriptase (Invitrogen). Two μL of the cDNA preparation was added to PowerUp SYBR Green Master Mix (Thermofisher Scientific) for qPCR analysis, $n=1$. Graphs indicate the cycling threshold values for chicken (A,B,C) or human (D,E,F) cDNA amplified with primers targeting GAPDH(A,D), RPL37a (B,E), or IL-6 (C,F). Graphs depict the cycling profiles of chicken (G) or human (H) cDNA over 40 cycles. CJ= *C. jejuni*.



Supplemental Figure 3: Cycling threshold values for cDNA generated from the co-culture of wild-type *C. jejuni* with host macrophages, rerun with modifications.

mRNA was prepared and reverse transcribed as in figure 10. Chicken (ch) cDNA was diluted by a factor of 3 or 9 after which 2 μ L of these samples were amplified with primers targeting GAPDH (A) or RPL37a (B). Two μ L of human (hu) cDNA was amplified with primers targeting IL-6 (C) or TNF α (D). Graphs depict the cycling profiles of chicken (E) or human (F) cDNA over 40 cycles. CJ= *C. jejuni*.

Appendix 2: Macrophage clearance work accomplished by Daniel Zimmermann

Supplemental Table 1: Macrophage clearance data generated by Daniel Zimmermann.

Assays	# of WT repeats	# of MlghB repeats	# of MlghC repeats	# of WcaG repeats	# of WcaG Δ repeats	# of KpsM repeats
THP-1 adhesion, inoculum, macrophage and monocyte output, 30 min macrophage control, 30 min monocyte control, 30 min media only control	n=6	n=3	n=3	n=3	n=3	n=1
THP-1 uptake inoculum, inoculum, 1- and 3-hour macrophage controls, and the 1- and 3-hour macrophage output	n=7	n=5	n=5	n=4	n=4	n=2
THP-1 uptake 1-hour monocyte control, 1- and 3-hour monocyte uptake output	n=5	n=3	n=3	n=2	n=2	n=2
THP-1 uptake 3-hour monocyte control	n=5	n=2	n=2	n=3	n=3	n=2
THP-1 uptake 1- and 3-hour media controls	n=4	n=4	n=4	n=3	n=3	n=0
MQ-NCSU uptake inoculum, 1- and 3-hour macrophage controls, 1- and 3- hour uptake output	n=3	n=3	n=3	n=3	n=3	n=3
THP-1 survival inoculum, 1- and 3-hour monocyte survival output and 1 hour macrophage survival output	n=7	n=4	n=4	n=2	n=2	n=1
THP-1 survival 3-hour macrophage survival output	n=7	n=3	n=3	n=2	n=2	n=1
THP-1 survival 2-hour media only control	n=5	n=3	n=3	n=4	n=4	n=2

Curriculum Vitae

Name: Matthew Myles

Post-secondary Education and Degrees: The University of Western Ontario
Windsor, Ontario, Canada
2016-2020 B.MSc. (Western Scholars) Honours specialization in microbiology and immunology with, minor in psychology

The University of Western Ontario
London, Ontario, Canada
2020- M.Sc. Candidate in microbiology and immunology, in the Creuzenet laboratory

Honours and Awards: Western Continuing Admission Scholarship
2016-2020

Dean's Honour List
2017- 2020

Natural Sciences and Engineering Research Council of Canada (NSERC), Undergraduate Student Research Award.
Kim Lab, 2018
Creuzenet Lab, 2019

Dr. FW Luney Graduate Entrance Scholarship in Microbiology and Immunology
2020

NSERC Canada Graduate Scholarships-Master's
2020-2021

Ontario Graduate Scholarship
2021-2022

Related Work Experience Teaching Assistant: Microimm 3620G (Immunology Lab)
The University of Western Ontario
2021-2022

Conference publications:

Creuzenet C. Barnawi H. Myles M. Zimmerman D. Naismith J. (2020). Making a dent in campylobacteriosis by biting in *Campylobacter jejuni*'s sugar coat. Abstract. Presented by Carole Creuzenet at FASEB 2020 Microbial Glycobiology Conference, Lisbon, Portugal, moved online due to the COVID-19 Pandemic.

Myles M. and Creuzenet C. (2020) *Campylobacter jejuni* Capsular Heptose: Moderation of Host Macrophage Activation and Substrate Channeling During Synthesis. Abstract and 3 minute thesis. Presented at the Infection and Immunity Research Forum, Western University, Online.

Myles M. and Creuzenet C. (2021) *Campylobacter jejuni* Capsular Heptose in the Moderation of Host Macrophages. Abstract and poster. Presented at London Health Research Day, Online.

Myles M. and Creuzenet C. (2021) *Campylobacter jejuni* Capsular Heptose in the Moderation of Host Macrophage Activation. Abstract and Poster. Presented at the Canadian Society of Microbiologists Conference, Online.

Myles M. and Creuzenet C. (2022) *Campylobacter jejuni* Capsular Heptose in the Moderation of Clearance by Host Macrophages. Presented at the Canadian Society of Microbiologists Conference, Guelph, Canada.